An integrative approach to investigate the textural properties and possible mechanisms in the formation of Woody Breast in broilers

by

Amelia Welter

B.S., Kansas State University, 2019

A THESIS

submitted in partial fulfillment of the requirements for the degree

MASTER OF SCIENCE

Department of Animal Science and Industry
College of Agriculture

KANSAS STATE UNIVERSITY
Manhattan, Kansas

2021

Approved by:

Major Professor
Dr. Michael Chao

Copyright

ABSTRACT

Woody breast (WB) is a myopathy observed in chicken breast meat (*Pectoralis* major), that is characterized by a tough and rubbery texture. The objective of this study was to investigate factors and enzymatic activities contributing to the abnormal texture seen in WB and utilize integrative omics (proteomics/lipidomics) to examine the functionality/integrity of WB sarcoplasmic reticulum (**SR**). Fourteen Ross line broiler breast fillets (7 severe WB and 7 normal) were collected at 3 h postmortem from a commercial processing plant. Around 8 h postmortem, each sample was trimmed, weighed, vacuum packaged and frozen at -20°C. A section of the cranial end of each fillet was pulverized in liquid nitrogen to measure pH, objective tenderness, sarcomere length, free calcium concentration, proteolysis, calpain activity, collagenase activity, collagen content, collagen crosslinks and peak transitional temperature measurements. The SR fractions of the samples were extracted via ultracentrifugation through discontinuous sucrose gradients. The SR factions were separated into lipid and protein for lipidomic and proteomic analysis. The WB fillets were heavier than normal chicken breast fillets (522.9 vs. 446.9g; $P<0.05$) and exhibited a higher pH (6.17 vs. 5.83; $P<0.05$). Objective tenderness was not significantly different (34.09 vs. 37.69 N; $P>0.10$), but WB samples tended to have shorter sarcomeres (1.70 vs. 2.02 μm; $P=0.05$) and less intact troponin-T compared to normal breast samples (relative intact troponin-T band density: 49.98 vs. 56.97%; $P=0.05$) at 8 hrs postmortem. For enzymatic activity, WB had more autolyzed μ/m calpain levels (71.05 vs. 59.12% calpain autolyzed; $P<0.01$) and more activated collagenase (13.24 vs. 7.84% activated MMP2; $P<0.05$). In addition, the purge from WB samples also had higher levels of free calcium compared to normal samples (6.2 vs. 4.2 nmol calcium/mg protein; $P<0.05$). There was increased collagen levles present in the WB samples compared to normal chicken breast samples

(3.89 vs. 2.08 mg collagen/g muscle tissue; $P<0.05$), as well as more mature crosslinks in WB (0.23 vs. 0.14 mol PYD/mol collagen; $P < 0.05$; 0.07 vs. 0.04 mol DPD/mol collagen; $P < 0.01$). Finally, WB had a higher peak transitional temperature compared to N (65.47 vs. 63.72°C; $P<0.05$). Lipidomics data revealed significant differences for 66 phospholipid species and WB SR had a less relative % of phosphatidylcholine (PC) and more phosphatidylethanolamine (PE), phosphatidylserine (PS) and lysophosphatidylcholine (LPC) ($P<0.05$). Proteomics data revealed 677 proteins with differential abundance with WB SR having an upregulation of calcium transport proteins (ex. sarcoplasmic/endoplasmic reticulum calcium ATPase), a downregulation of proteins responsible for calcium release and signaling (ex. ryanodine receptors), and no difference for calcium storage proteins (ex. Calsequestrin). There was a significant upregulation to stress response proteins in WB ($P<0.05$). As for membrane integrity, there was an upregulation of phospholipase A2 (PLA2) in WB SR ($P<0.01$) and membrane repair proteins ($P<0.05$). Interestingly, cholinesterase exhibited a 7.62-fold increase in WB SR ($P<0.01$). This study showed that the cause of texture abnormality of WB may be the combined effects of increased collagen and more calcium being released from the SR early postmortem. The elevated free calcium levels in WB meat may be due to alterations in lipid structure and increases in the breakdown of SR membrane phospholipids ultimately causing integrity issues. On the other hand, the upregulation of cholinesterase activity is an indicator of the presence of cholinesterase inhibitors. Perhaps, the action potential in WB is prolonged due to the inhibition of cholinesterase causing the additional release of calcium from the SR.

Table of Contents

List of Figures

List of Tables

Acknowledgements

First, I would like to thank Dr. Michael Chao, my major professor who has offered endless guidance throughout this process. Who knew when you first talked to me as an undergraduate that we would end up here? You really pushed me to challenge myself through my research and taught me lots of valuable life skills, as well as expanded my cultural knowledge. I can't even begin to show my gratitude for everything you have done for me over the past few years between answering tons of questions, reading loads of writing and lots of fun adventures along the way. I would also like to extend a thank you to Ying, Luke and Hans for some amazing meals, kindness, and fun memories at the Chao house, you truly have a wonderful family.

Additionally, I would like to thank my committee members Dr. Travis O'Quinn and Dr. Erika Geisbrecht for all your advice and support throughout my program at K-state. I would also like to thank David Brooks from the Department of Biochemistry and Molecular Biophysics for offering a lot of assistance in the development of protocols for my project, I really enjoyed working with you. I would also like to thank Dr. Steve Hartson from Oklahoma State, you provided exceptional guidance as I experienced proteomics work for the first time. Furthermore I would like to thank Sally Stroda, John Wolf and the meat lab employees for all their help and conversation during my program.

Everything I accomplished would not have been possible without the help of my wonderful peers. Wanjun, Colin, Abby and Larissa you guys have always been there for me whenever I needed help, someone to motivate me or simply a friend. We had some great times, made lots of amazing memories and I am so grateful I got to meet all of you. I would also like to thank our undergrads, Emily and Faith, you guys were always so willing to help whenever with

whatever. Moreover, I would like to thank the other meat science grad students, the office was always such a great environment to be a part of and you were all so willing to assist with projects and answer questions.

Finally, I would like to thank my parents, Myrna and Randy, as well as all of my siblings. You guys have always pushed me to follow my passion and I knew I could always call any of you for advice anytime. A huge thank you to my fiancé, Ethan, you have been my rock throughout this whole thing. All your love and support did not go unnoticed and was greatly appreciated, I would not be where I am today without all of you or your love for pork!

Dedication

I would like to dedication this thesis to my family and my fiancé Ethan, this would not have been possible without everyone's unending love and encouragement, from very close and very far away.

Chapter 1 - Literature Review

INTRODUCTION

Over the past few decades, there have been tremendous improvements seen in the poultry industry that have led to better yields with greater feed to gain conversion (Anthony, 1998). This has helped meet the ever growing demand for boneless broiler breast meat in the United States (Caldas-Cueva and Owens, 2020). Unfortunately, there were unexpected consequences from these grow efficiency enhancements, particularly in the area of broiler meat quality (Yalcin, et al., 2018). Woody Breast (**WB**) syndrome is a meat quality defect that produces highly undesirable textural characteristics for the *Pectoralis Major* muscle in chicken (Sihvo, et al., 2014). This defect alone has cost the poultry industry over $200 million per year in economic losses (Kuttappan, et al., 2016). Research has found that the broilers exhibiting WB suffer from oxidative stress promoting hypoxic conditions (Abasht, et al., 2016; Dridi and Kidd, 2016; Mutryn, et al., 2015). Hypoxia can lead to necrosis resulting in the generation of scar and connective tissue (Sihvo et al., 2014). Interestingly, there have been multiple studies showing high levels of sarcoplasmic calcium in WB samples (Soglia, et al., 2016b; Soglia, et al., 2018; Tasoniero, et al., 2016). Sarcoplasmic reticulum (**SR**) plays a key role in maintaining calcium homeostasis within the cell (Endo, 1977), and an imbalance in sarcoplasmic calcium levels can significantly alter meat quality, particularly, meat tenderness (Ertbjerg and Puolanne, 2017; Koohmaraie, 1988; Ren, et al., 2019). Hence, the aim of this literature review is to review the meat quality differences between WB and normal (**N**) meat and how the functionality of the SR and elevated calcium levels may play a role on the development of meat quality differences.

WB Syndrome

The meat texture abnormalities of WB have been identified as tough and rubbery with hardened ridge-like bulges along the caudal and cranial regions of the *Pectoralis Major* muscle (Kuttappan, et al., 2016). In severe WB cases, clear viscous fluids covering the meat and scattered hemorrhages in the meat have been described (Sihvo, et al., 2014). The incidence of WB within the United States was reported as 30-50% as of 2015 with a wide range of severity (Owens, 2016). The morphological changes from the WB myopathy can be observed in broilers around 2 weeks of age (Sihvo, et al., 2017). Studies have shown WB can demonstrate histological signs of myodegeneration, lymphocytic vasculitis, lipidosis, and fibrosis (Sihvo, et al., 2014; Sihvo, et al., 2017; Velleman and Clark, 2015; Velleman, et al., 2018). Due to these observed pathological changes, WB meat often contains higher level of fat, collagen and moisture with reduced levels of protein and ash (Baldi, et al., 2019; Soglia, et al., 2016a). Unfortunately, the exact etiology for WB has not been determined, but research has shed light on some possible causative mechanisms.

Textural Differences Between WB and N Meat

As mentioned earlier, WB produces many undesirable meat quality defects; however, this literature review will focus on the textural differences. One way to determine textural differences is to measure tenderness either objectively or subjectively. The most commonly utilized method to measure objective tenderness is Warner-Bratzler Shear Force (**WBSF**) (Destefanis, et al., 2008). Other studies have utilized textural profile analysis (**TPA**), Allo-Kramer shear cell (**AK**) and Meullenet-Owens Razor Shear (**MORS**) to evaluate WB meat's textural properties (Aguirre, et al., 2018; Cavitt, et al., 2004; Chatterjee, et al., 2016; Lee, et al., 2008b). As for subjective measurements of tenderness, trained panels, where the participants have been standardized to

discriminate among textural attributes or consumer panels, which consist of untrained consumers, have both been utilized to assess sensory tenderness for WB meat (Aguirre, et al., 2018; Solo, 2016).

All the described tenderness measurement methodology are commonly utilized in poultry meat industry. Aguirre, et al. (2018) utilized 6 expert panelists and noted WB meat to have higher values for springiness, hardness, denseness, cohesiveness, crunchiness, fracturability, fibrousness and chewiness, and Solo (2016) found that untrained consumers prefer the texture of N fillets over WB fillets. As expected, there is a lot of discrepancy between methodology for objective tenderness measurements. Many noted no difference in tenderness when utilizing WBSF and AK to compare the textural properties between N to WB (Aguirre, et al., 2018; Cai, et al., 2018; Dalgaard, et al., 2018; Gratta, et al., 2019; Soglia, et al., 2017). However, Bowker and Zhuang (2019) and Chatterjee, et al. (2016) noted higher peak shear force and shear energy for WB samples indicating increased toughness compared to N using MORS. Finally, Chatterjee, et al. (2016) and Aguirre, et al. (2018) both found WB meat to be harder and chewier than N samples using TPA.

It has been discussed previously that WB meat is described as tough and rubbery; however, the data does not offer consistent findings. No difference is observed for WBSF and AK methods, but MORS and TPA found WB meat to be described as tougher, harder, and chewier. The discrepancy between results could be attributed to methodology differences and measurement locations with the muscle. Kuttappan, et al. (2016) hypothesizes the textural differences observed in WB meat are due to the deposition of scar tissue resulting in more connective tissue. Therefore, the traditional WBSF peaks may not be able to distinguish tenderness differences as they represent the textural property from the myofibrillar components

(Girard, et al., 2012). However, shear force measurements such as MORS and TPA, may be a more appropriate method to determine textural characteristics of WB as they offer more consistent results (Aguirre, et al., 2018; Bowker and Zhuang, 2019), but more research is needed to fully understand the best method to define WB texture.

Chemical Differences Between WB and N Meat

pH. Multiple studies have shown higher pH values for WB meat, around 6.0, compared to N meat having an average value of approximately 5.8 (Bowker, et al., 2016; Cai, et al., 2018; Dalle Zotte, et al., 2014; Kuttappan, et al., 2017; Mudalal, et al., 2015). Unfortunately, the actual cause of the pH increase in WB meat has not yet been understood, but current literature posits two possible theories: 1. Aguirre, et al. (2018) suggested that myodegeneration as well as an increase in interstitial connective tissue may alter the pH of the meat; 2. Mudalal, et al. (2015) and Kuttappan, et al. (2017) hypothesized there may be disruptions to the rigor mortis process due to a downregulation of carbohydrate metabolism resulting a higher ultimate pH. Degeneration of muscle cells could reduce the glycogen content as glycogen is stored in muscle cells, and less glycogen can impact the pH decline process (Matarneh, et al., 2017; Mudalal, et al., 2015). However, no conclusion has been reached regarding the exact cause of the consistent finding for higher pH in WB meat. Again, more research is needed to fully understand the mechanism behind the increase pH in WB meat.

Proximate Analysis. The overall composition of muscle tissue can impact the quality of the meat as each component can influence different textural characteristics. Many studies have shown WB meat to have a higher moisture and fat and lower protein content compared to N breast meat (Cai, et al., 2018; Rigdon, et al., 2021; Soglia, et al., 2016b). It has been suggested that WB meat undergoes muscle degeneration, and some of the myofibrillar proteins are replaced

by connective tissue and fat, which resulted in the decrease in overall protein content (Dalle Zotte, et al., 2014). Additionally, there is an increased levels of fat because of lipidosis, or the deposition of fat, during regeneration of muscle tissue in WB broilers (Sihvo, et al., 2014; Trocino, et al., 2015). It is important to point out even though WB has been shown to have higher moisture content, the ability to retain the water is reduced possibly due to the increase in connective tissue and the reduced myofibrillar proteins as previously mentioned (Dalgaard, et al., 2018; Mazzoni, et al., 2015).

Collagen Characteristics. Connective tissue, with the main component being collagen, can impact meat texture because it is known to have a negative relationship with tenderness (Berry, et al., 1988). Collagen has been a topic of high interest in WB research as many have suggested that fibrosis is occurring, where muscle tissue is being broken down and regenerated as connective tissue (Sihvo, et al., 2014; Sihvo, et al., 2017; Velleman and Clark, 2015). Many studies have shown an increase in collagen content in WB meat compared to N (Baldi, et al., 2019; Soglia, et al., 2016a; Soglia, et al., 2016b). However, Morey, et al. (2020) found no difference in soluble and insoluble collagen content between N and WB samples. Interestingly, Rigdon, et al. (2021) found no difference in the soluble collagen content but noted a significant increase in insoluble collagen content for WB meat. High densities of collagen crosslinking, particularly pyridinoline (PYD), has been shown to have a strong impact on meat texture and collagen solubility (Wu, et al., 2021), which Baldi, et al. (2019) noted higher densities of PYD were found in WB compared to N samples. Brasselet, et al. (2005) has observed scar tissue possesses excessive collagen crosslinking in rabbit arterial tissue. Therefore, it is possible that the accumulation of scar tissue in WB meat resulted in higher collagen crosslinking and the higher content of insoluble collagen, which contributed to the textural defects seen in WB meat.

Free Calcium Concentration. Intracellular calcium levels are important to meat quality as it plays a key role during the rigor mortis process as well as the tenderization process in postmortem muscle (Gordon, et al., 2000; Koohmaraie, 1988). Increased calcium levels have been consistently observed in WB meat (Soglia, et al., 2016b; Soglia et al., 2018; Tasoniero, et al., 2016), where Soglia, et al. (2016b) recorded calcium levels for WB meat at approximately 20.8 mg/100 g of raw meat compared to roughly 8.40 mg /100 g raw meat for N samples. Calcium concentration within the cell is kept very low around less than 0.4 mM and is mostly stored in the SR, while the extracellular calcium concentration is typically around 2-4 mM (Kuo and Ehrlich, 2015). Therefore, any movement of calcium across the membrane can easily disrupt homeostasis. In order to preserve this strict concentration gradient, there is a very sophisticated system in place within the SR that serves primarily as a calcium cache (Szent-Györgyi, 1975). Soglia, et al. (2018) suggested that there may be dysfunctionality of WB SR, which possibly obstruct the SR's ability to properly resequester the calcium ions back into the SR, hence, the high levels of sarcoplasmic calcium. This theory will be discussed in more detail later in the literature review.

Protease Activity Differences Between WB and N Meat

Proteases are enzymes that catalyze peptide bond hydrolysis, ultimately degrading structural proteins in muscle tissue (Asghar and Bhatti, 1988). It warrants special attention for this literature review because many well-known proteases such as calpains and matrix metalloproteinases are calcium dependent. With the noted increase in the free calcium concentration in WB meat, it is likely the protease activity is also altered in WB compared to N meat.

Calpain Activity. The calcium-dependent protease calpain is the main enzyme system involved in meat tenderization (Bhat, et al., 2018). There are various isoforms of this protease, but in postmortem avian muscle, the major active calpain form is μ/m calpain (Lee, et al., 2008a). The most common way to measure calpain activity is through casein zymography (Lee, et al., 2008a; Soglia, et al., 2018), in which the degradation of the casein in gels represents the activity of the calpains (Biswas and Tandon, 2019). Soglia, et al. (2018) utilized casein zymography and noted increased amounts of activated μ/m calpain while also seeing a decrease in inactivated μ/m calpain in both WB and N meat as refrigerated storage time progressed. Unfortunately, no difference in calpain activity was found between WB and N samples. On the other hand, Hasegawa, et al. (2020) measured calpain activity through spectrophotometry in which calpain activity was determined by a calcium-dependent increase in absorbance, and they noted a significant increase in calpain activity for WB meat. These results are interesting since calpain is a calcium-dependent protease, and WB meat is known to have high levels of calcium. Therefore, we should expect to consistently observe more calpain activity in WB.

Calpain degradation products. Proteolysis refers to the weakening of the ultrastructure of the proteins which plays an important role in contributing to the tenderness of the meat (Kemp and Parr, 2012). There are different ways to measure proteolysis in meat, such as gravimetric fragmentation index (**GFI**) and western blotting. The GFI method utilizes vacuum-filtration of meat homogenate through nylon screens to compare the weight of the original sample to the residue weight (Sams, et al., 1991). It has an inverse relationship with the fragmentation index, which indicates the extent of myofibrillar fragmentation in muscle due to proteolysis (Owens and Sams, 1997). Alternatively, western blotting uses immunodetection to quantify specific proteins and its degradation products (Welinder and Ekblad, 2011). Sun, et al. (2018) utilized GFI and

noted a higher fragmentation index for WB samples compared to N samples indicating more proteolysis as well as increased proteolysis with WB severity. Other research has shown that proteolysis, particularly the degradation of the desmin, was found to be higher in WB meat as it was noted to have less intact desmin compared to N meat (Bowker, et al., 2016; Zhang, et al., 2020). Another protein typically observed with western blotting is troponin-T (**TNT**), but Tijare, et al. (2016) found no significant difference for TNT degradation between WB and N breast using western blotting. Overall, there appears to be increased proteolysis observed in WB meat which could be a result of increased calpain activity as previously discussed.

Sarcoplasmic Reticulum Functionality and Calcium

Muscle cells contain a multitude of organelles and proteins that are required for the process of contraction and relaxation to occur. During the excitation-contraction-coupling (**ECC**) reaction the SR organelle is vital as it is the calcium reservoir of the cell. Together the SR and calcium ions play a crucial role ensuring skeletal muscle activity transpires without complication.

Sarcoplasmic Reticulum Function. The SR is a domain of the endoplasmic reticulum (ER) organelle (MacLennan and Campbell, 1979) and is derived from rough-surface ER during the earliest myotube stage (Ezerman and Ishikawa, 1967). This SR tubule system indirectly wraps itself around myofibrils and are intimately associated with the transverse tubules (T-tubules) at the terminal cisternae in skeletal muscle. These two components interact with each other to form triads within the sarcomere of muscle cells (Ezerman and Ishikawa, 1967). The location and structure of the SR indicate it is involved in the activation for contraction specifically through the absorption, storage, and release of calcium.

Muscle contraction/relaxation is a calcium-dependent reaction. When contraction is initiated, calcium is released from the SR and binds to troponin C, causing a conformational change that allows for the binding between actin and myosin heads. As relaxation is instigated, the calcium is pumped back into the SR resulting in the breakage of the actin and myosin bonds. When neither contraction nor relaxation is happening, the calcium is simply stored in the SR until needed again for contraction or other biological pathways (Szent-Györgyi, 1975). Any disruption in SR proteins or membrane integrity can lead to aberrant muscle contraction and/or relaxation (Hirata, et al., 2006; Houser, 2001; Jungbluth, et al., 2018).

Effect of SR Protein Composition and SR Functionality

Calcium transportation. Sarco/endoplasmic reticulum calcium transport ATPase (**SERCA**) is a protein that serves as a pump to sequester calcium ions from the sarcoplasm into the SR. The pump is embedded in the membrane of the SR as a single polypeptide chain with three isoforms found in mammals, SERCA1 (~110kDa), SERCA2 (~100kDa) and SERCA3 (~97kDa), all of which have unique isoforms and functions (Zanotti, 2016). SERCA1 is commonly found in fast-twitching skeletal muscle, SERCA 2 in cardiac and slow-twitch skeletal muscle and SERCA3 in vascular endothelial cells, tracheal epithelium and pancreatic β-cells (Prasad, et al., 2004). Given that SERCA is an ATPase, it requires the hydrolysis of ATP for energy (Mueller, et al., 2004). Since this is an ATP-dependent protein, any inhibition of ATP synthesis can also impact the functionality of SERCA. Prasad, et al. (2004) showed that SERCA1 knockout mice had a significant reduction in calcium uptake activity, resulting in hyper contraction in various muscles. Additionally, there are known SERCA inhibitors, with a popular one being thapsigargin, that can induce calcium release from the SR and prevent calcium uptake through inhibiting the SERCA pump (Lytton, et al., 1991). This ultimately can alter calcium

homeostasis within the cells. Finally, Larsen, et al. (2001) added ethyleneglycolbis(β-aminomethylether)-N,N', tetraacetic acid and dithioteritol to PC12 neural cells to induce an ER/SR stress response and found an increase in SERCA pumping capacity. Clearly, many factors can impact the functionality of SERCA and the transportation of calcium in cells.

Calcium release. Ryanodine receptor (**RyR**) is a protein found in the membrane of the SR whose primary function is calcium release from the SR during ECC in muscle cells. This homotetramer protein is the largest known ion channel with a mass greater than 2,000 kDa (Lanner, et al., 2010). Just as SERCA, there are three isoforms of RyR found in mammals (RyR1, RyR2 and RyR3) that each serve a specific function in the process of calcium release. RyR1 is primarily found in skeletal muscles, while RyR2 is expressed in cardiac muscle and RyR3 in wide variety of cell types with low levels in skeletal muscle (Capes, et al., 2011). RyR is mainly controlled by the interaction with dihydropyridine receptors (**DHPR**) during an action potential in skeletal muscle (Fill and Copello, 2002). As the membrane depolarizes (excitation), there is a conformational change in DHPR that leads to the activation of RyR to release calcium from the SR (Fill and Copello, 2002). Finally, when calcium concentration inside of the SR is high (>100μM), the channel is locked in the open position to allow for the release of calcium through sarcolemma depolarization (Lanner, et al., 2010), which is known as calcium-induced calcium release.

Kushnir, et al. (2010) found poor muscle tone, muscle weakness and musculoskeletal abnormalities in RyR1 knockout mice throughout development. In addition, the skeletal muscle was not contracting under electrical stimulation due to the cells' inability to release calcium from the SR. On the other hand, hyperactivity of RyR1 can result in excessive release of calcium and is characterized by the development of muscle weakness, as seen in patients with malignant

hypothermia (**MH**) and central core disease (**CCD**) (Capes, et al., 2011). Durham, et al. (2008) and Boncompagni, et al. (2009) performed studies using mice whose gene sequence was modified to express a leaky RyR1 channel and found elevated calcium release as expected. Additionally, both noted an increase in reactive oxygen species (**ROS**) damage leading to further calcium leakage and thought it may be contributing to the progressive development of myopathies characterized by decreased muscle performance such as MH and CCD (Boncompagni, et al., 2009; Durham, et al., **2**008). Ultimately, they are suggesting that oxidative damage due to calcium leakage could be contributing to the progression of these diseases (Capes, et al., 2011).

Calcium storage. Calsequestrin (**CASQ**) is the most abundant calcium binding protein in the SR. Around 40-50 calcium ions (~20 mM) can bind to a single CASQ protein. This results in an increase of the total amount of calcium that can be held within the SR (Beard, et al., 2004). This acidic protein is a monomer with a molecular mass of around 40 kDa and is located at the cisternae of the SR. There are two isoforms of CASQ, CASQ1 found in fast skeletal muscle and CASQ2 in cardiac and slow skeletal muscle (Novák and Soukup, 2011). The protein CASQ plays an important role in controlling calcium release and uptake by sensing the concentration of calcium in both the sarcoplasm and SR. Although CASQ has a low affinity for calcium, the binding capacity is extremely high. The binding occurs through a conformation change in which the hydrophobicity of the protein is lost, allowing calcium to bind and stabilize the protein (Berchtold, et al., 2000). When calcium is needed for contraction, CASQ releases the bound calcium to allow it to flow through the RyR channel (Wang and Michalak, 2020). Paolini, et al. (2015) used CASQ1 knockout mice to investigate its role in the development of MH and CCD, and they found that CASQ1 knockout mice had structural disarray along with an increase in

mitochondrial numbers. This is interesting to note because ROS are mostly generated in the mitochondria, and ROS production leads to oxidative stress. In fact, Paolini, et al. (2015) documented higher levels of oxidative stress in the CASQ1 knockout mice compared to the wild type. This is concerning as oxidative stress can injure protein and membrane lipids due to the imbalance of oxidant production and antioxidant activity (Moylan and Reid, 2007). On the other hand, overexpression of CASQ will inhibit RyR function (Miller, et al., 2005), resulting in myopathies as previously discussed in the case on RYR knockout mice.

Effect of SR Phospholipid Profile on SR Functionality

Many proteins that are a part of the SR are anchored in the membrane of the organelle, so the phospholipid profile must also be considered. Biological membranes are vital because they act as barriers that house proteins required for various processes. Although all the phospholipid species serve an important role to cell/organelle membrane, we are specifically going to review phosphatidylcholine (**PC**), phosphatidylethanolamine (**PE**) and phosphatidylerine (**PS**) due to the specific findings from this research.

Phosphatidylcholine. The most abundant phospholipid in mammalian cells and tissues is PC, making up 45-55% of the total phospholipids (Vance, 2015). This phospholipid is composed of hydrocarbon chains attached to glycerolphosphocholine via acyl, alkyl, or alkenyl linkages (DeLong, et al., 1999). Besides its structural role, PC also serves as a major source of intracellular signaling molecules (Testerink, et al., 2009). There are two pathways to which PC can be synthesized, the most common being the cytidine diphosphate (CDP)-choline pathway (Li and Vance, 2008), but in liver cells, the process involves methylation of PE to PC (DeLong, et al., 1999). Animals mainly get choline from their diet but can also obtain it from pathways such as PC or acetylcholine catabolism (Li and Vance, 2008).

Unfortunately, phospholipids can undergo hydrolysis which alters the composition and functionality of the membranes. Pikuła, et al. (1994) showed the addition of phospholipase C resulted in PC hydrolysis, and that PC content has a positive relationship with SERCA activity. Andersen, et al. (1983) confirmed that PC content and SERCA have a positive relationship by showing high PC to SERCA ratio with more calcium being sequestered per mole of hydrolyzed ATP. This indicates that reduction in PC content in membranes can impact the SR functionality, particularly its ability to resesquester calcium. This may be due to PC being the main structural phospholipid in mammalian cell membranes (Kanno, et al., 2007), and the SERCA is a membrane embedded protein.

While there are multiple phospholipases that hydrolysis phospholipids, phospholipase A2 (**PLA2**) is an important one to investigate because it exhibits a preference for PC and converts PC into lysophosphatidylcholine (**LPC**) and a free fatty acid (Mouchlis, et al., 2018). This reaction can cause significant damage to cell membranes (Diaz and Arm, 2003). Any disruption to the phospholipid structure of cell membranes can impact the integrity of the membrane as well as trigger ER/SR stress affecting the functionality of the proteins as previously discussed (Fu, et al., 2011; Li, et al., 2006). Overall, PC plays a huge role in the functionality of the SR as it can impact the cell's ability to move calcium into the SR via the protein pumps embedded in the membrane.

Phosphatidylethanolamine. The second most abundant phospholipid in mammalian membranes is PE, constituting about 15-25% of the total phospholipids (Vance, 2015). It has been shown that PE is enriched in the inner membrane of the mitochondria and can alter the morphology of the mitochondria (Steenbergen, et al., 2005). In addition to being a membrane component, PE also plays an important role in apoptosis and cell signaling (Vance, 2008). In

mammalian cells PE is synthesized via two major pathways: the cytidine diphosphate (CDP)-ethanolamine and PS decarboxylation pathway (Vance, 2008). For the CDP- ethanolamine pathway, the enzyme ethanolamine kinase-1 utilizes ethanolamine as the substrate to undergo a series of reactions to produce PE (Vance and Tasseva, 2013). However, mammalian cells cannot synthesize ethanolamine and therefore must be provided by the diet (Vance and Tasseva, 2013). As for PS decarboxylation pathway, PS (produced in the ER) is converted to PE by phosphatidylserine decarboxylase (PSD), and this process occurs in the mitochondria and ER (Vance, 2008).

As with PC, alterations to the amount of PE present in the membrane of the SR can impact its functionality. Multiple studies have shown that reduced PE in SR results in the inhibition of SERCA activity and even muscle weakness (Funai, et al., 2016; Gustavsson, et al., 2011). Gustavsson, et al. (2011) showed that more PE species within the lipid bilayer leads to increased affinity for calcium by the SERCA pump. This is likely due to a protein-lipid interaction between the head group of PE and SERCA that results in an activating affect for the SERCA protein (Gustavsson, et al., 2011). There has also been much research centered around the importance of the ratio of PC:PE ratio in cells related to SERCA activity (Lee, et al., 2018; Paran, et al., 2015). Fajardo, et al. (2018) noted increases in PC but not PE can result in an increased PC:PE ratio, which negatively impacted SERCA activity. While the exact mechanism behind this anomaly remains unknown, Gustavsson, et al. (2011) found that increasing PE content can increase SERCA affinity for calcium and elevated maximal SERCA activity.

Phosphatidylserine. In mammalian cells, PS makes up about 5-10% of the total phospholipids (Vance, 2015). Research shows that PS is the major anionic phospholipid class that is mainly found in the inner leaflet of the plasma membrane of neural tissue (Kim, et al.,

2014). Typically, PS is enriched in the brain compared to other types of cells in mammalian tissue (Vance and Steenbergen, 2005). The location of PS allows it to participate in the activation of multiple signaling pathways since it can form part of the protein docking sites (Kim, et al., 2014). The synthesis process for PS involves a calcium dependent base-exchange reaction in which the head group of PC or PE is replaced by a serine through the activity of phosphatidylserine synthase (Vance and Tasseva, 2013).

As with PC and PE, PS can impact the functionality of the SR. Szymanska, et al. (1992) purified skeletal SERCA and reconstituted it with PS proteoliposomes and noted an increase in calcium uptake via the SERCA pump. These results were supported by another study which also saw an increase in SERCA activity in the presence of more PS (Dalton, et al., 1998). Therefore, the functionality of the SERCA is sensitive to the alteration of phospholipid profile of cell membranes as it is embedded in the SR membrane.

Potential Meat Quality Defects Due to Impacts Due to Elevated Free Calcium Levels

Xing, et al. (2017) assessed the effects of stress induced by transport on the oxidative state and expression of SERCA and RyR in chicken. After transport, the *pectoralis major* (**PM)** muscles from broilers were separated into normal or pale, soft and exudative-like (**PSE**). Their results indicated that after transport, the production of ROS increased with a decrease in the expression of SERCA1 and RyR in the PSE breasts. Mutryn, et al. (2015) compared the genomes of PM from WB and N chicken breast. Based on the differentially expressed genes, there was evidence to suggest intracellular calcium overload because of the noted upregulation of the ATPase calcium transporting cardiac muscle slow twitch 2 (**ATPA2**) gene and the parvalbumin (**PVALB**) gene in WB. The ATPA2 gene codes for the SERCA2a and 2b isoforms, therefore an upregulation for this gene could lead to quicker calcium uptake and larger amounts of calcium

loading in the SR (Kuo, et al., 1998). The PVALB gene is essential to calcium buffering and regulating calcium concentrations (Mitchell, 1999). The upregulation of these proteins is thought to increase calcium uptake into the SR to compensate for the high levels of extracellular calcium in the WB meat. However, it has yet to be determined how this upregulation contributes to the development of WB meat quality defects.

There is also concern for the upregulation of phospholipases that can breakdown membranes, which may also contribute to weaken membrane integrity. It has been shown that as membrane phospholipids are hydrolyzed, the calcium binding capabilities are depleted (Steinberg, et al., 1974). Mutryn, et al. (2015) observed greater expression of phospholipase A2 and phospholipase B1 in chicken suffering from WB. This upregulation resulted in disruption of membrane functionality due to the formation of lysophospholipids and free fatty acids. The researchers hypothesized that the elevated calcium levels noted in WB were activating phospholipases and causing damage to the sarcolemma membrane. Additionally, Moon, et al. (2012) found that in the presence of calcium ions, phospholipase A2 is activated and subsequently noted an increase in release of arachidonic acid. This is interesting to note because arachidonic acid has a pro-inflammatory response and increased inflammation has been seen in WB birds (Xing, et al., 2021; Young and Rasmussen, 2020). Increased phospholipase A2 activity caused by increased calcium levels in WB meat could be damaging the phospholipid membrane causing more calcium to leak out as well as an increase in the inflammation response.

CONCLUSION

Currently, WB is a major concern to the poultry industry as it produces less favorable texture and quality defects such as poor color, reduced water holding capacity, increased pH, and elevated levels of fat and collagen. Additionally, there are high levels of calcium present in the

WB meat which can impact protease activity which could be beneficial but also cause detrimental quality defects. Investigating how the extra calcium present in WB is affecting the meat as well as understanding why there is high calcium could provide insights to the mechanism behind WB formation. It is known that the SR serves as the main storage compartment for calcium within the cells making it an important organelle in live muscle contraction. Many proteins reside in the phospholipid membrane of the SR and are responsible for the movement of calcium in and out of the SR. The overall functionality of the SR is dependent on the proteins' ability to function properly and membrane integrity. Having any type of dysfunctionality to the SR can cause meat quality defects which leads to downgraded product and negative economic impact for the industry. Therefore, the aim of our research is to investigate WB quality deficiency and the functionality of the SR.

REFERENCES

Abasht, B., M. F. Mutryn, R. D. Michalek, and W. R. Lee. 2016. Oxidative stress and metabolic perturbations in wooden breast disorder in chickens. PloS one 11:e0153750.

Aguirre, M., C. Owens, R. Miller, and C. Alvarado. 2018. Descriptive sensory and instrumental texture profile analysis of woody breast in marinated chicken. Poultry science 97:1456-1461.

Andersen, J. P., E. Skriver, T. S. Mahrous, and J. V. Møller. 1983. Reconstitution of sarcoplasmic reticulum Ca2+-ATPase with excess lipid. Dispersion of the pump units. Biochimica et Biophysica Acta (BBA)-Biomembranes 728:1-10.

Anthony, N. 1998. A Review of Genetic Practices in Poultry: Efforts to Improve Meat Quality 1. Journal of Muscle foods 9:25-33.

Asghar, A., and A. Bhatti. 1988. Endogenous proteolytic enzymes in skeletal muscle: their significance in muscle physiology and during postmortem aging events in carcasses. Advances in food research 31:343-451.

Baldi, G., F. Soglia, L. Laghi, S. Tappi, P. Rocculi, S. Tavaniello, D. Prioriello, R. Mucci, G. Maiorano, and M. Petracci. 2019. Comparison of quality traits among breast meat affected by current muscle abnormalities. Food Research International 115:369-376.

Beard, N., D. R. Laver, and A. F. Dulhunty. 2004. Calsequestrin and the calcium release channel of skeletal and cardiac muscle. Progress in biophysics and molecular biology 85:33-69.

Berchtold, M. W., H. Brinkmeier, and M. Muntener. 2000. Calcium ion in skeletal muscle: its crucial role for muscle function, plasticity, and disease. Physiological reviews 80:1215-1265.

Berry, B., J. Smith, J. Secrist, and L. Douglass. 1988. Consumer response to restructured beef

steaks processed to have varying levels of connective tissue. Journal of Food Quality 11:15-25.

Bhat, Z. F., J. D. Morton, S. L. Mason, and A. E.-D. A. Bekhit. 2018. Role of calpain system in meat tenderness: A review. Food Science and Human Wellness 7:196-204.

Biswas, A. K., and S. Tandon. 2019. Casein Zymography for Analysis of Calpain-1 and Calpain-2 Activity. Pages 31-38 in CalpainSpringer.

Boncompagni, S., A. E. Rossi, M. Micaroni, S. L. Hamilton, R. T. Dirksen, C. Franzini-Armstrong, and F. Protasi. 2009. Characterization and temporal development of cores in a mouse model of malignant hyperthermia. Proceedings of the National Academy of Sciences 106:21996-22001.

Bowker, B., and H. Zhuang. 2019. Detection of razor shear force differences in broiler breast meat due to the woody breast condition depends on measurement technique and meat state. Poultry science 98:6170-6176.

Bowker, B., H. Zhuang, E. Barton, and J. A.-M. Sanchez. 2016. White striping and wooden breast defects influence meat quality and muscle protein characteristic in broiler breast meat. Proc. 62nd Int. Cong. Meat Sci. Tech. Bangkok, Thailand.

Brasselet, C., E. Durand, F. Addad, A. A. H. Zen, M. B. Smeets, D. Laurent-Maquin, S. Bouthors, G. Bellon, D. de Kleijn, and G. Godeau. 2005. Collagen and elastin cross-linking: a mechanism of constrictive remodeling after arterial injury. American Journal of Physiology-Heart and Circulatory Physiology 289:H2228-H2233.

Cai, K., W. Shao, X. Chen, Y. Campbell, M. Nair, S. Suman, C. Beach, M. Guyton, and M. Schilling. 2018. Meat quality traits and proteome profile of woody broiler breast (pectoralis major) meat. Poultry science 97:337-346.

Caldas-Cueva, J. P., and C. M. Owens. 2020. A review on the woody breast condition, detection methods, and product utilization in the contemporary poultry industry. Journal of Animal Science 98:skaa207.

Capes, E., R. Loaiza, and H. H. Valdivia. 2011. Ryanodine receptors. Skeletal muscle 1:18.

Cavitt, L., G. Youm, J. Meullenet, C. Owens, and R. Xiong. 2004. Prediction of poultry meat tenderness using razor blade shear, Allo-Kramer shear, and sarcomere length. Journal of food science 69:SNQ11-SNQ15.

Chatterjee, D., H. Zhuang, B. Bowker, G. Sanchez-Brambila, and A. Rincon. 2016. Instrumental texture characteristics of broiler pectoralis major with the wooden breast condition. Poultry science 95:2449-2454.

Dalgaard, L. B., M. K. Rasmussen, H. C. Bertram, J. A. Jensen, H. S. Møller, M. D. Aaslyng, E. K. Hejbøl, J. R. Pedersen, D. Elsser-Gravesen, and J. F. Young. 2018. Classification of wooden breast myopathy in chicken pectoralis major by a standardised method and association with conventional quality assessments. International Journal of Food Science & Technology 53:1744-1752.

Dalle Zotte, A., M. Cecchinato, A. Quartesan, J. Bradanovic, G. Tasoniero, and E. Puolanne. Year. How does" wooden breast" myodegeneration affect poultry meat quality. Proc. 60th International Congress of Meat.

Dalton, A. K., J. M. East, S. Mall, S. Oliver, P. A. Starling, and G. A. Lee. 1998. Interaction of phosphatidic acid and phosphatidylserine with the Ca2+-ATPase of sarcoplasmic reticulum and the mechanism of inhibition. Biochemical Journal 329:637-646.

DeLong, C. J., Y.-J. Shen, M. J. Thomas, and Z. Cui. 1999. Molecular distinction of

phosphatidylcholine synthesis between the CDP-choline pathway and phosphatidylethanolamine methylation pathway. Journal of Biological Chemistry 274:29683-29688.

Destefanis, G., A. Brugiapaglia, M. T. Barge, and E. Dal Molin. 2008. Relationship between beef consumer tenderness perception and Warner–Bratzler shear force. Meat science 78:153-156.

Diaz, B. L., and J. P. Arm. 2003. Phospholipase A2. Prostaglandins, leukotrienes and essential fatty acids 69:87-97.

Dridi, S., and M. Kidd. 2016. Molecular pathways involved in amino acid and phosphorous utilization. Ch 8:119-128.

Durham, W. J., P. Aracena-Parks, C. Long, A. E. Rossi, S. A. Goonasekera, S. Boncompagni, D. L. Galvan, C. P. Gilman, M. R. Baker, and N. Shirokova. 2008. RyR1 S-nitrosylation underlies environmental heat stroke and sudden death in Y522S RyR1 knockin mice. Cell 133:53-65.

Endo, M. 1977. Calcium release from the sarcoplasmic reticulum. Physiological reviews 57:71-108.

Ertbjerg, P., and E. Puolanne. 2017. Muscle structure, sarcomere length and influences on meat quality: A review. Meat Science 132:139-152. doi https://doi.org/10.1016/j.meatsci.2017.04.261

Ezerman, E. B., and H. Ishikawa. 1967. Differentiation of the sarcoplasmic reticulum and T system in developing chick skeletal muscle in vitro. The Journal of cell biology 35:405-420.

Fajardo, V. A., J. S. Mikhaeil, C. F. Leveille, A. R. Tupling, and P. J. LeBlanc. 2018. Elevated

whole muscle phosphatidylcholine: phosphatidylethanolamine ratio coincides with reduced SERCA activity in murine overloaded plantaris muscles. Lipids in health and disease 17:1-8.

Fill, M., and J. A. Copello. 2002. Ryanodine receptor calcium release channels. Physiological reviews 82:893-922.

Fu, S., L. Yang, P. Li, O. Hofmann, L. Dicker, W. Hide, X. Lin, S. M. Watkins, A. R. Ivanov, and G. S. Hotamisligil. 2011. Aberrant lipid metabolism disrupts calcium homeostasis causing liver endoplasmic reticulum stress in obesity. Nature 473:528-531.

Funai, K., I. J. Lodhi, L. D. Spears, L. Yin, H. Song, S. Klein, and C. F. Semenkovich. 2016. Skeletal muscle phospholipid metabolism regulates insulin sensitivity and contractile function. Diabetes 65:358-370.

Girard, I., H. Bruce, J. Basarab, I. Larsen, and J. Aalhus. 2012. Contribution of myofibrillar and connective tissue components to the Warner–Bratzler shear force of cooked beef. Meat science 92:775-782.

Gordon, A., E. Homsher, and M. Regnier. 2000. Regulation of contraction in striated muscle. Physiological reviews 80:853-924.

Gratta, F., L. Fasolato, M. Birolo, C. Zomeño, E. Novelli, M. Petracci, A. Pascual, G. Xiccato, and A. Trocino. 2019. Effect of breast myopathies on quality and microbial shelf life of broiler meat. Poultry science 98:2641-2651.

Gustavsson, M., N. J. Traaseth, and G. Veglia. 2011. Activating and deactivating roles of lipid bilayers on the Ca2+-ATPase/phospholamban complex. Biochemistry 50:10367-10374.

Hasegawa, Y., T. Hara, T. Kawasaki, M. Yamada, T. Watanabe, and T. Iwasaki. 2020. Effect of wooden breast on postmortem changes in chicken meat. Food Chemistry 315:126285.

Hirata, Y., M. Brotto, N. Weisleder, Y. Chu, P. Lin, X. Zhao, A. Thornton, S. Komazaki, H. Takeshima, and J. Ma. 2006. Uncoupling store-operated Ca2+ entry and altered Ca2+ release from sarcoplasmic reticulum through silencing of junctophilin genes. Biophysical journal 90:4418-4427.

Houser, S. R. 2001. Reduced abundance of transverse tubules and L-type calcium channels: another cause of defective contractility in failing ventricular myocytesElsevier Science.

Jungbluth, H., S. Treves, F. Zorzato, A. Sarkozy, J. Ochala, C. Sewry, R. Phadke, M. Gautel, and F. Muntoni. 2018. Congenital myopathies: disorders of excitation–contraction coupling and muscle contraction. Nature Reviews Neurology 14:151-167.

Kanno, K., M. K. Wu, E. F. Scapa, S. L. Roderick, and D. E. Cohen. 2007. Structure and function of phosphatidylcholine transfer protein (PC-TP)/StarD2. Biochimica et Biophysica Acta (BBA)-Molecular and Cell Biology of Lipids 1771:654-662.

Kemp, C. M., and T. Parr. 2012. Advances in apoptotic mediated proteolysis in meat tenderisation. Meat Science 92:252-259.

Kim, H.-Y., B. X. Huang, and A. A. Spector. 2014. Phosphatidylserine in the brain: metabolism and function. Progress in lipid research 56:1-18.

Koohmaraie, M. Year. The role of endogenous proteases in meat tenderness. Proc. Proc. Recip. Meat Conf.

Kuo, I. Y., and B. E. Ehrlich. 2015. Signaling in muscle contraction. Cold Spring Harbor perspectives in biology 7:a006023.

Kuo, T. H., H.-R. C. Kim, L. Zhu, Y. Yu, H.-M. Lin, and W. Tsang. 1998. Modulation of endoplasmic reticulum calcium pump by Bcl-2. Oncogene 17:1903-1910.

Kushnir, A., M. J. Betzenhauser, and A. R. Marks. 2010. Ryanodine receptor studies using

genetically engineered mice. FEBS letters 584:1956-1965.

Kuttappan, V., B. Hargis, and C. Owens. 2016. White striping and woody breast myopathies in the modern poultry industry: a review. Poultry Science 95:2724-2733.

Kuttappan, V. A., W. Bottje, R. Ramnathan, S. D. Hartson, C. N. Coon, B.-W. Kong, C. M. Owens, M. Vazquez-Añon, and B. M. Hargis. 2017. Proteomic analysis reveals changes in carbohydrate and protein metabolism associated with broiler breast myopathy. Poultry science 96:2992-2999.

Lanner, J. T., D. K. Georgiou, A. D. Joshi, and S. L. Hamilton. 2010. Ryanodine receptors: structure, expression, molecular details, and function in calcium release. Cold Spring Harbor perspectives in biology 2:a003996.

Larsen, A. H., A. Frandsen, and M. Treiman. 2001. Upregulation of the SERCA-type Ca 2+ pump activity in response to endoplasmic reticulum stress in PC12 cells. BMC biochemistry 2:4.

Lee, H., V. Sante-Lhoutellier, S. Vigouroux, Y. Briand, and M. Briand. 2008a. Role of calpains in postmortem proteolysis in chicken muscle. Poultry Science 87:2126-2132.

Lee, S., F. Norheim, H. L. Gulseth, T. M. Langleite, A. Aker, T. E. Gundersen, T. Holen, K. I. Birkeland, and C. A. Drevon. 2018. Skeletal muscle phosphatidylcholine and phosphatidylethanolamine respond to exercise and influence insulin sensitivity in men. Scientific reports 8:1-12.

Lee, Y., C. Owens, and J. Meullenet. 2008b. The meullenet-owens razor shear (mors) for predicting poultry meat tenderness: its applications and optimization. Journal of texture studies 39:655-672.

Li, Z., L. B. Agellon, T. M. Allen, M. Umeda, L. Jewell, A. Mason, and D. E. Vance. 2006. The

ratio of phosphatidylcholine to phosphatidylethanolamine influences membrane integrity and steatohepatitis. Cell metabolism 3:321-331.

Li, Z., and D. E. Vance. 2008. Thematic review series: glycerolipids. Phosphatidylcholine and choline homeostasis. Journal of lipid research 49:1187-1194.

Lytton, J., M. Westlin, and M. R. Hanley. 1991. Thapsigargin inhibits the sarcoplasmic or endoplasmic reticulum Ca-ATPase family of calcium pumps. Journal of Biological Chemistry 266:17067-17071.

MacLennan, D. H., and K. P. Campbell. 1979. Structure, function and biosynthesis of sarcoplasmic reticulum proteins. Trends in Biochemical Sciences 4:148-151.

Matarneh, S. K., E. M. England, T. L. Scheffler, and D. E. Gerrard. 2017. The conversion of muscle to meat. Pages 159-185 in Lawrie´ s Meat ScienceElsevier.

Mazzoni, M., M. Petracci, A. Meluzzi, C. Cavani, P. Clavenzani, and F. Sirri. 2015. Relationship between pectoralis major muscle histology and quality traits of chicken meat. Poultry Science 94:123-130.

Miller, S. L., S. Currie, C. M. Loughrey, S. Kettlewell, T. Seidler, D. F. Reynolds, G. Hasenfuss, and G. L. Smith. 2005. Effects of calsequestrin over-expression on excitation–contraction coupling in isolated rabbit cardiomyocytes. Cardiovascular research 67:667-677.

Mitchell, M. 1999. Muscle abnormalities-pathophysiological mechanisms. Poultry Meat Science:65-98.

Moon, S. H., C. M. Jenkins, X. Liu, S. Guan, D. J. Mancuso, and R. W. Gross. 2012. Activation of Mitochondrial Calcium-independent Phospholipase A2γ (iPLA2γ) by Divalent Cations Mediating Arachidonate Release and Production of Downstream Eicosanoids*♦. Journal of Biological Chemistry 287:14880-14895.

Morey, A., M. L. Johnson, J. Kataria, and J. M. Gonzalez. 2020. Studying the Effects of Collagenase (Type 1) on the Collagen in Woody Breast Meat. Animals 10:1602.

Mouchlis, V. D., Y. Chen, J. A. McCammon, and E. A. Dennis. 2018. Membrane allostery and unique hydrophobic sites promote enzyme substrate specificity. Journal of the American Chemical Society 140:3285-3291.

Moylan, J. S., and M. B. Reid. 2007. Oxidative stress, chronic disease, and muscle wasting. Muscle & Nerve: Official Journal of the American Association of Electrodiagnostic Medicine 35:411-429.

Mudalal, S., M. Lorenzi, F. Soglia, C. Cavani, and M. Petracci. 2015. Implications of white striping and wooden breast abnormalities on quality traits of raw and marinated chicken meat. Animal 9:728-734.

Mueller, B., M. Zhao, I. V. Negrashov, R. Bennett, and D. D. Thomas. 2004. SERCA structural dynamics induced by ATP and calcium. Biochemistry 43:12846-12854.

Mutryn, M. F., E. M. Brannick, W. Fu, W. R. Lee, and B. Abasht. 2015. Characterization of a novel chicken muscle disorder through differential gene expression and pathway analysis using RNA-sequencing. BMC genomics 16:399.

Novák, P., and T. Soukup. 2011. Calsequestrin distribution, structure and function, its role in normal and pathological situations and the effect of thyroid hormones. Physiological research 60:439.

Owens, C. Year. Woody breast meat. Proc. 69th Reciprocal Meat Conference Proceedings. June 18th-23rd, San Angelo, Texas.

Owens, C. M., and A. Sams. 1997. Muscle metabolism and meat quality of pectoralis from turkeys treated with postmortem electrical stimulation. Poultry science 76:1047-1051.

Paolini, C., M. Quarta, L. Wei-LaPierre, A. Michelucci, A. Nori, C. Reggiani, R. T. Dirksen, and F. Protasi. 2015. Oxidative stress, mitochondrial damage, and cores in muscle from calsequestrin-1 knockout mice. Skeletal muscle 5:10.

Paran, C. W., K. Zou, P. J. Ferrara, H. Song, J. Turk, and K. Funai. 2015. Lipogenesis mitigates dysregulated sarcoplasmic reticulum calcium uptake in muscular dystrophy. Biochimica et Biophysica Acta (BBA)-Molecular and Cell Biology of Lipids 1851:1530-1538.

Pikuła, S., L. Epstein, and A. Martonosi. 1994. The relationship between phospholipid content and Ca2+-ATPase activity in the sarcoplasmic reticulum. Biochimica et Biophysica Acta (BBA)-Biomembranes 1196:1-13.

Prasad, V., G. W. Okunade, M. L. Miller, and G. E. Shull. 2004. Phenotypes of SERCA and PMCA knockout mice. Biochemical and biophysical research communications 322:1192-1203.

Ren, X., G. D. Lamb, and R. M. Murphy. 2019. Distribution and activation of matrix metalloproteinase-2 in skeletal muscle fibers. American Journal of Physiology-Cell Physiology 317:C613-C625.

Rigdon, M., A. M. Stelzleni, R. W. McKee, T. D. Pringle, B. Bowker, H. Zhuang, and H. Thippareddi. 2021. Texture and quality of chicken sausage formulated with woody breast meat. Poultry Science 100:100915.

Sams, A., S. Birkhold, and K. Mills. 1991. Fragmentation and tenderness in breast muscle from broiler carcasses treated with electrical stimulation and high-temperature conditioning. Poultry Science 70:1430-1433.

Sihvo, H.-K., K. Immonen, and E. Puolanne. 2014. Myodegeneration with fibrosis and regeneration in the pectoralis major muscle of broilers. Veterinary pathology 51:619-623.

Sihvo, H.-K., J. Lindén, N. Airas, K. Immonen, J. Valaja, and E. Puolanne. 2017. Wooden breast myodegeneration of pectoralis major muscle over the growth period in broilers. Veterinary Pathology 54:119-128.

Soglia, F., J. Gao, M. Mazzoni, E. Puolanne, C. Cavani, M. Petracci, and P. Ertbjerg. 2017. Superficial and deep changes of histology, texture and particle size distribution in broiler wooden breast muscle during refrigerated storage. Poultry Science 96:3465-3472.

Soglia, F., L. Laghi, L. Canonico, C. Cavani, and M. Petracci. 2016a. Functional property issues in broiler breast meat related to emerging muscle abnormalities. Food Research International 89:1071-1076.

Soglia, F., S. Mudalal, E. Babini, M. Di Nunzio, M. Mazzoni, F. Sirri, C. Cavani, and M. Petracci. 2016b. Histology, composition, and quality traits of chicken Pectoralis major muscle affected by wooden breast abnormality. Poultry Science 95:651-659.

Soglia, F., Z. Zeng, J. Gao, E. Puolanne, C. Cavani, M. Petracci, and P. Ertbjerg. 2018. Evolution of proteolytic indicators during storage of broiler wooden breast meat. Poultry science 97:1448-1455.

Solo, J. 2016. Meat quality and sensory analysis of broiler breast fillets with woody breast muscle myopathy.

Steenbergen, R., T. S. Nanowski, A. Beigneux, A. Kulinski, S. G. Young, and J. E. Vance. 2005. Disruption of the phosphatidylserine decarboxylase gene in mice causes embryonic lethality and mitochondrial defects. Journal of Biological Chemistry 280:40032-40040.

Steinberg, J., E. Masoro, and B. P. Yu. 1974. Role of sarcoplasmic reticulum phospholipids in calcium ion binding activity. Journal of Lipid Research 15:537-543.

Sun, X., D. Koltes, C. Coon, K. Chen, and C. Owens. 2018. Instrumental compression force and

meat attribute changes in woody broiler breast fillets during short-term storage. Poultry science 97:2600-2606.

Szent-Györgyi, A. 1975. Calcium regulation of muscle contraction. Biophysical journal 15:707-723.

Szymanska, G., H. W. Kim, J. Cuppoletti, and E. G. Kranias. 1992. Regulation of the skeletal sarcoplasmic reticulum Ca 2+-ATPase by phospholamban and negatively charged phospholipids in reconstituted phospholipid vesicles. Molecular and cellular biochemistry 114:65-71.

Tasoniero, G., M. Cullere, M. Cecchinato, E. Puolanne, and A. Dalle Zotte. 2016. Technological quality, mineral profile, and sensory attributes of broiler chicken breasts affected by white striping and wooden breast myopathies. Poultry science 95:2707-2714.

Testerink, N., M. H. van der Sanden, M. Houweling, J. B. Helms, and A. B. Vaandrager. 2009. Depletion of phosphatidylcholine affects endoplasmic reticulum morphology and protein traffic at the Golgi complex. Journal of lipid research 50:2182-2192.

Tijare, V. V., F. Yang, V. Kuttappan, C. Alvarado, C. Coon, and C. Owens. 2016. Meat quality of broiler breast fillets with white striping and woody breast muscle myopathies. Poultry Science 95:2167-2173.

Trocino, A., A. Piccirillo, M. Birolo, G. Radaelli, D. Bertotto, E. Filiou, M. Petracci, and G. Xiccato. 2015. Effect of genotype, gender and feed restriction on growth, meat quality and the occurrence of white striping and wooden breast in broiler chickens. Poultry science 94:2996-3004.

Vance, J. E. 2008. Thematic Review Series: Glycerolipids. Phosphatidylserine and phosphatidylethanolamine in mammalian cells: two metabolically related

aminophospholipids. Journal of lipid research 49:1377-1387.

Vance, J. E. 2015. Phospholipid synthesis and transport in mammalian cells. Traffic 16:1-18.

Vance, J. E., and R. Steenbergen. 2005. Metabolism and functions of phosphatidylserine. Progress in lipid research 44:207-234.

Vance, J. E., and G. Tasseva. 2013. Formation and function of phosphatidylserine and phosphatidylethanolamine in mammalian cells. Biochimica et Biophysica Acta (BBA)-Molecular and Cell Biology of Lipids 1831:543-554.

Velleman, S. G., and D. L. Clark. 2015. Histopathologic and myogenic gene expression changes associated with wooden breast in broiler breast muscles. Avian Diseases 59:410-418.

Velleman, S. G., D. L. Clark, and J. R. Tonniges. 2018. The effect of the wooden breast myopathy on sarcomere structure and organization. Avian diseases 62:28-35.

Wang, Q., and M. Michalak. 2020. Calsequestrin. Structure, function, and evolution. Cell calcium 90:102242.

Welinder, C., and L. Ekblad. 2011. Coomassie staining as loading control in Western blot analysis. Journal of proteome research 10:1416-1419.

Wu, W. J., A. A. Welter, E. A. Rice, B. A. Olson, T. G. O'Quinn, E. A. Boyle, G. Magnin-Bissel, T. A. Houser, M. D. Chao, and T. G. O'Quinn. 2021. Biochemical Factors Affecting East Asian Consumers' Sensory Preferences of Six Beef Shank Cuts. Meat and Muscle Biology 5.

Xing, T., X. Pan, L. Zhang, and F. Gao. 2021. Hepatic oxidative stress, apoptosis and inflammation in broiler chickens with wooden breast myopathy. Frontiers in physiology 12:415.

Xing, T., X. Zhao, P. Wang, H. Chen, X. Xu, and G. Zhou. 2017. Different oxidative status and

expression of calcium channel components in stress-induced dysfunctional chicken muscle. Journal of animal science 95:1565-1573.

Yalcin, S., S. Ozkan, M. C. Acar, and O. Meral. 2018. The occurrence of deep pectoral myopathy in broilers and associated changes in breast meat quality. British poultry science 59:55-62.

Young, J. F., and M. K. Rasmussen. 2020. Differentially expressed marker genes and glycogen levels in pectoralis major of Ross308 broilers with wooden breast syndrome indicates stress, inflammation and hypoxic conditions. Food Chemistry: Molecular Sciences 1:100001.

Zanotti, G. 2016. The Ca 2+ ATPase of the Sarco-/Endoplasmic Reticulum (SERCA): Structure and Control. Pages 137-151 in Regulation of Ca2+-ATPases, V-ATPases and F-ATPasesSpringer.

Zhang, X., D. Antonelo, J. Hendrix, V. To, Y. Campbell, M. Von Staden, S. Li, S. P. Suman, W. Zhai, and J. Chen. 2020. Proteomic Characterization of Normal and Woody Breast Meat from Broilers of Five Genetic Strains. Meat and Muscle Biology 4.

Chapter 2 - A Proposed Mechanism for the Altered Texture Property of Woody Breast in Broilers

ABSTRACT

Woody breast (WB) is a myopathy observed in chicken *Pectoralis major* characterized by its tough and rubbery texture. Unfortunately, the exact causation of WB texture remains unknown. The objective of this study was to investigate factors and enzymatic activities that may contribute to the abnormal texture observed in WB. Fourteen Ross line broiler breast fillets (7 severe WB and 7 normal) were collected at 3 h postmortem from a commercial processing plant. Each sample was trimmed, weighed, vacuum packaged and frozen at -20°C at approximately 8 h postmortem. One 1.9 cm strip across the cranial end of each fillet was fabricated and pulverized in liquid nitrogen to measure pH, objective tenderness, sarcomere length, proteolysis, calpain activity, collagenase activity, collagen content, collagen crosslinks and peak transitional temperature measurements. Purge was collected from each sample to evaluate free calcium concentration. The WB fillets were heavier (522.9 vs. 446.9g; $P<0.05$) and had a higher pH (6.17 vs. 5.83; $P<0.05$). Objective tenderness was not significantly different (34.09 vs. 37.69 N; $P>0.10$), but WB tended to have shorter sarcomeres (1.70 vs. 2.02 µm; $P=0.0543$) and less intact troponin-T (relative intact troponin-T band density: 49.98 vs. 56.97%; $P=0.0515$). The WB had more autolyzed µ/m calpain (71.05 vs. 59.12% calpain autolyzed; $P<0.01$) and more activated collagenase (13.24 vs. 7.84% activated MMP2; $P<0.05$). Purge from WB had higher levels of free calcium (6.2 vs. 4.2 nmol calcium/mg protein; $P<0.05$). There was increased collagen in WB (3.89 vs. 2.08 mg collagen/g muscle tissue; $P<0.05$), as well as more mature crosslinks in WB (0.23 vs. 0.14 mol PYD/mol collagen; $P < 0.05$; 0.07 vs. 0.04 mol DPD/mol collagen; $P < 0.01$). Finally, WB had a higher peak transitional temperature (65.47 vs. 63.72°C;

P<0.05). The results indicated that the cause of texture abnormality of WB may be the combined effects of more calcium being released from the sarcoplasmic reticulum early postmortem resulting in shorter sarcomere length and more collagen being deposited in the chicken breast meat.

Key Words: woody breast, calcium, sarcomere, calpain activity, troponin-T

INTRODUCTION

The poultry industry has seen many improvements in the growth efficiency of broilers, such as a reduction to the time of slaughter, and increases in overall body weight, muscle yield and feed conversion efficiency in the past couple decades (Anthony, 1998). However, the improvement in production efficiency have also led to the increased incidence of a number of meat quality issues (Yalcin, et al., 2018), most notably, the Woody Breast (**WB**) syndrome. Meat suffering from WB is characterized by hardened areas and ridge-like bulges at both the caudal and cranial regions of the *Pectoralis Major* muscle of broilers (Sihvo, et al., 2014). It is also known that WB results in lowered water-holding/binding capacity, lighter color, less red, more yellow, and greater raw weights compared to normal chicken breast (Dalle Zotte, et al., 2014; Mudalal, et al., 2015). As of 2015 in the United States, the incident rates of WB ranged from 30 to 50% (Owens, 2016), and costs the industry over $200 million per year in economic losses (Kuttappan, et al., 2016).

The apparent tough and rubbery texture abnormalities in WB are well defined (Mudalal, et al., 2015; Sihvo, et al., 2014), but the exact cause of WB in broilers remains unknown. Studies have shown that WB occurrence may be the result of oxidative stress and metabolic disorders associated with the development of hypoxic conditions in the *Pectoralis Major* muscle (Abasht, et al., 2016; Dridi and Kidd, 2016; Mutryn, et al., 2015) ; as a consequence, this condition may lead to multifocal regenerative myodegeneration and necrosis resulting in increased scar tissues

and collagen content in the breast meat (Sihvo, et al., 2014). Furthermore, other studies have consistently shown elevated levels of free cytoplasmic calcium (Soglia, et al., 2016b) and increased pH (Brambila, et al., 2017; Cai, et al., 2018) in WB meat compared to N breast meat. Huang and Ahn (2018) hypothesized myodegeneration in WB broilers may damage the sarcoplasmic reticulum leading to the increase in free calcium content, which further increased the usage of glycogen reserve from the enhanced glycolytic activity, thus resulting in greater ultimate pH in meat.

It is well established that collagen characteristics, free calcium concentration and pH all play significant roles on the textural development of meat (Coro, et al., 2002; Ertbjerg and Puolanne, 2017; Soglia, et al., 2016b; Wu, 2020). In addition, proteolytic enzyme activity during the postmortem storage of meat is calcium and pH-dependent (Koohmaraie and Geesink, 2006; Maddock, et al., 2005; Whipple and Koohmaraie, 1993). However, the effect of increased free cytoplasmic calcium and pH on muscle contraction and proteolytic enzyme activity as well as muscle necrosis on collagen characteristics are not well understood in WB meat. Examining biochemical changes of muscle fibers and intramuscular connective tissue between normal (**N**) and WB samples could shed light on the formation of WB textural defects (Dransfield and Sosnicki, 1999; Nishimura, 2010). Therefore, the objective of this study was to investigate factors contributing to the abnormal texture observed in WB and enzymatic activities that may influence WB texture during postmortem aging.

MATERIALS AND METHODS

Sample Collection, Fabrication and Preparation

Fourteen broiler breasts (*pectoralis major)* fillet samples were collected from a commercial processing facility that slaughters large broilers. All breasts samples were collected post-chill from

the deboning line at approximately 3 h postmortem. The breasts were trimmed, weighed, and scored for woody breast and white striping at approximately 6 h postmortem. Each sample was assigned a normal, moderate or severe score for woody breast based on the degree of observable hardness and white striping based on prevalence and thickness of white striation on the surface of the fillet. Seven breasts that exhibited severe woody breast and white striping and seven breasts exhibiting zero signs of woody breast or white striping were selected for analysis. At 8 h postmortem, samples were vacuum package and stored at -20 ºC until shipped to Kansas State University Meat and Muscle Biology Laboratory.

All breast fillets were thawed in a refrigerator at 4°C for 24 h. The exudate (~10 mL) was collected from each sample for further analysis. A 1.9 cm strip across the cranial end of each fillet was fabricated, frozen in liquid nitrogen, pulverized using a blender (model 51BL32; Warring Commercial, Torring, CT) and stored at -80ºC until further analysis. The remainder of the breast fillet was repackaged and stored at -80ºC until further analysis.

pH Determination

Five g of powdered meat and 50 mL of ultrapure water were homogenized at 10,000 rpm for 20 s using a bench top homogenizer (Fisherbrand 850 homogenizer: Fisher Scientific, Pittsburgh, PA) in duplicates. The pH value was determined using a pH probe (InLab® Solids Pro-ISM; Mettler Toledo) attached to a pH meter (SevenCompact pH; Mettler Toledo) while solution was stirred constantly using a magnetic stir bar. The pH probe was calibrated using reference solutions at pH 4 and 7 prior to the measurement. Between each sample, the electrode was cleaned with ultrapure water and dried with kimwipes.

Free Calcium Concentration

Free calcium was quantified using the methods described by (Parrish, et al., 1981) with modifications. One mL of purge from each sample was transferred to a microcentrifuge tube. Protein concentration was determined using a Pierce bicinchoninic acid (**BCA**) protein assay kit (Thermo Fisher Scientific, Waltham, MA). The purge was treated with 0.2 mL of 27.5% trichloroacetic acid, vortexed thoroughly and incubated for 10 min at room temperature. After the incubation period, the samples were centrifuged at 10,000 x g for 10 min (Eppendorf centrifuge 5810 R, F45-30-11 rotor; Eppendorf, Hamburg, Germany). Five hundred μL of the supernatant was transferred to a 5 mL centrifuge tube, and the volume was brought to 5 mL with ultrapure water. The diluted supernatant was filtered through a 13 mm diameter Millex-LG 0.45 μm syringe filter (Millipore, Bedford, MA) into a new centrifuge tube and capped. Calcium concentrations (ppm) of the filtered samples were quantified via atomic absorption spectroscopy (AAnalyst 200; Perkin-Elmer, Norwalk, CT) at a wavelength of 422.7 nm with appropriate calcium concentration standards. Calcium concentrations were calculated by multiplying by the dilution factor and expressed as nmol of free calcium/mg protein.

Objective Tenderness (Warner-Bratzler Shear Force)

Warner-Bratzler Shear Force (**WBSF**) was used to measure tenderness of the samples according to Zhuang and Savage (2009). Breast fillets were removed from the freezer and thawed at 4°C for 24 h prior to cooking. Two 1.9 cm x 1.9 cm strips were removed from the cranial end of the breast fillets. A Cuisine Art Griddle Deluxe Clamshell (Cuisine Art, Stamford, CT) was used to grill the strips to an internal temperature of 78°C. Temperature of the samples were monitored with a Thermapen MK4 thermometer (Thermoworks, American Fork, UT) which was placed in the geometric center of the sample. The strips were chilled at 4°C overnight.

Each strip was sheared three times perpendicular to the muscle fiber orientation at 250 mm/min using an Instron testing machine (Model 5569; Instron, Norwood, MA) with a WBSF blade attachment (G-R Elec. Mfg., Manhattan, KS). The mean peak shear force (N) of six shears was calculated for each breast.

Sarcomere Length

Sarcomere length was determined as described by Girard, et al. (2012a) with modifications. One hundred mg of powdered meat was homogenized with 1 mL 0.25M sucrose and 0.02M EGTA solution for 15 s at 8,000 rpm (Fisherbrand 850 homogenizer: Fisher Scientific). Fifty μL of the mixed solution was pipetted onto a microscope slide and sealed with a coverslip. Slides were imaged with a Zeiss-axioplan 2 using a 100 x 1.4/f objective. Operating system used to image was LSM 5 Pascal V.3.2SP2 (Zeiss, Oberkochen, Germany). ImageJ software (version 1.52k; National Institute of Health) with the LSM Toolbox plugin was used to analyze the images. For each sample, three images were captured and 10 sarcomeres per image were measured for an average of 30 sarcomere lengths per sample.

Proteolysis

Myofibrillar proteins were isolated according the method described by Pietrzak, et al. (1997) with modifications. Three g of powdered meat was added to 15 mL ice-cold rigor buffer (0.1 M KCl, 2 mM $MgCl_2$, 1 mM EGTA, and 10 mM K_2HPO_4) at pH 7.4 and homogenized for 20 s at 15,000 rpm (Fisherbrand 850 homogenizer; Fisher Scientific). Homogenate was filtered through double-layered cheese cloth to eliminate fat and connective tissue, and 1.4 mL of homogenate was transferred into a microcentrifuge tube and centrifuged at 4,000 x g for 5 min (Eppendorf centrifuge 5810 R, F45-30-11 rotor; Eppendorf). The supernatant was decanted and the pellet was resuspended in 1 mL of ultrapure water. The pellet washing step was repeated

twice until the supernatant was free of myoglobin. The washed pellet was re-suspended in one mL of extraction buffer (0.1 M Tris-HCl, 1.25 mM EDTA, 1% SDS), vortexed thoroughly for 10 s and centrifuged at 4,000 x g for 5 min (Eppendorf centrifuge 5810 R; Eppendorf). The supernatant was transferred to a new microcentrifuge tube as the protein stock. Protein concentration was determined using a Pierce BCA protein assay kit (Thermo Fisher Scientific). All myofibrillar protein samples were diluted to 4 mg/mL with extraction buffer.

Degree of proteolysis was measured by troponin-T (**TNT**) degradation according to the method described by Chao, et al. (2017) with modifications. Seventy-five µL of the 4 mg/mL myofibrillar protein samples were mixed with 4x Laemmli SDS sample buffer (Alfa Aesar, Haverhill, MA) at 3:1 ratio. All samples were heated at 95°C for 5 min (Isotemp; Fischer Scientific). Ten µL of SeeBlue Pre-Stained Standard (Novex Life technologies Carlsbad, CA) and 60 µg of prepared myofibrillar protein samples were loaded into pre-cast RunBlue SDS 4-20% Mini Gels (BCG42012; Expedeon, San Diego, CA). Proteins were separated using a SE 260 Hoefer Mighty Small II electrophoresis unit (Hoefer Scientific Instruments, San Francisco, CA) and ice-cold 1X RunBlue SDS running buffer (Expedeon). The system was run at constant voltage of 180 V until the blue dye reached the bottom of the gel (approximately 45 min). Following gel electrophoresis, gels were equilibrated in 1X transfer buffer (Expedoen) and transferred onto a PVDF membrane (iBlot 2 PVDF Transfer Stack; Invitrogen, Carlsbad, CA) using an iBlot 2 Gel Transfer Device (Invitrogen) with settings of 20V for 1 min, 23V for 4 min, and 25V for 2 min.

Membranes were blocked for 90 min in 10 mL of 5% non-fat dry milk in 10mM Tris Base, 150 mM NaCl and 0.1% Tween-20 (**TBS-T**) at room temperature. Membranes were incubated overnight in mouse IgG monoclonal primary antibody (anti-TNT, JLT-12; Booster Bio,

Pleasanton, CA) at a dilution of 1:20 with the blocking solution at 4°C. Membranes were washed three times for 10 min each with TBS-T and incubated for 60 min with Peroxidase Conjugated Goat Anti-Mouse IgF1 (BA1050; Booster Bio) diluted 1:1,000 with the blocking solution at room temperature while protected from light. Membranes were washed three times for 10 min each with TBS-T and a final 5 min wash with TBS.

Before imaging, the membrane was incubated for 5 min in 6 mL of Amersham ECL Prime Western Blotting Detection Reagent (GE Healthcare, Chicago, IL) at room temperature while protected from light. A ChemiDoc-It 415 Imaging System (UVP, Upland, CA) was used to image the membranes. Band intensities were measured using VisionWorksLS Image Acquisition and Analysis Software (UVP). Intact and degraded forms of TNT were found at 35 and 28 kDA, respectively. Percent TNT degraded was measured by band intensities of degraded bands divided by band intensities of all bands in a specific lane.

Calpain Activity

Sarcoplasmic proteins were isolated according the method described by Veiseth, et al. (2001) with modifications. Five hundred mg of powdered meat was added to 15 mL ice-cold extraction buffer [1% Triton X, 50mM Tris-base, 10 mM EDTA and 0.05% β-mercaptoethanol (**BME**)] at pH 8.3 and homogenized for 20 s at 15,000 rpm (Fisherbrand 850 homogenizer; Fisher Scientific). Homogenate was filtered through double-layered cheese cloth to eliminate fat and connective tissue, and 1.4 mL of homogenate was transferred into an microcentrifuge tube and centrifuged at 20,000 x g for 30 min at 4°C (Eppendorf centrifuge 5810 R; Eppendorf). The supernatant was transferred into a new microcentrifuge tube as the protein stock. Protein concentration was determined using a Pierce BCA protein assay kit (Thermo Fisher Scientific). All sarcoplasmic protein samples were diluted to 2 mg/mL with extraction buffer.

Calpain activity was measured by casein zymography according to the method described by Biswas and Tandon (2019) with modifications. Sarcoplasmic proteins were mixed with Native Tris-Glycine sample buffer (Novex Life Technologies) with 0.75% BME at a ratio of 1:1. Five µL of SeeBlue Pre-Stained Standard (Novex Life technologies) and 30 µg of prepared sarcoplasmic protein samples were loaded into a resolving gel (10% acrylamide: bis-acrylamide = 37.5:1, wt/wt, that contained 0.2% casein) that was polymerized with 0.72% ammonium persulfate (**APS**) and 0.11% tetramethylethylenediamine (**TEMED**) with a stacking gel (5% acrylamide: bis-acrylamide = 37.5:1, wt/wt, contained no casein) that was polymerized with 1.53% APS and 0.31% TEMED. Proteins were separated using a SE 260 Hoefer Mighty Small II electrophoresis unit (Hoefer Scientific Instruments) and ice-cold 1X Native-PAGE running buffer (192 mM glycine, 25 mM Tris-base and 1 mM EDTA) with 0.05% BME. The system was run at constant voltage of 125 V at 4°C until the blue tracking dye reached the bottom of the gel, approximately 4 h.

Following gel electrophoresis, gels were incubated for 1 h in 5mM $CaCl_2$ and 50mM Tris-HCl (pH 7.5) at room temperature with one change of buffer at 30 min. Gels were incubated overnight (16 h) in 5 mM $CaCl_2$, 50mM Tris-HCl and 10 mM dithiothreitol (**DTT**) (pH 7.5) at 25°C. After the overnight incubation, gels were stained for 30 min in Coomassie blue stain (2.3 mM Coomassie blue G250, 40% methanol, 10% glacial acetic acid and 50% ultrapure water) at room temperature. Finally, gels were destained using a destaining solution (30% methanol, 10% glacial acetic acid and 60% ultrapure water) at room temperature until the bands appeared, approximately 2 h.

A ChemiDoc-It 415 Imaging System (UVP) was used to image the membranes. Band intensities were measured using VisionWorksLS Image Acquisition and Analysis Software (UVP).

Intact and degraded forms of calpain were measured, and percent activated calpain was calculated by band intensities of degraded bands divided by band intensities of all bands in a specific lane.

Collagenase Activity

Sarcoplasmic proteins were isolated according the method described by Tajhya, et al. (2017) with modifications. Five hundred mg of powdered meat sample were added to 15 mL ice-cold extraction buffer (20 mM Tris-HCl, 125 mM NaCl and 1% TritonX) and homogenized for 15 s at 10,000 rpm (Fisherbrand 850 homogenizer; Fisher Scientific). Homogenate was filtered through double-layered cheese cloth to eliminate fat and connective tissue, and 1.4 mL of homogenate was transferred into an microcentrifuge tube and centrifuged at 16,000 x g for 20 min at 4°C (Eppendorf centrifuge 5810 R; Eppendorf). The supernatant was transferred into a new microcentrifuge tube as the protein stock. Protein concentration was determined using a Pierce BCA protein assay kit (Thermo Fisher Scientific). All sarcoplasmic protein samples were diluted to 2 mg/mL with extraction buffer.

Degree of collagenase activity was measured by gelatin-zymography according to the method described by Tajhya, et al., (2017) with modifications. Sarcoplasmic proteins were mixed with Tris-glycine SDS sample buffer (Novex Life Technologies) at a ratio of 1:1. Five µL of SeeBlue Pre-Stained Standard (Novex Life Technologies), 1 ng of positive control (MMP-2 902-MP; R&D Systems, Minneapolis, MN) and 15 µg of prepared sarcoplasmic protein samples were loaded into a 10% Zymogram Plus (gelatin) pre-casted gel (Invitrogen). Proteins were separated using a Novex mini-cell XCellSure Lock electrophoresis cell (Invitrogen) in ice-cold 1XRunBlue SDS running buffer (Expedoen). The system was run at constant voltage of 125 V at 4°C until the blue tracking dye reached the bottom of the gel, approximately 150 min.

Following gel electrophoresis, gels were incubated for 1 h in 1X Renaturing Buffer

(Novex) at room temperature with one change of the same buffer at 30 min. After renature, gels were incubated for 1 h in 1X Developing Buffer (Novex) at 25°C with one change of the developing buffer at 30 min. Gels were incubated for 36 h in 1X Developing Buffer (Novex) at 37°C in an incubator (Symphony general forced air incubator; VWR, Radnor, PA). After incubation, gels were stained for 30 min in Coomassie blue stain (2.3 mM Coomassie blue G250, 40% methanol, 10% glacial acetic acid and 50% ultrapure water) at room temperature. Finally, gels were destained using a destaining solution (30% methanol, 10% glacial acetic acid and 60% ultrapure water) at room temperature until the bands appeared, approximately 1 h. Imaging process was identical as described in the calpain activity section.

Collagen Extraction

Collagen was reduced and hydrolyzed according to the method described by Avery, et al. (2009) with modifications. Five hundred mg of powdered meat was weighed out into 15 x 125 mm glass tubes with polytetrafluoroethylene coated caps. Two and a half mL of phosphate buffered saline (**PBS**) with 0.04% of sodium borohydride were added to each tube and incubated in the fume hood for 60 min as a reduction step to avoid the loss of crosslinks. Two hundred µl of glacial acetic acid was added to stop the reduction step. Samples were centrifuged at 1,000 x g for 5 min (Eppendorf centrifuge 5810 R; Eppendorf) and washed 3 times using 5 mL ultrapure water to eradicate residual sodium borohydride and acetic acid. Samples were dried under a vacuum evaporator (RapidVap; Labconco, Kansas City, MO) at 80°C at 53% speed with 200 mbar vacuum for 15 min. Ten mL of 6N hydrocholoric acid (HCl) was added to each sample, and the samples were hydrolyzed in a forced air oven (Isotemp 737F; Fisher Scientific) at 115°C for 24 h. Samples were cooled to room temperature and the HCl was evaporated from the samples using a vacuum evaporator (RapidVap; Labconco) at 40-50°C at 53% speed with 0 mbar vacuum until all residual

HCl was gone. Samples were rehydrated with 0.5 mL of ultrapure water and stored at -80°C preceding hydroxyproline and crosslink analysis.

Collagen Content

Collagen content was determined by the hydroxyproline assay described by Bergman and Loxley (1963) with modifications. Fifty µL of rehydrated samples were diluted with 4.95 mL ultrapure water and 0.5 mL of diluted sample was transferred to 15 x 125 mm glass tubes. To each sample 1.5 mL of ultrapure water was added and the samples incubated in a 60°C water bath. One mL of Chloramine-T Oxidant Reagent (6 mM of chloramine-t hydrate in buffer solution (140 mM citric acid monohydrate, 37.5 mM sodium hydroxide, 660 mM sodium acetate trihydrate, and 29% 1-proponal, pH 6.0) was added. The samples were vortexed and incubated for 20 min at room temperature. One mL of dimethylaminobenzaldehyde (**DMBA**) color reagent (60mM DMBA, dissolved in 21% perchloric acid, 65% two-proponal and 14% ultrapure water) was added to each tube. The samples were vortexed and incubated in a 60°C water bath for 90 min shielded from light. Samples were placed in a cold-water bath for 3 min. A spectrophotometer equipped with a microplate reader (BioTek Eon; BioTek Instruments Inc., Winooski, VT) was used to determine hydroxyproline concentration at an absorbance of 588 nm. An appropriate hydroxyproline standard curve and samples were plated in duplicate on each plate. A conversion factor of 7.14 for hydroxyproline to collagen ratio was used. Collagen content was displayed as mg of collagen per g of wet tissue.

Collagen Crosslinks

Samples were purified and analyzed following methods described by Viguet-Carrin, et al. (2009) with modifications. Ultrapure water was used to diluted extracted collagen at 8%. Diluted samples were centrifuged at 4,000 x g for 20 min (Eppendorf centrifuge 5810 R; Eppendorf) and

the residue was discarded. In a 5 mL glass tube, 400 µL of diluted sample was combined with 2.8 mL of sample buffer (6:1 acetonitrile and acetic acid) for a final volume of 3.2 mL. Samples were cleaned using a Bond Elut Cellulose cartridge 300 mg, 3 mL (12102095; Agilent Technologies, Santa Clara, CA) through a PrepSep 24-port solid phase extraction vacuum manifold (Fisher Scientific). Each cellulose cartridge was equilibrated with 2.5 mL of wash buffer (8:1:1, acetonitrile, acetic acid, and ultrapure water), followed by the diluted samples. The cellulose cartridge was washed 4 times with 2.5 mL of wash buffer and then with 0.2 mL of ultrapure water. The wash was discarded, and a clean glass tube was placed in the vacuum manifold before elution of crosslinks. Six hundred µL of 1% heptafluorobutyric acid (**HFBA**) ran through the cellulose cartridge twice to elute the crosslinks. Cleaned samples were vortexed and transferred to 2 mL amber vials (*P/N* 5188-6535; Agilent Technologies) capped with 9 mm pre0-slite PTFE screw caps (*P/N* 5185-5865; Agilent Technologies).

An ultra-high-pressure liquid chromatography system (Acquity UPLC H-Class; Waters Corporation, Milford, MA) equipped with a degasser, quaternary pump, sample manager and an Acquity UPLC Fluorescence Detector (Waters Corporation) was used to determine mature crosslinks pyridinoline (**PYD**) and deoxypyridinoline (**DPD**). A PYD/DPD standard (*P/N* 4101; Quidel Co., San Deigo, CA) was used to produce a standard curve to determine linearity range of assays and detection limits. The crosslinks were separated using an HSS T3 2.1 x 100 mm, 1.8 µm column (Waters Corporation), at a flow rate of 0.5 mL/min with a column temperature of 60°C. Solvent A (0.2% HFBA in ultrapure water) and solvent B (100% acetonitrile) were used as a gradient solution. After a 10 min isocratic step at 100% solvent A, PYD/DPD were eluted with 85% solvent A and 15 % solvent B for a total run time of 20 min for each sample. The PYD and DPD were measured for fluorescence at an excitation of 297 nm and emission of 395 nm.

Between each sample, 100% solvent B was used to rinse off residues of previous samples followed by 100% solvent A to equilibrate the column. Quantification of the PYD and DPD crosslinks were determined by a calibration curve by plotting the peak area ratio (crosslink area/standard area). The concentration of PYD and DPD were multiplied by the dilution factors to get final concentration in ppm. To calculate the levels of crosslinks in mol/mol of collagen, the chemical masses of 428.44, 412.44 and 300,000 g/mol were used for PYD, DPD and collagen, respectively.

Perimysial Extraction

Perimysial fraction extraction was conducted following the method described by Light and Champion (1984) with modifications. Approximately 30 g of muscle tissue on the distal end of the breast fillets was removed and homogenized two times in 0.05M $CaCl_2$ using a blender (model 51BL32; Warring Commercial). The homogenate was filtered through a 1 mm mesh screen into a small beaker. The connective tissue collected on the screen was rehomogenized with the same volume of 0.05M $CaCl_2$. This process was repeated twice, and anything that remained on the mesh screen after the final homogenization was considered the perimysial fraction. The perimysial fractions were transferred to a tube containing 1X PBS and hydrated overnight at 4°C for peak transitional temperature measurement.

Peak Transitional Temperature Measurement

Collagen denaturation temperature was assessed according to methods described by Vierck, et al. (2018) with modifications. Prior to the measurement, perimysial fractions was removed from the PBS, and the non-bound water was removed by blotting the samples with filter paper. Five to 10 mg of hydrated samples was placed in a hermetic aluminum crucible (S201-53090; Shimadzu, Kyoto, Japan), and the aluminum crucible was sealed using a sealing press

(SSC-30; Shimadzu). The sample crucible and a sealed empty crucible, for a reference crucible, were placed at the stage of the differential scanning calorimeter (DSC-60; Shimadzu). The temperature program was set from room temperature to 100°C with a 5°C/min temperature increase. To analyze the data the TA-60WS software (Shimadzu) was used to determine the peak transitional temperature (°C).

Statistical Analysis

All data were analyzed as a completely randomized design. Each animal was considered the experimental unit. Tukey's test was used for multiple comparisons. Data were analyzed using the GLIMMIX procedure of SAS (version 9.4, Cary, NC). For all analysis, separation of means was conducted using LSMEANS procedure (least significant differences) at $P < 0.05$.

RESULTS AND DISCUSSION

As expected, WB fillets were heavier than the N fillets (522.9 vs. 446.9 g; P < *0.05*; Figure 2.5A). These results are supported by many other studies (Bowker, et al., 2019; Sihvo, et al., 2014; Sun, et al., 2018), which they all found a strong positive relationship between the severity of the WB myopathy and the raw weight of the breast fillets. However, Kuttappan, et al. (2017) showed that only fillets harvested from birds at 6 weeks had a strong positive relationship between bird weight and WB incidence, whereas birds harvested at 9 weeks only had a minor relationship between the two parameters. This finding suggested that incidence of WB may be influenced by a combination of factors including age and bird weight.

The pH values for WB were higher compared to the N samples (6.17 vs. 5.83; P < *0.05*; Figure 2.5B). This again is supported by other studies (Cai, et al., 2018; Mudalal, et al., 2015), who also found elevated pH in the WB fillets. While the actual cause of the pH increase in WB is not known, there are several hypotheses. Aguirre, et al. (2018) and Kuttappan, et al. (2017)

suggested that there is a down regulation of carbohydrate metabolism in WB, which would play a role in the rigor mortis process and leading to the higher ultimate pH. On the other hand, Mudalal, et al. (2015) suggested the presence of excessive scar tissue may lower the glycogen content in WB breast fillets, resulting in a higher ultimate pH. However, more research would be needed to confirm these hypotheses.

There was no significant difference for WBSF between the WB and N samples (34.09 vs. 37.69 N; $P > 0.10$; Figure 2.5D). A WB fillet is typically described as tough and rubbery, so this result was not anticipated. However, Cai, et al. (2018) and Dalgaard, et al. (2018) also did not find a difference in WBSF between WB and N fillets. The WB texture described above has been hypothesized to be a result of the deposition of additional connective tissue from scarring (Kuttappan, et al., 2016). Therefore, WBSF may not be the best textural analysis method for WB texture as the peak shear force detected by WBSF mostly represents the myofibrillar components (Girard, et al., 2012b). On the other hand, the use of compression based texture analysis has been noted to offer more consistent results in WB research (Bowker and Zhuang, 2019). Aguirre, et al. (2018) utilized texture profile analysis (**TPA**) and documented that marinated severe WB were harder, more cohesive, springier, and chewier than marinated N breast. Chatterjee, et al. (2016) also found that both raw and cooked WB fillets had greater hardness and chewiness compared to N samples using TPA.

There is a tendency for sarcomere lengths to be longer in N samples in comparison to WB (2.02 vs. 1.70 μm; $P = 0.05$; Figure 2.5C). A representative image for sarcomere length measurements is displayed in Figure 2.1. It is interesting to note that many past studies observed longer sarcomeres in the WB compared to N fillets (Solo, 2016; Sun, et al., 2018; Tijare, et al., 2016). The variation of deboning and freezing times as well as the WB severity could explain

some of the differences observed. The samples in the current study were deboned at 3 h postmortem and frozen around 8 h, whereas Tijare, et al.,(2016) deboned at 4 h postmortem and frozen around 24 h. In addition, Solo (2016) deboned and immediately froze their samples at 4 h postmortem, and Sun, et al. (2018) deboned at 2 h postmortem and only utilized chilled storage for 1, 2 and 8 d. In poultry, the rate of rigor mortis can vary depending on various factors both pre- and post-mortem but may take as long as 6 h to complete (Li, et al., 2012; Schreurs, 2000). During the rigor mortis process, free calcium plays a critical role in the formation of actomyosin bonds and the ultimate sarcomere length. Perhaps, there are free calcium concentration differences between the N and WB samples resulting in the observed tendency. The shorter sarcomere may ultimately contribute to the contracted appearance and texture of WB fillets.

Purge from WB had greater free calcium concentration compared to purge from N fillets (6.20 vs. 4.20 nmol calcium/mg protein; $P < 0.05$; Figure 2.6A). Many other studies have also found higher free calcium concentrations in the WB samples (Soglia, et al., 2016b; Soglia, et al., 2018; Tasoniero, et al., 2016). This data supported the shorter sarcomere phenomenon observed in this study as it is possible that the higher free calcium in WB samples allowed for the additional development of actomyosin complexes during the rigor mortis process and resulted in the observed tendency for shorter sarcomere lengths in WB (Ertbjerg and Puolanne, 2017). Calcium plays an important role in rigor mortis as well as the following tenderization process as many proteolytic enzymes require calcium for activation (Koohmaraie, 1988). However, the exact cause for the increase in free calcium in WB samples are not fully understood. One of the hypotheses suggested that the calcium sequestering capabilities of the sarcoplasmic reticulum (**SR**) may be compromised in WB broilers (Soglia, et al., 2018). The SR's number one role is to maintain calcium homeostasis within the cells to ensure the proper balance between muscle

contraction and relaxation. This function is mainly controlled by three major protein groups that are responsible for calcium storage, sequestering and release in the SR (Barone, et al., 2015). Minor defects in any of the above protein groups can result in higher levels of free calcium in the sarcoplasm. Additionally, Lee, et al. (2015) suggested that extra calcium may activate lipases such as phospholipase A2 (**PLA2**) which could cause the weakening of the SR membrane phospholipid layer via the formation of lysophospholipids as the same group of researchers noted an upregulation of the gene *PLA2G4A* which encodes for PLA2 in WB samples. The increase in PLA2 activity may further weaken SR membrane integrity and could result in additional calcium leakage.

At 8 hrs postmortem, more μ/m calpain was autolyzed in WB samples compared to the N samples, indicating greater calpain activity in WB than N fillets (71.05 vs. 59.12 % calpain autolyzed; $P < 0.01$; Figure 2.6C). A representative image for the calpain activity measurement is displayed in Figure 2.2. In addition, WB samples tended to have less intact TNT compared to N samples (49.88 vs. 56.97 % relative intact troponin-T band density; $P = 0.05$; Figure 2.6B). A representative image for the TNT degradation measurement is displayed in Figure 2.3. Calpain autolysis has been shown to have a positive relationship to storage time and myofibrillar protein degradation (Koohmaraie, 1992). Soglia, et al. (2018) observed an increase in autolyzed μ/m calpain simultaneously with a decrease in native μ/m calpain in both the WB and N samples as they were stored for 10, 24, 72, 120 and 168 h postmortem at 5°C. Hasegawa, et al. (2020) also found WB samples to have higher calpain activity and less intact TNT measured at 12 h postmortem compared to the N samples. Furthermore, Bowker, et al. (2016) and Zhang, et al. (2020) reported 24 hr post-mortem WB fillets to have less intact desmin compared to N samples. It is important to point out that μ/m calpain has been shown to be the dominant active calpain

form in avian muscles (Soglia, et al., 2018), while μ-calpain become inactive within 6 h postmortem (Lee, et al., 2008). We were not able to identify any μ-calpain activity through immunoblotting in this study (data not shown). Therefore, it is very likely that the calpain activity identified through the casein zymography in the current study was from μ/m calpain. The calpain system is calcium-dependent, and it has been repeatedly documented that WB samples have higher free calcium concentration compared to N samples (Lee, et al., 2008; Soglia, et al., 2016b; Soglia, et al., 2018; Tasoniero, et al., 2016). The increased free calcium available in WB samples likely contributed to the enhanced proteolytic activity (Tasoniero, et al., 2016).

The WB samples had greater relative percentage of activated matrix metalloproteinases 2 demonstrating greater collagenase activity compared to the N samples (13.24 vs. 7.84 % activated MMP2; $P < 0.05$; Figure 2.6D). A representative image for the collagenase activity measurement is displayed in Figure 2.4. Currently, there is little research investigating collagenase activity in WB fillet through gelatin-zymography. Matrix metalloproteinases (**MMPs**) are a group of calcium dependent proteases that degrade components of the extracellular matrix, such as collagen and gelatin (Visse and Nagase, 2003). Like the calpain system, the MMP activity is also enhanced in WB samples due to the increased levels of free calcium present as MMPs also require calcium for activation (Kohn, et al., 1994; Munshi, et al., 2002). Byron (2019) found that visual WB defects such as the hard rigid appearance began to dissipate, and the flexibility of the fillet improved after refrigerated storage of 5 d and mitigate the severity of WB. It is possible that the enhanced collagenase activity in WB samples may play a role in the dissipation of WB during chilled storage.

The WB had more collagen content compared to N samples (3.89 vs. 2.08 mg collagen/g wet tissue; $P < 0.01$; Figure 2.7A). In addition, WB samples had greater PYD and DPD

crosslinks density than the N samples (0.23 vs. 0.14 mol PYD/mol collagen; $P < 0.05$; Figure 2.7C; 0.07 vs. 0.04 mol DPD/mol collagen; $P < 0.01$; Figure 2.7D). Many others have also found WB fillets to have more intramuscular collagen compared to N samples (Baldi, et al., 2019; Soglia, et al., 2016a; Soglia, et al., 2016b). Baldi, et al. (2019) attributed the cause of the increased collagen content in WB samples as progressive myodegeneration, which results in the deposit of scar tissue instead of muscle fibers. Soglia, et al. (2016a) also suggested that fibrosis may also be occurring in WB broilers, which leads to the thickening of connective tissue throughout the breast fillet. On the other hand, Baldi, et al. (2019) also showed that WB samples had greater PYD density than the N samples. Observing the development of scar tissue and constrictive remodeling of arterial tissue is rabbits has been shown to impact excessive crosslinking (Brasselet, et al., 2005). Therefore, the scar tissue and fibrosis in WB filets could potentially be leading to the promotion of high densities of collagen crosslinking. Finally, Wu, et al. (2021) documented a strong positive correlation between PYD density in raw beef shank cuts and WBSF and connective tissue texture evaluated by East Asian consumers. It is likely the increase in mature collagen crosslink density in WB samples may contribute to the rubbery texture observed in WB.

The WB samples had a greater collagen denaturation temperature compared to N samples (65.47 vs. 63.72 °C; $P < 0.05$; Figure 2.7B). The differential scanning calorimeter (**DSC**) is a commonly used thermal analysis technique to understand the structural and functional properties of different meat components (Tamilmani and Pandey, 2016). Baldi, et al. (2019) associated the peak at 60.4 ± 1.5°C as the stromal protein denaturation temperature in poultry meat. Torrescano, et al. (2003) associated higher transitional temperature DSC reading for beef muscles with greater shear force, and many studies have shown that the peak transitional temperature of

connective tissue is an indicator of greater concentration of thermally stable collagen cross-links (Horgan, et al., 1990; Lepetit, 2008; Tornberg, 2005). Therefore, the DSC result further supported those elevated levels of heat-stable crosslinks such as PYD and DPD can result in increased tension and thermal denaturation temperature of the connective tissue, which potentially play a role in the development of WB fillets texture.

CONCLUSION

The development of WB has been an issue confounding the poultry industry for over a decade. While there have been many novel research studies in the area of WB myopathy development, there remains a multitude of unknowns. This research begins to fill in the blanks of many texture defects observed in WB fillets, particularly around collagen characteristics. Understanding the composition of mature collagen crosslinks in WB may partly explain the tough/rubbery texture of WB meat. Finally, it also appears that SR functionality/integrity may be compromised in WB broilers with accumulation of calcium in the sarcoplasm. Future research looking into the integrity and functionality of the SR may further shed light on the causation of WB myopathy.

REFERENCES

Abasht, B., M. F. Mutryn, R. D. Michalek, and W. R. Lee. 2016. Oxidative stress and metabolic perturbations in wooden breast disorder in chickens. PloS one 11:e0153750.

Aguirre, M., C. Owens, R. Miller, and C. Alvarado. 2018. Descriptive sensory and instrumental texture profile analysis of woody breast in marinated chicken. Poultry science 97:1456-1461.

Anthony, N. 1998. A Review of Genetic Practices in Poultry: Efforts to Improve Meat Quality 1. Journal of Muscle foods 9:25-33.

Avery, N. C., T. J. Sims, and A. J. Bailey. 2009. Quantitative determination of collagen cross-links. Pages 103-121 in Extracellular Matrix ProtocolsSpringer.

Baldi, G., F. Soglia, L. Laghi, S. Tappi, P. Rocculi, S. Tavaniello, D. Prioriello, R. Mucci, G. Maiorano, and M. Petracci. 2019. Comparison of quality traits among breast meat affected by current muscle abnormalities. Food Research International 115:369-376.

Barone, V., D. Randazzo, V. Del Re, V. Sorrentino, and D. Rossi. 2015. Organization of junctional sarcoplasmic reticulum proteins in skeletal muscle fibers. Journal of muscle research and cell motility 36:501-515.

Bergman, I., and R. Loxley. 1963. Two improved and simplified methods for the spectrophotometric determination of hydroxyproline. Analytical Chemistry 35:1961-1965.

Biswas, A. K., and S. Tandon. 2019. Casein Zymography for Analysis of Calpain-1 and Calpain-2 Activity. Pages 31-38 in CalpainSpringer.

Bowker, B., and H. Zhuang. 2019. Detection of razor shear force differences in broiler breast meat due to the woody breast condition depends on measurement technique and meat

state. Poultry science 98:6170-6176.

Bowker, B., H. Zhuang, E. Barton, and J. A.-M. Sanchez. 2016. White striping and wooden breast defects influence meat quality and muscle protein characteristic in broiler breast meat. Proc. 62nd Int. Cong. Meat Sci. Tech. Bangkok, Thailand.

Bowker, B., H. Zhuang, S. Yoon, G. Tasoniero, and K. Lawrence. 2019. Relationships between attributes of woody breast and white striping myopathies in commercially processed broiler breast meat. Journal of Applied Poultry Research 28:490-496.

Brambila, G. S., D. Chatterjee, B. Bowker, and H. Zhuang. 2017. Descriptive texture analyses of cooked patties made of chicken breast with the woody breast condition. Poultry Science 96:3489-3494.

Brasselet, C., E. Durand, F. Addad, A. A. H. Zen, M. B. Smeets, D. Laurent-Maquin, S. Bouthors, G. Bellon, D. de Kleijn, and G. Godeau. 2005. Collagen and elastin cross-linking: a mechanism of constrictive remodeling after arterial injury. American Journal of Physiology-Heart and Circulatory Physiology 289:H2228-H2233.

Byron, M. 2019. Impact of refrigerated storage on the dissipation of woody broiler breast meat.

Cai, K., W. Shao, X. Chen, Y. Campbell, M. Nair, S. Suman, C. Beach, M. Guyton, and M. Schilling. 2018. Meat quality traits and proteome profile of woody broiler breast (pectoralis major) meat. Poultry science 97:337-346.

Chao, M. D., K. Domenech-Pérez, and C. R. Calkins. 2017. Feeding vitamin E may reverse sarcoplasmic reticulum membrane instability caused by feeding wet distillers grains plus solubles to cattle. The Professional Animal Scientist 33:12-23.

Chatterjee, D., H. Zhuang, B. Bowker, G. Sanchez-Brambila, and A. Rincon. 2016. Instrumental

texture characteristics of broiler pectoralis major with the wooden breast condition. Poultry science 95:2449-2454.

Coro, F. A., E. Y. Youssef, and M. Shimokomaki. 2002. Age related changes in poultry breast meat collagen pyridinoline and texture. Journal of food biochemistry 26:533-541.

Dalgaard, L. B., M. K. Rasmussen, H. C. Bertram, J. A. Jensen, H. S. Møller, M. D. Aaslyng, E. K. Hejbøl, J. R. Pedersen, D. Elsser-Gravesen, and J. F. Young. 2018. Classification of wooden breast myopathy in chicken pectoralis major by a standardised method and association with conventional quality assessments. International Journal of Food Science & Technology 53:1744-1752.

Dalle Zotte, A., M. Cecchinato, A. Quartesan, J. Bradanovic, G. Tasoniero, and E. Puolanne. Year. How does" wooden breast" myodegeneration affect poultry meat quality. Proc. 60th International Congress of Meat.

Dransfield, E., and A. Sosnicki. 1999. Relationship between muscle growth and poultry meat quality. Poultry science 78:743-746.

Dridi, S., and M. Kidd. 2016. Molecular pathways involved in amino acid and phosphorous utilization. Ch 8:119-128.

Ertbjerg, P., and E. Puolanne. 2017. Muscle structure, sarcomere length and influences on meat quality: A review. Meat science 132:139-152.

Girard, I., J. Aalhus, J. Basarab, I. Larsen, and H. Bruce. 2012a. Modification of beef quality through steer age at slaughter, breed cross and growth promotants. Canadian Journal of Animal Science 92:175-188.

Girard, I., H. Bruce, J. Basarab, I. Larsen, and J. Aalhus. 2012b. Contribution of myofibrillar and

connective tissue components to the Warner–Bratzler shear force of cooked beef. Meat science 92:775-782.

Hasegawa, Y., T. Hara, T. Kawasaki, M. Yamada, T. Watanabe, and T. Iwasaki. 2020. Effect of wooden breast on postmortem changes in chicken meat. Food Chemistry 315:126285.

Horgan, D. J., N. L. King, L. B. Kurth, and R. Kuypers. 1990. Collagen crosslinks and their relationship to the thermal properties of calf tendons. Archives of biochemistry and biophysics 281:21-26.

Huang, X., and D. U. Ahn. 2018. The Incidence of Muscle Abnormalities in Broiler Breast Meat - A Review. Korean J Food Sci Anim Resour 38:835-850. doi 10.5851/kosfa.2018.e2

Kohn, E. C., W. Jacobs, Y. S. Kim, R. Alessandro, W. G. Stetler-Stevenson, and L. A. Liotta. 1994. Calcium influx modulates expression of matrix metalloproteinase-2 (72-kDa type IV collagenase, gelatinase A). Journal of Biological Chemistry 269:21505-21511.

Koohmaraie, M. Year. The role of endogenous proteases in meat tenderness. Proc. Proc. Recip. Meat Conf.

Koohmaraie, M. 1992. The role of Ca2+-dependent proteases (calpains) in post mortem proteolysis and meat tenderness. Biochimie 74:239-245.

Koohmaraie, M., and G. Geesink. 2006. Contribution of postmortem muscle biochemistry to the delivery of consistent meat quality with particular focus on the calpain system. Meat science 74:34-43.

Kuttappan, V., B. Hargis, and C. Owens. 2016. White striping and woody breast myopathies in the modern poultry industry: a review. Poultry Science 95:2724-2733.

Kuttappan, V., C. Owens, C. Coon, B. Hargis, and M. Vazquez-Anon. 2017. Incidence of broiler

breast myopathies at 2 different ages and its impact on selected raw meat quality parameters. Poultry Science 96:3005-3009.

Lee, H., V. Sante-Lhoutellier, S. Vigouroux, Y. Briand, and M. Briand. 2008. Role of calpains in postmortem proteolysis in chicken muscle. Poultry Science 87:2126-2132.

Lee, W. R., E. M. Brannick, M. F. Mutryn, W. Fu, and B. Abasht. 2015. Characterization of a novel chicken muscle disorder through differential gene expression and pathway analysis using RNA-sequencing.

Lepetit, J. 2008. Collagen contribution to meat toughness: Theoretical aspects. Meat Science 80:960-967.

Li, S., X. Xu, and G. Zhou. 2012. The roles of the actin-myosin interaction and proteolysis in tenderization during the aging of chicken muscle. Poultry science 91:150-160.

Light, N., and A. E. Champion. 1984. Characterization of muscle epimysium, perimysium and endomysium collagens. Biochemical Journal 219:1017-1026.

Maddock, K., E. Huff-Lonergan, L. Rowe, and S. M. Lonergan. 2005. Effect of pH and ionic strength on μ-and m-calpain inhibition by calpastatin. Journal of Animal Science 83:1370-1376.

Mudalal, S., M. Lorenzi, F. Soglia, C. Cavani, and M. Petracci. 2015. Implications of white striping and wooden breast abnormalities on quality traits of raw and marinated chicken meat. Animal 9:728-734.

Munshi, H. G., Y. I. Wu, E. V. Ariztia, and M. S. Stack. 2002. Calcium regulation of matrix metalloproteinase-mediated migration in oral squamous cell carcinoma cells. Journal of Biological Chemistry 277:41480-41488.

Mutryn, M. F., E. M. Brannick, W. Fu, W. R. Lee, and B. Abasht. 2015. Characterization of a

novel chicken muscle disorder through differential gene expression and pathway analysis using RNA-sequencing. BMC genomics 16:399.

Nishimura, T. 2010. The role of intramuscular connective tissue in meat texture. Animal science journal 81:21-27.

Owens, C. Year. Woody breast meat. Proc. 69th Reciprocal Meat Conference Proceedings. June 18th-23rd, San Angelo, Texas.

Parrish, F., C. Selvig, R. Culler, and M. Zeece. 1981. CAF Activity, Calcium Concentration, Andy the 30,000-Dalton Component of Tough and Tender Bovine Longissimus Muscle. Journal of Food Science 46:308-311.

Pietrzak, M., M. Greaser, and A. Sosnicki. 1997. Effect of rapid rigor mortis processes on protein functionality in pectoralis major muscle of domestic turkeys. Journal of Animal Science 75:2106-2116.

Schreurs, F. 2000. Post-mortem changes in chicken muscle. World's poultry science journal 56:319-346.

Sihvo, H.-K., K. Immonen, and E. Puolanne. 2014. Myodegeneration with fibrosis and regeneration in the pectoralis major muscle of broilers. Veterinary pathology 51:619-623.

Soglia, F., L. Laghi, L. Canonico, C. Cavani, and M. Petracci. 2016a. Functional property issues in broiler breast meat related to emerging muscle abnormalities. Food Research International 89:1071-1076.

Soglia, F., S. Mudalal, E. Babini, M. Di Nunzio, M. Mazzoni, F. Sirri, C. Cavani, and M. Petracci. 2016b. Histology, composition, and quality traits of chicken Pectoralis major muscle affected by wooden breast abnormality. Poultry Science 95:651-659.

Soglia, F., Z. Zeng, J. Gao, E. Puolanne, C. Cavani, M. Petracci, and P. Ertbjerg. 2018. Evolution

of proteolytic indicators during storage of broiler wooden breast meat. Poultry science 97:1448-1455.

Solo, J. 2016. Meat quality and sensory analysis of broiler breast fillets with woody breast muscle myopathy.

Sun, X., D. Koltes, C. Coon, K. Chen, and C. Owens. 2018. Instrumental compression force and meat attribute changes in woody broiler breast fillets during short-term storage. Poultry science 97:2600-2606.

Tajhya, R. B., R. S. Patel, and C. Beeton. 2017. Detection of matrix metalloproteinases by zymography. Pages 231-244 in Matrix MetalloproteasesSpringer.

Tamilmani, P., and M. C. Pandey. 2016. Thermal analysis of meat and meat products. Journal of Thermal Analysis and Calorimetry 123:1899-1917.

Tasoniero, G., M. Cullere, M. Cecchinato, E. Puolanne, and A. Dalle Zotte. 2016. Technological quality, mineral profile, and sensory attributes of broiler chicken breasts affected by white striping and wooden breast myopathies. Poultry science 95:2707-2714.

Tijare, V. V., F. Yang, V. Kuttappan, C. Alvarado, C. Coon, and C. Owens. 2016. Meat quality of broiler breast fillets with white striping and woody breast muscle myopathies. Poultry Science 95:2167-2173.

Tornberg, E. 2005. Effects of heat on meat proteins–Implications on structure and quality of meat products. Meat science 70:493-508.

Torrescano, G., A. Sanchez-Escalante, B. Gimenez, P. Roncales, and J. A. Beltrán. 2003. Shear values of raw samples of 14 bovine muscles and their relation to muscle collagen characteristics. Meat Science 64:85-91.

Veiseth, E., S. Shackelford, T. Wheeler, and M. Koohmaraie. 2001. Effect of postmortem

storage on μ-calpain and m-calpain in ovine skeletal muscle. Journal of animal science 79:1502-1508.

Vierck, K. R., T. G. O'Quinn, J. A. Noel, T. A. Houser, E. A. Boyle, and J. M. Gonzalez. 2018. Effects of marbling texture on muscle fiber and collagen characteristics. Meat and Muscle Biology 2.

Viguet-Carrin, S., E. Gineyts, C. Bertholon, and P. Delmas. 2009. Simple and sensitive method for quantification of fluorescent enzymatic mature and senescent crosslinks of collagen in bone hydrolysate using single-column high performance liquid chromatography. Journal of Chromatography B 877:1-7.

Visse, R., and H. Nagase. 2003. Matrix metalloproteinases and tissue inhibitors of metalloproteinases: structure, function, and biochemistry. Circulation research 92:827-839.

Whipple, G., and M. Koohmaraie. 1993. Calcium chloride marination effects on beef steak tenderness and calpain proteolytic activity. Meat science 33:265-275.

Wu, W. J., A. A. Welter, E. A. Rice, B. A. Olson, T. G. O'Quinn, E. A. Boyle, G. Magnin-Bissel, T. A. Houser, M. D. Chao, and T. G. O'Quinn. 2021. Biochemical Factors Affecting East Asian Consumers' Sensory Preferences of Six Beef Shank Cuts. Meat and Muscle Biology 5.

Yalcin, S., S. Ozkan, M. C. Acar, and O. Meral. 2018. The occurrence of deep pectoral myopathy in broilers and associated changes in breast meat quality. British poultry science 59:55-62.

Zhang, X., W. Zhai, S. Li, S. P. Suman, J. Chen, H. Zhu, D. S. Antonelo, and M. W. Schilling.

2020. Early Postmortem Proteome Changes in Normal and Woody Broiler Breast Muscles. Journal of Agricultural and Food Chemistry 68:11000-11010.

Zhuang, H., and E. Savage. 2009. Variation and Pearson correlation coefficients of Warner-Bratzler shear force measurements within broiler breast fillets. Poultry science 88:214-220.

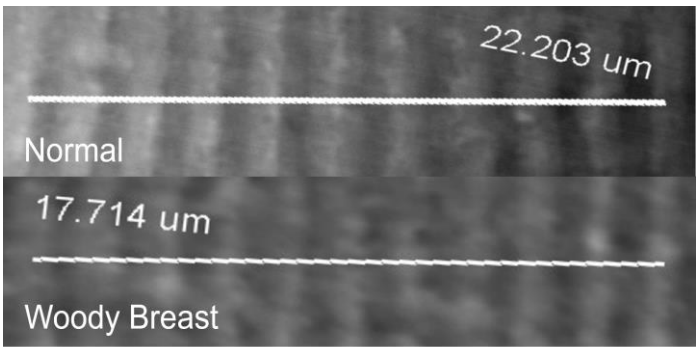

Figure 2.1 Representative normal and woody breast samples used to quantify sarcomere length

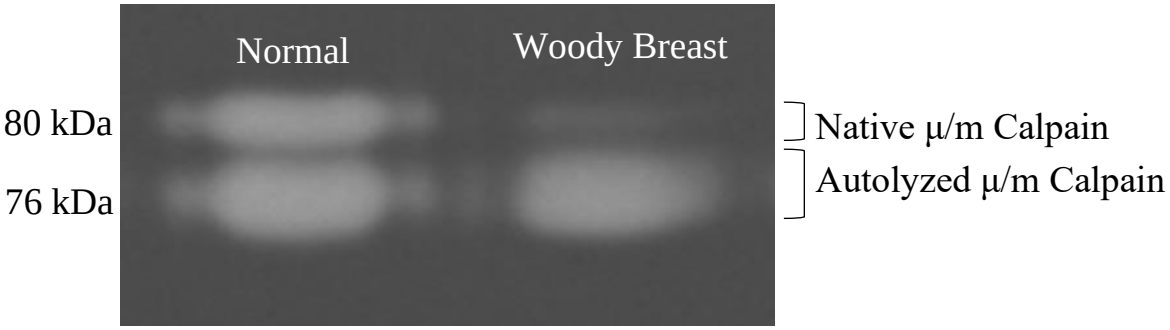

Figure 2.2.2 Representative normal and woody breast samples used to quantify calpain activity

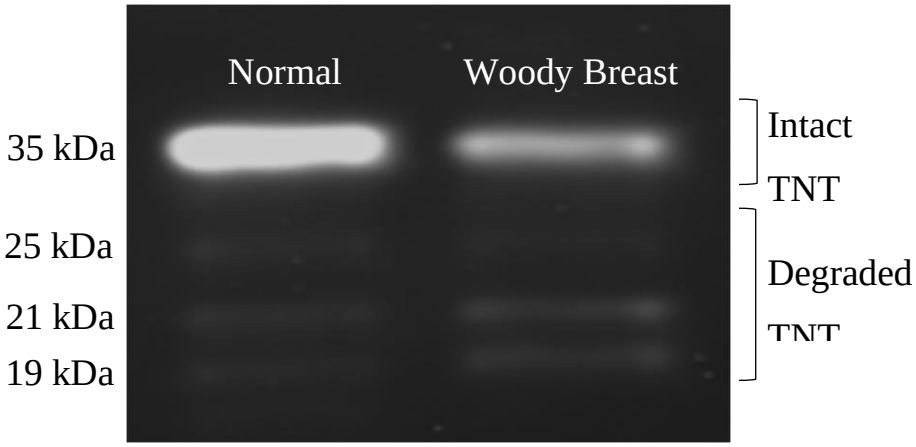

Figure 2.3 Representative normal and woody breast samples used to quantify proteolysis

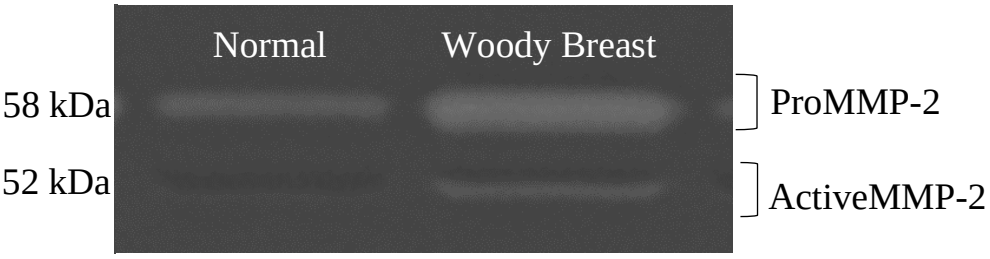

Figure 2.4 Representative normal and woody breast samples used to quantify collagenase activity

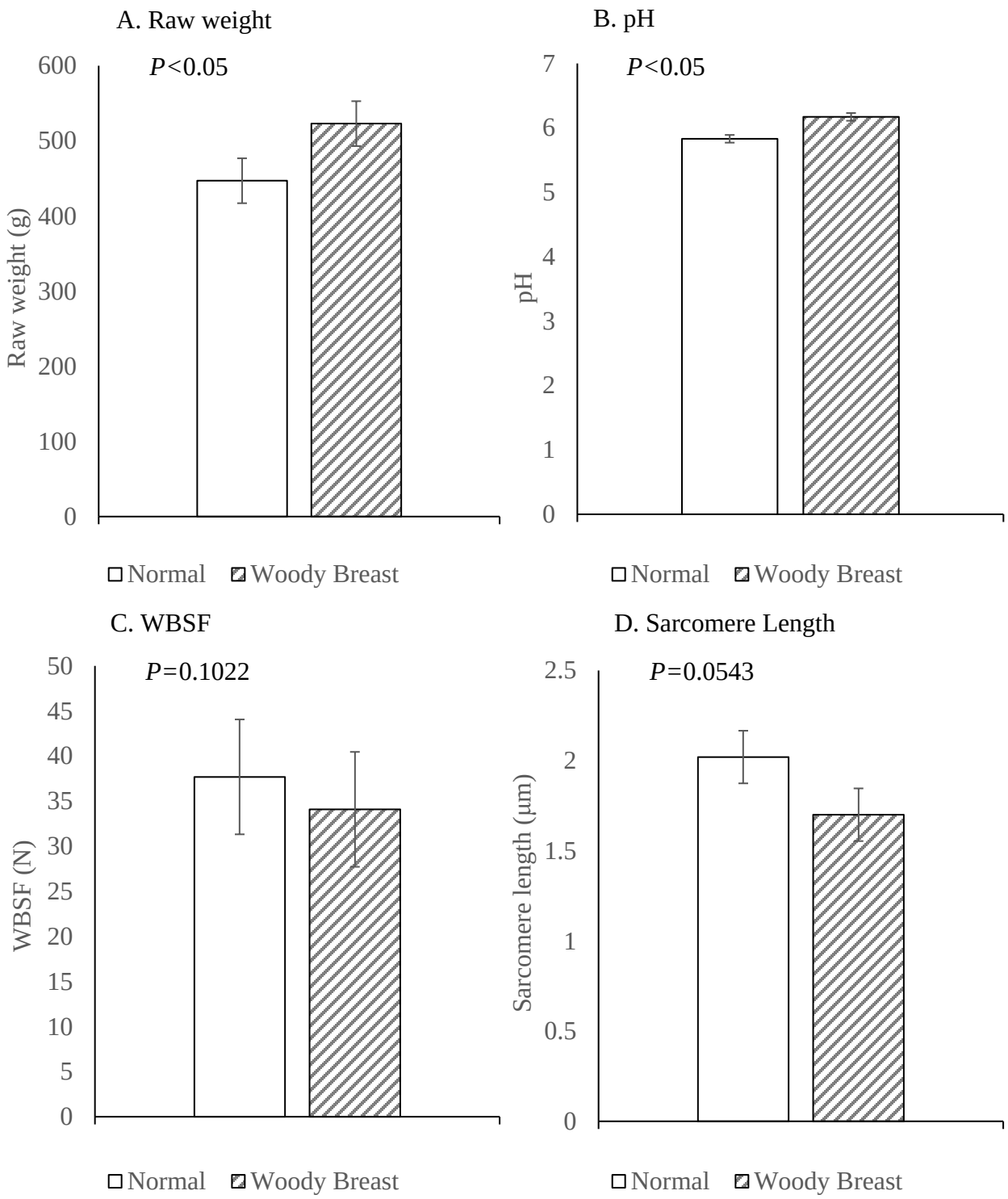

Figure 2.5 Effects of WB abnormality on (A) raw weight (g), (B) pH, (C) Warner Bratlzer shear force (N) and (D) sarcomere length (µm) compared to N breast fillet. Each bar represents the mean ± standard error; *n* = 14.

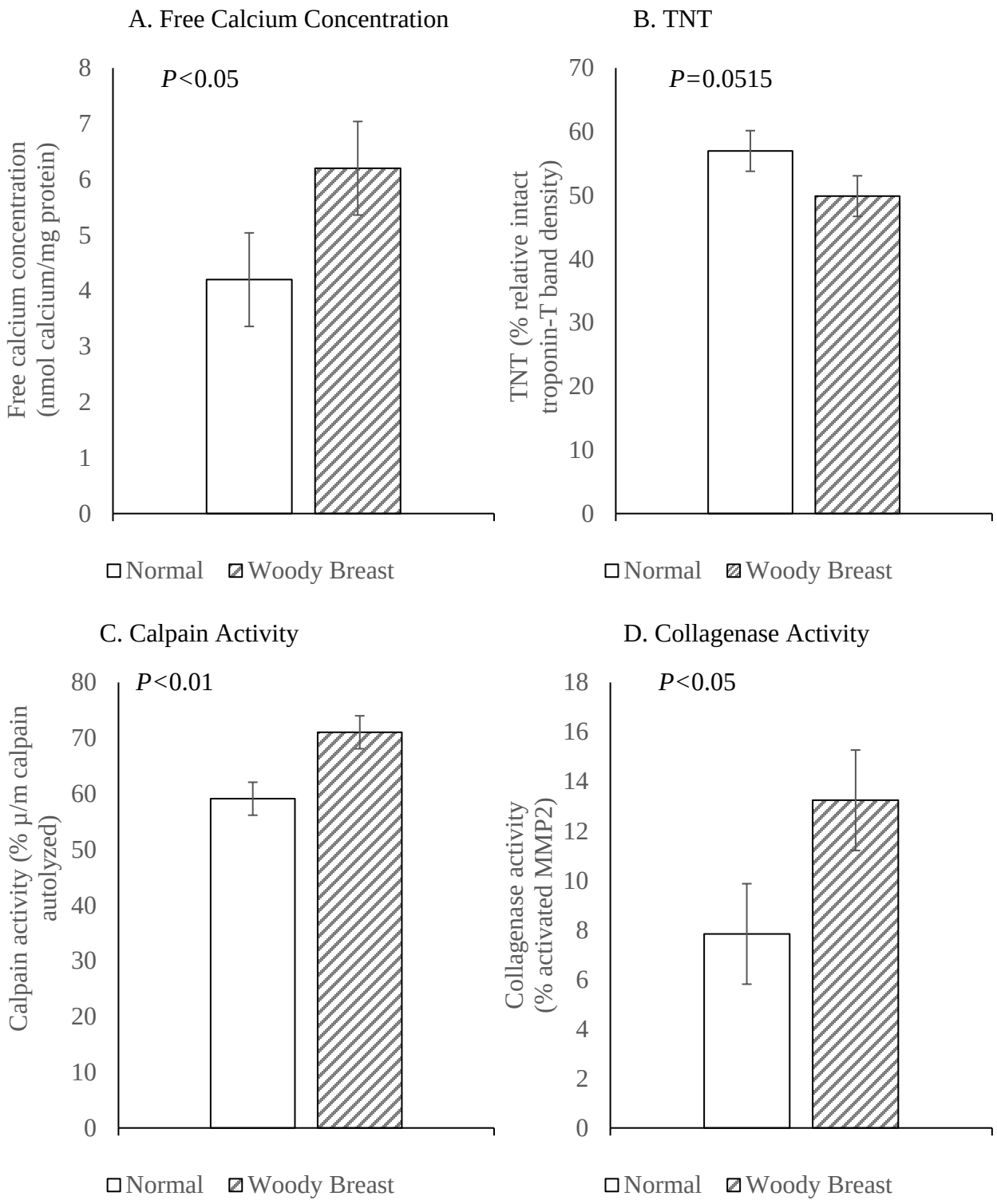

Figure 2.6 Effects of WB abnormality on (A) free calcium concentration (nmol calcium/mg protein), (B) troponin-T degradation (% relative intact troponin-T band density), (C) calpain activity (% calpain autolyzed) and (D) collagenase activity (% activated MMP2) compared to N breast fillet. Each bar represents the mean ± standard error; *n* = 14.

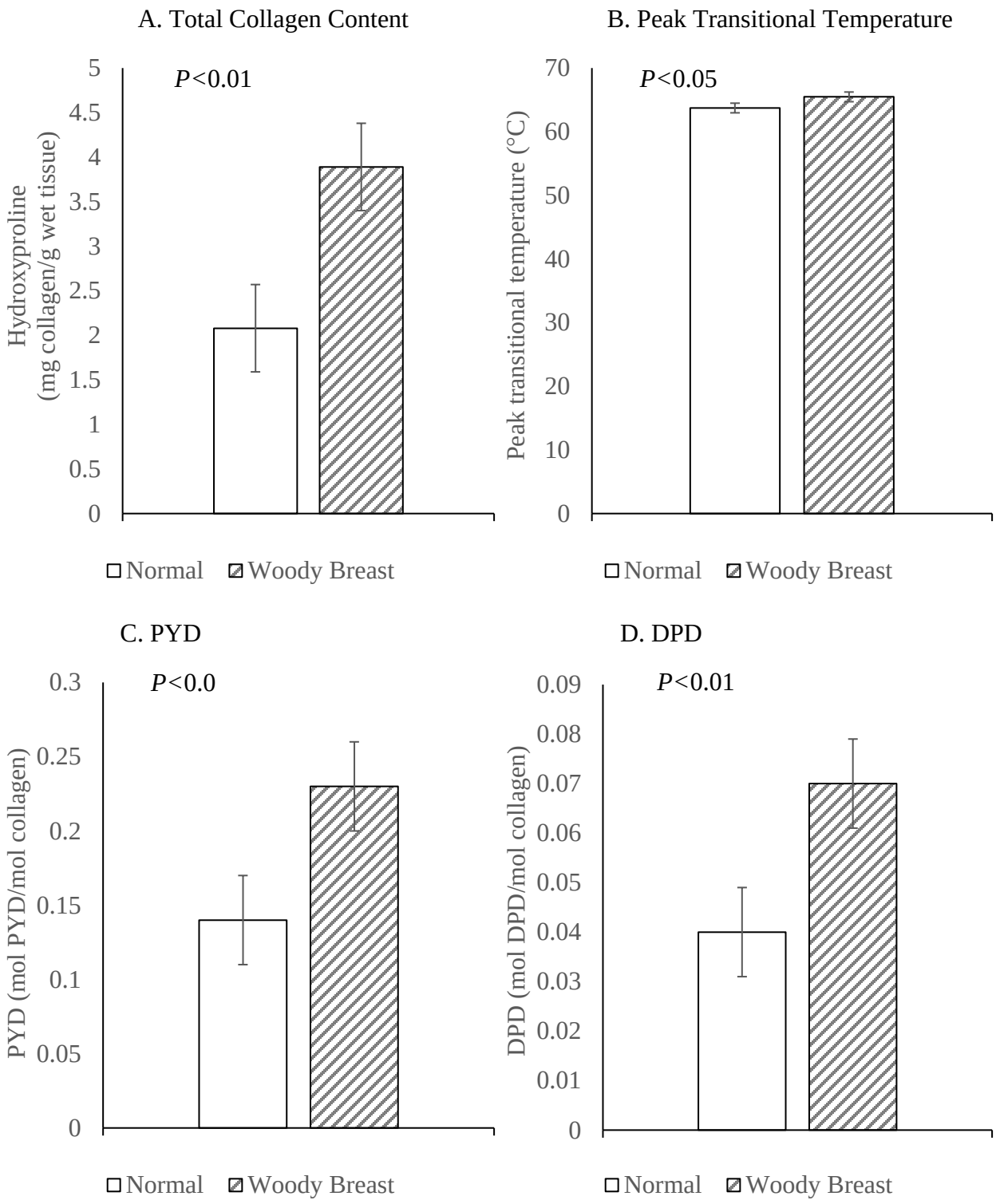

Figure 2.7 Effects of WB abnormality on (A) hydroxyproline (mg collagen/g wet tissue), (B) peak transitional temperature (°C), (C) pyridinoline (mol PYD/mol collagen) and (D) deoxypyridinoline (mol DPD/mol collagen) compared to N breast fillet. Each bar represents the mean ± standard error; *n* = 14.

Chapter 3 - An Integrative Omics Approach to Understand Sarcoplasmic Reticulum's Role in Elevated Levels of Free Calcium in Broiler Woody Breast

ABSTRACT

Woody breast (WB) is a myopathy observed in broiler *Pectoralis major* resulting in a rubbery texture. We hypothesize that a sarcoplasmic reticulum (SR) dysfunctionality associated with WB may lead to additional leakage of intracellular calcium into the sarcoplasm. The objective of this study was to utilize an integrative omics (lipidomics/proteomics) approach to investigate the functionality/integrity of WB SR. Fourteen Ross line broiler breast fillets (7 severe WB and 7 normal) were collected, packaged and frozen at 8 hrs postmortem from a commercial processing plant. The SR fractions of the samples were extracted via ultracentrifugation through discontinuous sucrose gradients. The proteins and lipids were extracted from SR fractions and utilized for proteomic and lipidomic analysis, respectively. Lipidomics data revealed WB SR had less relative % of phosphatidylcholine (PC) and more phosphatidylethanolamine (PE), phosphatidylserine (PS) and lysophosphatidylcholine (LPC) ($P<0.05$). Proteomics data revealed an upregulation of calcium transport proteins (ex. sarcoplasmic/endoplasmic reticulum calcium ATPase; $P<0.05$) and a downregulation of proteins responsible for calcium release (ex. ryanodine receptors; $P<0.05$) in WB SR. There was no difference in protein abundance for calcium storage proteins (ex. Calsequestrin; $P>0.05$). Interestingly, cholinesterase exhibited a 7.62-fold increase in WB SR ($P<0.01$), and there was also an upregulation of phospholipase A2 (PLA2) in WB SR ($P<0.01$). Changes in lipid composition and increases in lipid catabolism in SR may be partly responsible for the increased

free calcium levels in WB meat. WB SR membrane integrity may be compromised due to an upregulation of PLA2, resulting in the hydrolysis of PC, the main building block of lipid bilayers, into LPC. The upregulation of cholinesterase activity is a typical indicator of elevated cholinesterase inhibitors as found in Alzheimer's and Parkinson's disease patients. Perhaps, the inhibition of cholinesterase extended the length of action potential and calcium release from the SR. The upregulation of calcium transport proteins and downregulation of calcium release proteins in WB SR may be its attempt to regulate this proposed excessive signaling of calcium release.

Key Words: Calcium, lipidomics, proteomics, sarcoplasmic reticulum, woody breast

INTRODUCTION

The United States is the top consumer of chicken breasts in the world (Caldas-Cueva and Owens, 2020). To keep up with the demand, the poultry industry selected for birds with large and rapid growing breast muscles (Petracci, et al., 2015), which resulted in an emerging myopathy known as woody breast (**WB**) (Tijare, et al., 2016). This abnormality is typically identified by its tough, rubbery texture and hard ridges along the caudal and cranial regions of the *Pectoralis Major* muscle (Kuttappan, et al., 2016; Sihvo, et al., 2014). While the exact mechanism of WB development remains unknown, there are many theories circulating the literature such as oxidative stress, metabolic disorders and myodegeneration in the breast muscle (Abasht, et al., 2016; Dridi and Kidd, 2016; Kuttappan, et al., 2017; Mutryn, et al., 2015; Sihvo, et al., 2014).

Many studies, including a previous study by our lab, have noted high levels of free sarcoplasmic calcium concentrations in WB samples (Soglia, et al., 2016; Soglia, et al., 2018; Tasoniero, et al., 2016; Welter, et al., 2019). Calcium plays an important role during the rigor

mortis and the later tenderization process, as it aids in the formation of actomyosin bonds and activates the calcium dependent proteases such as calpains and matrix metalloproteinases (**MMPs**) following rigor mortis (Ertbjerg and Puolanne, 2017; Koohmaraie, 1988; Ren, et al., 2019). Therefore, elevated levels of calcium in WB samples could result in an overactive calcium dependent protease system (Ohlendieck, 2013), which can be detrimental to homeostasis of muscle cells as it can lead to myodegeneration and necrosis, both of which identified as potential etiologies for WB texture defects (de Brot, et al., 2016; Sihvo, et al., 2014; Trocino, et al., 2015).

The sarcoplasmic reticulum (**SR**) is an organelle that is responsible for the uptake, storage, and release of calcium within muscle cells. Various proteins are involved in the reuptake, storage and release of calcium from the SR, with the main ones being sarco(endo)plasmic reticulum Ca^{2+}-ATPase (**SERCA**), calsequestrin (**CASQ**) and ryanodine receptors (**RyR**), respectively (Rossi and Dirksen, 2006). In addition to the proteins, loss in phospholipid bilayer membrane integrity could also be a source of calcium leakage and affecting the functionality of the proteins anchored to the membrane (Rossi, et al., 2008). Phospholipase A2 (**PLA2**) is an ubiquitous enzymes that is activated by calcium resulting in phospholipid cleavage into lysophospholipids and free fatty acids release (Burke and Dennis, 2009). It is possible that one or more proteins/phospholipids are accountable for the alteration of SR functions, resulting in the accumulation of cytoplasmic free calcium. Therefore, the objective of this study was to utilize integrative omics (lipidomics/proteomics) approach to investigate the functionality/integrity of WB SR.

MATERIALS AND METHODS

Sample Collection, Fabrication and Preparation

Fourteen broiler breasts (*pectoralis major)* fillet samples were collected from a commercial processing facility that slaughters large broilers. All breasts samples were collected post-chill from the deboning line at approximately 3 h postmortem. The breasts were trimmed, weighed, and scored for woody breast and white striping at approximately 6 h postmortem. Each sample was assigned a normal, moderate or severe score for woody breast based on the degree of observable hardness and white striping based on prevalence and thickness of white striation on the surface of the fillet. Seven breasts that exhibited severe woody breast and white striping and seven breasts exhibiting zero signs of woody breast or white striping were selected for analysis. At 8 h postmortem, samples were vacuum package and stored at -20 ºC until shipped to Kansas State University Meat and Muscle Biology Laboratory.

All breast fillets were thawed in a refrigerator at 4°C for 24 h. The exudate (~10 mL) was collected from each sample for further analysis. A 1.9 cm strip across the cranial end of each fillet was fabricated, frozen in liquid nitrogen, pulverized using a blender (model 51BL32; Warring Commercial, Torring, CT) and stored at -80ºC until further analysis. The remainder of the breast fillet was repackaged and stored at -80ºC until further analysis.

Sarcoplasmic Reticulum (SR) Membrane Extraction

The SR membrane was extracted from muscle tissue according to the method described by Wilkie and Schirmer (2008) with modifications. Approximately 20 g of raw breast filet was cut into small 1 cm x 1 cm x 1 cm cubes and homogenized in 80 mL of ice-cold homogenization buffer (50 mM HEPES, 24 mM KCl, 5 mM $MgCl_2$ and 250 mM sucrose with 0.1% protease inhibitor (Halt Protease Inhibitor Sing-Use Cocktail (100X); Thermo Scientific, Waltham, MA) using a

hand-held homogenizer with 3 x 15 s bursts. Content was transferred into two separate 50 mL plastic centrifuge tube and centrifuged at 1000 × g for 10 min at 4ºC (Eppendorf centrifuge 5810 R, A-4-81 rotor; Eppendorf, Hamburg, Germany). The supernatant was filtered through four layers of cheesecloth into an 85 mL Nalgene high-speed centrifuge tube (Thermo Scientific). To pellet the mitochondria, the samples were centrifuged at 10,000 x g for 20 min at 4ºC (Eppendorf centrifuge 5810 R, F-34-6-38 rotor; Eppendorf). The supernatant was transferred to a 70 mL ultracentrifuge tube (part #355622; Beckman Coulter, Brea, CA) and centrifuged at 100,000 x g for 45 min at 4ºC (Optima XE-90 Ultracentrifuge, Type 45 Ti rotor; Beckman Coulter) to pellet the microsome. The supernatant was discarded, and the pellet was re-suspended in 7 mL of ice-cold homogenization buffer. Nineteen mL of ice-cold 2.8 M SHKM buffer (2.8 M sucrose, 50 mM HEPES, 25 mM KCl and 5 mM $MgCl_2$) was added to the sample, and the content was transferred to a 38 mL thin wall ultracentrifuge tube (part #344058; Beckman Coulter). In addition, seven mL ice-cold 1.85 M SHKM (1.85 M sucrose, 50 mM HEPES, 25 mM KCl and 5 mM $MgCl_2$) and three mL of ice-cold homogenization buffer was added to the same thin wall ultracentrifuge tube. The samples were centrifuged at 57,000 x g for 4 h at 4ºC (Optima XE-90 Ultracentrifuge, SW32 Ti rotor; Beckman Coulter) using the principle of density gradient centrifugation to move the less dense SR to the layer with less sucrose while pelleting the denser components of the microsome. The SR was removed from the interphase between the 1.85 M SHKM and homogenization buffer as shown in Figure 3.1 and transferred to a 32 mL thick wall ultracentrifuge tube (part #355631; Beckman Coulter). Twenty-five mL of ice-cold homogenization buffer was added, and the sample was centrifuged at 152,000 x g for 75 min at 4ºC (Optima XE-90 Ultracentrifuge, SW32 Ti rotor; Beckman Coulter). The supernatant was discarded, and the pellet was resuspended in 0.5 mL of homogenization buffer. Half of it was used for proteomic analysis, and the other half was used for

lipidomics analysis.

Protein Extraction

Microcentrifuge tubes containing the SR proteomic samples were centrifuged at 6,000 x g for 10 min at 4ºC (Eppendorf centrifuge 5810 R, F45-30-11 rotor; Eppendorf) to pellet the SR. The supernatant was discarded, and the pellet was resuspended and vortexed in 100 µL of 0.1% Triton X-100 in 1 X PBS and 150 µL of 8 M urea. The samples were centrifuged at 6,000 x g for 2 min at 4ºC to re-pellet the insoluble material. The supernatant was transferred to a new microcentrifuge tube, and the protein concentration was determined using a Pierce BCA protein assay kit (Thermo Fisher Scientific). The protein stock was stored at -80ºC until further analysis.

Shotgun Proteomics

The SR protein stock containing 50 µg of protein were reduced with the addition of 5 mM tris(2-carboxyethyl) phosphine for 30 min at RT. The reduced samples were further alkylated for 30 min in the dark at RT by the addition of 10 mM iodoacetamide. The solutions were diluted with 3 volumes of 100 mM Tris-HCl at pH 8.5 and digested by the addition of one µg/mL of trypsin/LysC (Promega, Madison, WI). After overnight digestion, an additional 0.5 µg/mL of trypsin/LysC were added and digested for another 6 h. Peptides were desalted by solid phase extraction using a C18 pipet tip (Pierce 87784; ThermoFisher) and eluted with 70:30:0.1 acetonitrile/water/trifluoroacetic acid.

Peptides were injected into an Acclaim PepMap RSLC nano-C18 column (2 µm C18 particles, 75 µm ID x 50 cm, ThermoFisher) in a vented trap configuration and separated using a gradient of 0.1% formic acid / acetonitrile (3-30 %) for 120 min. The peptides were eluted into a Nanospray Flex ion source coupled to an Orbitrap Fusion mass spectrometer (Thermo Scientific). The mass spectrometer was programmed to perform “Top-Speed” data-dependent

MS/MS using quadrupole filtration, HCD collision, and ion trap analysis of fragment ions.

Instrument RAW files were analyzed using MaxQuant v1.6.10.43 to compare observed ions of peptides and peptide fragments to a database of 27,542 Gallus gallus sequences downloaded from Uniprot on 01/19/20. The database searches utilized default MaxQuant settings, supplemented with the variable following modifications: oxidation of Met, N-terminal acetylation, and cyclization of Gln to pyro-glutamate.

Lipid Extraction

The SR lipid was extracted according to the method described by Bligh and Dyer (1959) with modifications. Two hundred and fifty µL of SR stock was transferred to a 13x100 mm glass tube, and 3.75 mL of 1:2 chloroform:methanol (v/v) was added. The samples were vortexed, capped and left to sit under the fume hood overnight. The next morning, 1.25 mL of chloroform was added and shaken for 1 min, followed by the addition of 1.25 mL of ultrapure water and shaken for another minute using a wrist action shaker (Model 75, Burrell, Pittsburgh, PA). Following shaking, the samples were centrifuged at 1,000 x g for 5 min (Eppendorf centrifuge 5810 R, A-4-62 rotor; Eppendorf). The aqueous phase was aspirated off, and the bottom layer was dried under nitrogen at 40ºC (REACTI-VAP III #TS-18826; Thermo Scientific). Finally, one ml of chloroform was added to redissolve the extracted lipid, and the content was transferred to a 1.8 ml glass vial with PTFE-lined cap and stored at -80 ºC until sample preparation.

Lipid Sample Preparation

Using a Hamilton syringe (Hamilton Co., Reno, NV), a predetermined volume of lipid stock in chloroform ranging from 4 to 13 µL, corresponding to approximately 2.5 µL diluted lipid in chloroform per mg of protein was transferred to an amber GC vial. Precise amounts of phospholipid internal standards were added to each vial in the following quantities: 0.66 nmol of

di14:0-phosphatidylcholine (**PC**), 0.66 nmol of di24:1-PC, 0.66 nmol of 13:0-lysophosphatidylcholine (**LPC**), 0.66 nmol of 19:0-LPC, 0.36 nmol of di14:0-phosphatidylethanolamine (**PE**), 0.36 nmol of di24:1-PE, 0.36 nmol of 14:0-lysophosphatidylethanolamine (**LPE**), 0.36 nmol of 18:0-lysoPE, 0.36 nmol of di14:0-PG, 0.36 nmol of di24:1- phosphatidylglycerol (**PG**), 0.36 nmol of 14:0- lysophosphatidylglycerol (**LPG**), 0.36 nmol of 18:0-LPG, 0.36 nmol of di14:0- phosphatidic acid (**PA**), 0.36 nmol of di20:0(phytanoyl)-PA, 0.24 nmol of di14:0- phosphatidylserine (**PS**), 0.24 nmol of di20:0(phytanoyl)-PS, 0.20 nmol of 16:0–18:0- phosphatidylinositol (**PI**), and 0.16 nmol of di18:0-PI. The sample and internal standard mixture in each vial were combined with solvent (chloroform: methanol: 300mM ammonium acetate in water, 300:665:35, v/v/v) for a final volume at 1.25 ml.

Electrospray Ionization (ESI)-Triple Quadrupole Mass Spectrometry

Lipidomics analysis of prepared lipid samples were analyzed at the Kansas Lipidomic Research Center (Kansas State University) through the methods described by Brügger, et al. (1997) and Welti, et al. (2002) with modifications. Using an autosampler (LC MiniPAL; CTC Analytics AG, Zwingen, Switzerland) fitted with the required injection loop for acquisition time, the samples were loaded by continuous infusion to the ESI source at 300 μL min^{-1} on a triple quadrupole MS/MS (Applied Biosystems API 4000, Foster City, CA). Scan speed was set to 100 μ sec^{-1}. The collision gas pressure was set at 2 (arbitrary units). The mass analyzers were adjusted to a resolution of 0.7 μ full width at half height. For each spectrum, 9 to 150 continuum scans were averaged in multiple channel analyzer (**MAC**) mode. The source temperature (heated nebulizer) was 100°C. The interface heater was on, and + 5.5 kV or – 4.5 kV was applied to the electrospray capillary. The collision gas was set at “low”. The curtain gas was set at 20 (arbitrary units), and

the two ion source gases were set at 45 (arbitrary units).

Each sample underwent a precursor and neutral loss scan to create a set of spectra with each spectrum exposing a set of lipid species containing a common head group or fatty acids fragment. The parameters used to detect phospholipid species were as described by Xiao, et al. (2010) particularly the intact ion analyzed, fragment type, scan mode, polarity, collision energy, declustering potentials, entrance potentials and exit potentials (Table 3.1). The sphingomyelin (SM) was determined from the same mass spectrum as PC and by comparison with PC internal standards using a conversion factor for SM in comparison with PC (determined experimentally to be 0.39). Ether-linked PCs and PEs (**ePCs** and **ePEs**) were determined in relation (less in masses compared to their ester-linked counterparts) to the same standards as other PC and PE species.

To adjust the spectrum, the background was subtracted to calculate the peak areas which were incorporated into a custom script in the Applied Biosystems Analyst software (Applied Biosystems). Within each phospholipid class, the lipid peak areas were uploaded to an online processing software for direct-infusion mass spectral data for lipid profile (LipidomDB Data Calculation Environment; (Zhou, et al., 2011)). Isotopic overlay, or the presence of a double bond creating a peak area >1, was corrected by the LipidomeDB software. A second peak of one species might generate a signal at the equivalent mass as the main peak of another more saturated lipid species. Hence, the signal from the second peak must be subtracted to determine the signal of the main peak. The signals produced by the internal standards were used to create a linear calibration curve (signal vs. mass/charge) that was used to rectify mass-dependent variation in instrument response. Last, the corrected signals were converted to nmol based on the signals from the 2 internal standards and the corresponding internal standard amounts indicated by the user (Zhou, et

al., 2011). Using the dried lipid weight for each sample, the lipid classes were normalized and recorded as nmol lipid class/mg lipid to compute the quantity of phospholipid. Data was also conveyed as mole percent (mol%); allocation of each phospholipid species in relative % of total phospholipid. This was accomplished by multiplying each nanomolar value by 100% and dividing by the total of the nanomolar amounts of the lipids analyzed.

Every 10 samples an "internal standards only" sample was introduced, and the mass spectra were obtained for these samples. These values were used to correct for chemical and instrumental noise in the rest of the samples. Any lipid metabolite discovered in the "internal standards only" samples was treated as contaminations and for the next 10 samples the molar amount of the lipid metabolite was subtracted to correct the molar amount of each lipid metabolite. Additionally, the eight QC samples prepared according to the details listed above were introduced to the system and the values for the first three QC samples were removed to account for prospective instrument variability. Data was removed if the lipid analytes variation (standard deviation divided by mean of the amount of the analyte in the QC) was >30%, leaving the final average variation being 2.5%. Finally, each evident lipid molecular species is exhibited as total acyl carbons: total double bonds.

Statistical Analysis

The Perseus software (v1.6.1.1) was used to analyze the label-free quantification (**LFQ**) protein intensities data files to perform t-tests with a random permutation false-discovery rate correction (**FDR**) set to 0.05 with an S0 factor of 0.1 to determine proteins with significant expression ($P<0.05$). Differences between protein intensities were validated with $\log_2$ transformed LQF protein intensities. Following statistical analysis, DAVID (v6.8, https://david.ncifcrf.gov/) software was utilized to classify gene ontology enrichment analysis of

the functional classes of the significantly abundant proteins. To analyze the lipidomic data, which included >100 phospholipid species identified, a SAS macro automatically completed the analyses repeatedly. Throughout the statistical analysis, only significant results ($P<0.05$) were reported and presented in this paper.

RESULTS AND DISCUSSION

Proteomics

With our unique objective focusing on understanding the calcium homeostasis process in chicken muscle, direct proteomic analysis of skeletal muscles posed a significant analytical challenge due to the high abundance of myofibrillar and stromal proteins (Deshmukh, et al., 2021). Therefore, we decided to maximize the detection effort by measuring the proteome of the SR. From the proteomics data, over 2,700 proteins were identified from the SR samples, with 677 proteins having significant differential expression ($P < 0.05$) between WB and N. Of those proteins demonstrating differential expression, 431 were up-regulated and 246 proteins were down-regulated in WB samples compare to N as demonstrated by the volcano plot where the red dots represent significantly different proteins and the gray dots as not significantly different proteins (Figure 3.2). The proteomics results are listed as Log2 fold changes, where a positive value indicates more expression in WB and a negative value more expression in N. Log2 fold change can be converted to fold change by taking 2 to the power of the Log2 fold change value. As demonstrated in many past SR proteomic studies (Babu, et al., 2004; Chu, et al., 2004; Liu, et al., 2013), our SR proteome coverage goes beyond proteins involved in calcium homeostasis including glycolysis/gluconeogenesis, aerobic respiration, and proteolysis. In order to achieve our objective, we will focus our effort to discuss the proteins involved in calcium regulation, stress response, membrane integrity, acetylcholinesterase activity and action potential regulation.

Table 3.2 displays a cluster of known proteins associated with SR that play significant roles in calcium regulation. Proteins involved in calcium transport were found to be upregulated 3.2 times greater in WB samples compared to N ($P<0.05$), with the most notable one being the sarcoplasmic/endoplasmic reticulum calcium ATPase 2 (**SERCA**). Soglia, et al., (2016) also observed a greater relative abundance of SERCA in WB compared to N samples. Other notable calcium pumps such as the calcium-transporting ATPase and plasma membrane calcium-transporting ATPase 1 were also found to be upregulated in WB compared to N samples. These proteins are responsible for the rapid removal of calcium from the sarcoplasm to induce muscle relaxation and to replenish calcium stores within the cell (Periasamy and Kalyanasundaram, 2007). On the other hand, a downregulation was observed for proteins responsible for calcium release in the WB compared to the N samples ($P <0.05$). Particularly, the ryanodine receptors (**RYR**) 2 and 3 were both downregulated 1.97 and 1.56 times less in WB samples respectively. Other proteins such as the calcium load-activated calcium channel and Junctophilin 1 are also downregulated in WB compared to N samples. These proteins are embedded in the plasma membrane and are responsible for the release of calcium from the SR during excitation-contraction coupling (Lanner, et al., 2010). Finally, no difference was found between WB and N for major calcium storage proteins such as calsequestrin and calmodulin ($P > 0.05$). However, an upregulation of sarcalumenin was observed for the WB samples compared to N ($P < 0.05$), which also serves a calcium storage function in striated muscle (Manring, et al., 2014; Papah, et al., 2018). These proteins exhibit strong affinity to calcium in the SR, so calcium can be stored and regulated for later contraction response (Walsh, 1983; Wang and Michalak, 2020).

There has been ample research linking calcium level imbalance to myopathies (Bellinger, et al., 2008; Chelu, et al., 2004). In the case of muscle cells failing to maintain calcium

homeostasis, Morel, et al. (2004) documented an upregulation of SERCA as the SR attempts to resequester more calcium from the sarcoplasm and a downregulation of RYRs as the SR decreases the calcium release rate in X-chromosome-linked muscular dystrophy mice or mxd mice used to study Duchenne muscular dystrophy. Meanwhile, no major modifications in calcium storage proteins were observed, so the storage capabilities for WB and N birds are likely unaltered from the myopathy. Duchenne muscular dystrophy has shown to reduce the expression of calcium storage proteins such as calsequestrin and calmodulin (Doran, et al., 2004; Pertille, et al., 2010). Calsequestrin is an endogenous regulator of the RYR complex via conformational changes (Ohkura, et al., 1998), so the unaltered/upregulation of calcium storage proteins in WB again indicates that there is no modification in RYR complex functionality. Therefore, the data suggested that the SR of WB birds is most likely functioning properly. The observed upregulation of calcium transport proteins in WB birds suggests that the SR may be compensating for the extra calcium in the sarcoplasm by increasing the protein synthesis of calcium transport proteins while decreasing the protein synthesis of calcium release proteins in attempt to maintain calcium homeostasis.

Table 3.3 provides a list of proteins found in this study that are related to endoplasmic reticulum (**ER**) stress response, protein disulfide-isomerase, protein disulfide-isomerase A3, protein disulfide-isomerase A4 and thioredoxin related transmembrane protein 4 were upregulated in the WB compared to N samples ($P<0.05$). In muscle tissue, the SR is a specialized form of the ER and is in charge of controlling calcium fluxes during the excitation-contraction coupling process and storage of calcium (Michalak and Opas, 2009; Villa, et al., 1993). Having increased expression of the ER stress proteins indicates that the ER/SR of WB meat may be undergoing stress factors attributed to localized hypoxia from poor vascularization

(Inagi, 2010; Mutryn, et al., 2015). When ER/SR endures stress, protein misfolding and aggregation of misfolded proteins have been documented to result in diseases such as cancer and neurodegeneration (Rao and Bredesen, 2004). Fortunately, the ER/SR has various stress response pathways that can be activated to combat protein misfolding. Protein disulfide isomerases combat ER/SR stress by rearranging and replacing disulfide bonds within misfolded proteins to correct the folding error (Gilbert, 1997), and thioredoxin related transmembrane protein 4 provides necessary quality control for ER/SR protein folding (Roth, et al., 2010).

Table 3.4 provides a list of proteins found in this study that are related to the membrane integrity of the SR, which points to potential membrane damage. The membrane of the SR is made up of a phospholipid bilayer in which multiple proteins are embedded, particularly those involved in translocating calcium (Toyoshima, 2009; Zhang, et al., 1997). Phospholipase A2 (**PLA2**) is a ubiquitous enzyme that hydrolyzes the phospholipids into lysophospholipids and can result in significant damage to the cell membranes (Diaz and Arm, 2003). In this study, we observed an upregulation of PLA2 in WB compared to the N samples ($P<0.05$) as observed in Mutryn, et al. (2015). Many inflammatory-mediated pathology research has revealed overactive PLA2 playing a role in the pathogenesis (Casale, et al., 2020). Increased activity of PLA2 is likely due to its response to an activating stimuli such as hormones, calcium mobilizing agents, oxidative stress or osmotic challenges (Lambert, et al., 2006; Rubio, et al., 2015). Interestingly, there have also been studies linking the production of reactive oxygen species (**ROS**) to the activation of PLA2 through the activation of mitogen-activate protein kinase cascades (Korbecki, et al., 2013). Many WB studies have noted increased levels of ROS, which is likely linked to the upregulation of PLA2 (Greene, et al., 2020; Xing, et al., 2021). Additionally, multiple PLA2 suppressor proteins such annexin A1, A2, A4 and A5 were significantly upregulated in the WB

samples ($P<0.05$). These proteins are responsible for inhibiting PLA2 activity (Buckland and Wilton, 2003; Kim, et al., 1994), which further confirmed our findings on the overexpression of PLA2 in this study.

Furthermore, annexin A6 and myoferlin, proteins involved in plasma membrane repair, have a significant upregulation for WB compared to N samples ($P<0.05$). When cells identify injury to the membrane, a plasma membrane repair system is activated (Boye and Nylandsted, 2016). Annexin A6 is a protein that is often recruited after membrane disruption and has been noted to be required for the repair process (Boye and Nylandsted, 2016). Another key protein, myoferlin, is responsible for aiding in membrane repair specifically via plasma membrane fusion during regeneration (Cipta and Patel, 2009). Overall, the results imply that the SR membrane is undergoing some level of damage from PLA2 hydrolysis, and other regulatory proteins are attempting to inhibit PLA2 activity, while the upregulation of membrane repair proteins demonstrated the cells effort to restore SR membrane integrity. However, it is possible that SR membrane has sustained enough damage from PLA2 hydrolysis, which could lead to calcium leakage from the SR.

Table 3.5 provides a list of key proteins involved in nerve impulse transmission, were upregulated in WB compared to N samples ($P<0.05$). It was brought to our attention that one specific protein, cholinesterase, had almost an eight-fold increase in WB compared to N ($P<0.05$). This protein exhibited the highest fold change of the proteomics data collected for this study. Cholinesterase is responsible for the breakdown of acetylcholine into choline and acetic acid (Quinn, 1987; Trang and Khandhar, 2020). The hydrolysis of acetylcholine plays a key role in muscle contraction as it terminates the action potential and begins the membrane repolarization process, which allows for the relaxation of muscle (Colovic, et al., 2013).

Upregulation of cholinesterase is often associated with neurodegenerative disorders such as dementia (Yang, et al., 2020) specifically Alzheimer's (McGleenon, et al., 1999) and Parkinson's disease (Ruberg, et al., 1986) as well as cell apoptosis (Jiang and Zhang, 2008). Multiple studies have also observed increased cholinesterase expression due to a disturbance in calcium homeostasis, particularly with elevated cytoplasmic calcium levels (Bursztajn, et al., 1991; Houenou, et al., 1993; Sberna, et al., 1997). This is of interest to the current study as WB is known to have higher levels of sarcoplasmic calcium compared to N birds. Additionally, there are many reversible/irreversible cholinesterase inhibitors such as organophosphorus insecticides (Colovic, et al., 2013) can also result in the dramatic upregulation of cholinesterase (Fulton and Key, 2001; Ranjbar, et al., 2002; Trang and Khandhar, 2020). With such unique data found in this study, we hypothesize there may be cholinesterase inhibitors present within the system, resulting in the increase production of cholinesterase in WB birds to combat the inhibitors to prevent the prolonged calcium release from the SR.

Additionally, there is a significant upregulation of the proteins guanine nucleotide binding protein (G- protein) G11 alpha-subunit and G-protein, q polypeptide that participate in G-protein coupled acetylcholine receptor signaling pathways for the WB samples ($P<0.05$). The main function of these proteins is the transmission of chemical signals across the membrane, which occurs by the binding of guanosine triphosphate (**GTP**) to induce a conformational change leading to the activation of phospholipase C (Oldham and Hamm, 2008), which signals to the SR to release calcium and elevating the sarcoplasmic calcium level (Alvarez-Curto, et al., 2016; Putney and Tomita, 2012). Wagner, et al. (2010) found that knockout G- protein G11 alpha-subunit and G-protein q polypeptide mice had shorter action potential compared to the wild type. Therefore, the observed upregulation for the proteins related to G-protein coupled acetylcholine

receptor signaling pathway in this study could translate into prolonged action potential leading to potentially more calcium release from the SR. On the other hand, one protein, synaptophysin-like protein 2 (**SYPL2**), was found to be downregulated in WB compared to the N samples (Table 3.5; $P<0.05$). The main function of this protein is to maintain calcium homeostasis as it controls calcium release via communication between the T-tubule and the junctional SR membrane (Kurebayashi, et al., 2003; Woo, et al., 2015). Papah, et al. (2018) also noted a downregulation of SYPL2 in WB meat and attributed this phenomenon to excitation-contraction coupling disruption and alteration of calcium homeostasis. In combination with the downregulation of RYR found in this study, it appears that the WB SR is regulating calcium homeostasis by withholding calcium release from the SR.

Table 3.6 shows a list of proteins found in this study that are related to membrane polarization. Action potential is a process that is driven by a change in the polarity of the plasma membrane by the movement of potassium and sodium ions (Chen and Lui, 2019). This is first accomplished by depolarization in which sodium enters the cell causing the membrane potential to become positive. Then repolarization occurs when potassium exits the cell, which returns the membrane potential to negative (Grider, et al., 2019). In this study, we found that the sodium voltage-gated channel beta subunit 2 (**SCN2B**) was downregulated in WB samples, and there was a significant upregulation for potassium channel tetramerization domain containing 12 (**KCTD12**) in WB samples ($P < 0.05$). The SCN2B protein encodes the β2 subunit of the sodium voltage gated channel which is an auxiliary subunit responsible for regulating the gating, kinetics, and expression in the plasma membrane (Bouza and Isom, 2017). As for KCTD12, this protein is an auxiliary subunit of the gamma-aminobutyric acid type B (**GABA-B**) receptor and regulates the signaling of GABA-B as well as aid in rapid desensitization (Zuo, et al., 2019).

Moreover, there was an upregulation for proteins involved in electrochemical gradient homeostasis such as Sodium/potassium-transporting ATPase subunit alpha1 (**ATP1A1**) and beta3 (**ATP1B3**) ($P < 0.05$). The sodium/potassium-transporting ATPase is responsible for the extraction of sodium ions and insertion of potassium ion into the cell via ATP hydrolysis to maintain sodium and potassium ion concentration gradients across the plasma membrane (Blanco, 2005; Holm and Lykke-Hartmann, 2016). ATP1A1 establishes and maintains ion electrochemical gradients of sodium and potassium across the cell membrane (Lin, et al., 2021), and ATP1B3 acts as part of the regulatory subunit of the sodium/potassium-transporting ATPase (Zheng, et al., 2020).

These findings are interesting as the reduced expression of SCNB2 indicated the muscle cells are limiting the amount of sodium ions entering the cell, making it difficult for action potential to fire. Chen, et al. (2002) used SCN2B deficient mice and observed abnormal excitability and action potential conduction, particularly a reduction in sodium current density and increased threshold for action potential generation. This is of concern because if the threshold level is not met, action potential will not fire. Additionally, upregulation of KCTD12 has been shown to accelerate the kinetics of GABA in human cells (Li, et al., 2017). The GABA-B receptors are inhibitory neurotransmitter receptors that causes hyperpolarization, which in turn activates inward rectifying potassium channels that encourage the uptake of potassium ions to return the membrane potential to back to resting (Evenseth, et al., 2020; Zheng, et al., 2019). The stage of hyperpolarization signifies the end of the action potential, but it reduces electrical membrane excitability because another action potential cannot be generated under these conditions (Biga, et al., 2020). Based on this information, it appears WB birds could be altering the expression of these proteins as a corrective action to reduce action potential firing and

encourage termination to combat extended action potential and increased calcium release. The upregulation of the sodium/potassium-transporting ATPase may also play a role by attempting to maintain the electrochemical gradient of WB muscle cell membrane.

Lipidomics

The ESI MS/MS characterized 352 different polar lipid species in chicken breast SR with the major lipid classes identified being LPC, PC, ePC, SM, LPE, PE, ePE, PI and PS . Sixty-six of those identified lipid species were significantly different ($P < 0.05$) between WB and N samples. Figure 3.3 displays the mol% of the SR phospholipid classes for WB and N samples. There was less PC and ePC and more PE and PS in WB compared to N SR ($P<0.05$). The decrease of PC mol % in WB SR is largely due to the decrease of PC 34:1, 36:3, 36:4 and 38:5 (Figure 3.4A; $P<0.05$). The ePC mol % followed a similar trend as the PC, in which mol % for ePC 36:4, 36:5, 38:4, 38:5 and 38:6 were reduced for WB SR compared to N (Figure 3.4B; $P<0.05$). For both PC and ePC, there was in increase in mol% for 32:0 for WB SR (Figure 3.4A & 3.4B; $P<0.05$). Elevated levels of PE in WB SR is due to the mol % increase in PE 34:1, 36:1, 36:2 and 40:4 (Figure 3.4C; $P<0.05$). The higher PS mol % in WB SR is mainly caused by an increase in mol% of PS 36:1 (Figure 3.4D; $P<0.05$).

Like other cell membrane, SR membrane contains many proteins embedded within that function to transport of molecules across the membrane (Bennett, et al., 1980). Disturbance of the phospholipid structure can alter the integrity of the membrane (Li, et al., 2006) and trigger ER/SR stress (Fu, et al., 2011). Investigating the phospholipid profile of the SR not only allow us to investigate membrane integrity, but also the functionality modifications contributing to the additional calcium release of WB SR. Unfortunately, there is little research focused directly on

the phospholipid profile of WB meat, and the current study is the first to utilize cutting edge lipidomics to characterize the SR phospholipid bilayer of WB birds.

The main structural component of membranes is PC, and it is the major phospholipid class that makes up mammalian cell membranes (Kanno, et al., 2007). Mouchlis, et al. (2018) found that PLA2 exhibited greater activity toward PC over other phospholipid classes, which explained the decrease in both PC and ePC classes, but not in other phospholipid classes. Vu, et al. (2015) found that phospholipids are particularly sensitive to hydrolysis by the PLA2 when the cells are undergoing stress response, which is further supported by the fact that PLA2 was upregulated in WB compared to the N samples as described earlier. The phospholipid class PC can be further divided into two groups. One is the traditional PC that contains an ester bond between the glycerol backbone and fatty acid side chains, and the other one is ePC which contains an ether bond instead of ester bond (da Silva, et al., 2012). It has also been shown that decreased ether lipid synthesis is linked to multiple metabolic abnormalities such as type 1 diabetes (Dean and Lodhi, 2018). In addition, Dorninger, et al. (2020) suggested ether-linked phospholipids may have the ability to influence signal transduction pathways by altering the function of plasma membrane receptors. Acetylcholine receptors were found to be upregulated in WB meat in this study. Perhaps, the reduction of ePC for WB samples is an indication of metabolic abnormalities and resulted in dysfunctionality in the signaling cascades. Finally, Chun et al. (2021) found similar lipidomic results in an *in vitro* PLA2 liposome study, which they also found a decrease in 36:3, 36:4 and 36:5 due to PLA2 hydrolysis that are consistent with the results from the current study.

The second most abundant phospholipid in mammalian cells is PE and is particularly concentrated in the inner membrane of the cell (Vance, 2015). This phospholipid class plays a

role in autophagy, cell division and protein folding (Farine, et al., 2015), and is a non-bilayer forming phospholipid, which functions to stimulate tight packing of membrane bilayer forming phospholipids such as PC (Calzada, et al., 2016). Due to the organizational structure of PE, it can also serve to stabilize membrane proteins and protein complexes within the bilayer (Farine and Bütikofer, 2013). Interestingly, many studies have found a high PC:PE ratio contributes to reduced SERCA activity (Fajardo, et al., 2018; Fu, et al., 2011; van der Veen, et al., 2017). In this current study, we found lower PC:PE ratio for WB compared to N, which coincided with the upregulation of SERCA proteins in WB samples as found in our proteomic data. More specifically, we observed increases in PE 36:2 and 40:4. Chun et al. (2021) found that PE 36:2 is almost exclusively 18:0/18:2, and PE 40:4 is likely a combination of 20:0/20:4 using product ion analysis methodology. Both 18:2 and 20:4 are omega 6 fatty acids that are characterized by their pro-inflammatory response (McNamara, et al., 2010; Yadav, et al., 2018). Increased inflammation has been observed in WB birds (Xing, et al., 2021; Young and Rasmussen, 2020), and the increase in the omega 6 fatty acids found in these PE species may be contributing to this phenomenon. It is interesting to note that PLA2 is well known to be highly selective for 18:2 and 20:4 containing phospholipid molecular species (Burdge, et al., 1995). Additionally, Patel and Witt (2017) showed that excess PE species with polyunsaturated acyl chains such as 20:4 and 22:4 in the ER membrane can trigger the formation of hydroperoxides and induce cell apoptosis. Hydroperoxides in lipids can be deleterious to cells because they have the ability to disrupt the structure and function of the membrane (Girotti, 1998). In the current study, the PE data shows WB SR to have more 20:4 indicating WB cells membranes could be suffering from distress.

The main anionic phospholipid is PS, typically enriched in the plasma membrane of neural tissue (Kim, et al., 2014). In order to synthesize PS, a calcium-dependent reactions must

occur to convert PC or PE into PS by replacing the head group with a serine (Vance and Vance, 2004). This reaction is catalyzed by enzymes such as phosphatidylserine synthase 1 and phosphatidylserine synthase 2 (Kim, et al., 2014). However, our proteomic data indicated a downregulation of phosphatidylserine synthase 1 for the WB samples ($P<0.05$; data not shown). This may be the muscle cells way to compensate for the overproduction of PS due to the high calcium levels found in WB samples. Chao, et al. (2020) also noted an increase in relative percentage of PS 36:1 in extended aged pork loins. Unlike PC, PS has been demonstrated to be resistant to PLA2 enzyme hydrolysis (Astudillo, et al., 2019). Perhaps, the high sarcoplasmic calcium level in WB and PS's ability to resist phospholipase hydrolysis both contributed to the increase in the relative percentage of PS for WB samples.

Figure 3.5 provides the mol% for phospholipid hydrolysis products LPC and LPE, where WB had significantly more total LPC compared to N samples ($P<0.05$). The WB SR had greater LPC mainly due to an increase in mol% for LPC 16:0 and 18:1 (Figure 3.6; $P<0.05$). Due to PLA2 activity, LPC is derived from the cleaving of PC (Law, et al., 2019). Chun et al. (2021) also found an increase in the mol % of LPC 16:0 and 18:1 when phospholipids were incubated with PLA2. Our findings on the LPC is further supported by the previously discussed proteomics data on the upregulation of PLA2 in WB samples. Furthermore, PLA2 activity is calcium-dependent (Murakami and Kudo, 2002), and WB has been consistently shown to have elevated levels of calcium in our and many other studies (Soglia, et al., 2016; Soglia, et al., 2018; Tasoniero, et al., 2016). Therefore, we hypothesize that the high calcium level in WB meat may lead to the increase in PLA2 activity resulting in SR membrane phospholipid hydrolysis. This membrane integrity damage could play a role in the increased calcium release from the SR and

potentially affect the function of the proteins embedded in the SR membrane (Cournia, et al., 2015).

CONCLUSION

The elevated levels of calcium found in WB meat is an issue of concern that could potentially play a role in the mechanism behind WB texture abnormalities. Our data indicated WB SR proteins are likely functioning properly and attempting to mitigate the noted calcium imbalance. However, there are noted alterations to the phospholipid membrane composition and increased lipid catabolism in the WB SR, which could be contributing to increased calcium release due to a compromised structure. Finally, the significant upregulation of cholinesterase suggested there may be a source of cholinesterase inhibitors preventing the breakdown of acetylcholine and delaying the termination of action potential. If action potential is prolonged, more calcium would be expected to be released from the SR and could aid in explaining the high calcium levels observed in WB. While the current study provided some novel data and shed light into the functionality of the SR of WB meat, ample of unknowns remain, which warrant further investigation to fully understand the cause of elevated calcium level in WB meat.

REFERENCES

Abasht, B., M. F. Mutryn, R. D. Michalek, and W. R. Lee. 2016. Oxidative stress and metabolic perturbations in wooden breast disorder in chickens. PloS one 11:e0153750.

Alvarez-Curto, E., A. Inoue, L. Jenkins, S. Z. Raihan, R. Prihandoko, A. B. Tobin, and G. Milligan. 2016. Targeted elimination of G proteins and arrestins defines their specific contributions to both intensity and duration of G protein-coupled receptor signaling. Journal of Biological Chemistry 291:27147-27159.

Astudillo, A. M., M. A. Balboa, and J. Balsinde. 2019. Selectivity of phospholipid hydrolysis by phospholipase A2 enzymes in activated cells leading to polyunsaturated fatty acid mobilization. Biochimica et Biophysica Acta (BBA)-Molecular and Cell Biology of Lipids 1864:772-783.

Babu, G. J., D. Wheeler, O. Alzate, and M. Periasamy. 2004. Solubilization of membrane proteins for two-dimensional gel electrophoresis: identification of sarcoplasmic reticulum membrane proteins. Analytical biochemistry 325:121-125.

Bellinger, A. M., M. Mongillo, and A. R. Marks. 2008. Stressed out: the skeletal muscle ryanodine receptor as a target of stress. The Journal of clinical investigation 118:445-453.

Bennett, J., K. McGill, and G. Warren. 1980. The role of lipids in the functioning of a membrane protein: the sarcoplasmic reticulum calcium pump. Pages 127-164 in Current topics in membranes and transportElsevier.

Biga, L. M., S. Dawson, A. Harwell, R. Hopkins, J. Kaufmann, M. LeMaster, P. Matern, K. Morrison-Graham, D. Quick, and J. Runyeon. 2020. Anatomy & physiology.

Blanco, G. Year. Na, K-ATPase subunit heterogeneity as a mechanism for tissue-specific ion regulation. Proc. Seminars in nephrology.

Bligh, E. G., and W. J. Dyer. 1959. A rapid method of total lipid extraction and purification. Canadian journal of biochemistry and physiology 37:911-917.

Bouza, A. A., and L. L. Isom. 2017. Voltage-gated sodium channel β subunits and their related diseases. Voltage-Gated Sodium Channels: Structure, Function and Channelopathies:423-450.

Boye, T. L., and J. Nylandsted. 2016. Annexins in plasma membrane repair. Biological chemistry 397:961-969.

Brügger, B., G. Erben, R. Sandhoff, F. T. Wieland, and W. D. Lehmann. 1997. Quantitative analysis of biological membrane lipids at the low picomole level by nano-electrospray ionization tandem mass spectrometry. Proceedings of the National Academy of Sciences 94:2339-2344.

Buckland, A. G., and D. C. Wilton. 2003. Annexins and phospholipases. Annexins. Kluwer Academic/Plenum, London:207-217.

Burdge, G. C., A. Creaney, A. D. Postle, and D. C. Wilton. 1995. Mammalian secreted and cytosolic phospholipase A2 show different specificities for phospholipid molecular species. The international journal of biochemistry & cell biology 27:1027-1032.

Burke, J. E., and E. A. Dennis. 2009. Phospholipase A2 structure/function, mechanism, and signaling. Journal of lipid research 50:S237-S242.

Bursztajn, S., L. W. Schneider, Y.-J. Jong, and S. A. Berman. 1991. Calcium and ionophore A23187 stimulates deposition of extracellular matrix and acetylcholinesterase release in cultured myotubes. Cell and tissue research 265:95-103.

Caldas-Cueva, J. P., and C. M. Owens. 2020. A review on the woody breast condition, detection

methods, and product utilization in the contemporary poultry industry. Journal of Animal Science 98:skaa207.

Calzada, E., O. Onguka, and S. M. Claypool. 2016. Phosphatidylethanolamine metabolism in health and disease. International review of cell and molecular biology 321:29-88.

Casale, J., S. E. O. Kacimi, and M. Varacallo. 2020. Biochemistry, phospholipase A2. StatPearls [Internet].

Chao, M., E. Donaldson, W. Wu, A. Welter, T. O'Quinn, W.-W. Hsu, M. Schulte, and S. Lonergan. 2020. Characterizing membrane phospholipid hydrolysis of pork loins throughout three aging periods. Meat science 163:108065.

Chelu, M. G., C. I. Danila, C. P. Gilman, and S. L. Hamilton. 2004. Regulation of ryanodine receptors by FK506 binding proteins. Trends in cardiovascular medicine 14:227-234.

Chen, C., V. Bharucha, Y. Chen, R. E. Westenbroek, A. Brown, J. D. Malhotra, D. Jones, C. Avery, P. J. Gillespie, and K. A. Kazen-Gillespie. 2002. Reduced sodium channel density, altered voltage dependence of inactivation, and increased susceptibility to seizures in mice lacking sodium channel β2-subunits. Proceedings of the National Academy of Sciences 99:17072-17077.

Chen, I., and F. Lui. 2019. Neuroanatomy, neuron action potential.

Chu, G., J. P. Kerr, B. Mitton, G. F. Egnaczyk, J. A. Vazquez, M. Shen, G. W. Kilby, T. I. Stevenson, J. E. Maggio, and J. Vockley. 2004. Proteomic analysis of hyperdynamic mouse hearts with enhanced sarcoplasmic reticulum calcium cycling. The FASEB journal 18:1725-1727.

Chun, C., R. Welti, M. R. Roth, M. Richards, and M. Chao. Year. Exploring the Potential Effect

of Anti-Phospholipase A2 Antibody to Extend Beef Shelf-life in a Beef Liposome Model System. Proc. 74th Reciprocal Meat Conference Proceedings. August 15th-18th, Reno, Nevada.

Cipta, S., and H. H. Patel. 2009. Molecular bandages: Inside-out, outside-in repair of cellular membranes. Focus on “myoferlin is critical for endocytosis in endothelial cells”American Physiological Society Bethesda, MD.

Colovic, M. B., D. Z. Krstic, T. D. Lazarevic-Pasti, A. M. Bondzic, and V. M. Vasic. 2013. Acetylcholinesterase inhibitors: pharmacology and toxicology. Current neuropharmacology 11:315-335.

Cournia, Z., T. W. Allen, I. Andricioaei, B. Antonny, D. Baum, G. Brannigan, N.-V. Buchete, J. T. Deckman, L. Delemotte, and C. Del Val. 2015. Membrane protein structure, function, and dynamics: a perspective from experiments and theory. The Journal of membrane biology 248:611-640.

da Silva, T. F., V. F. Sousa, A. R. Malheiro, and P. Brites. 2012. The importance of ether-phospholipids: a view from the perspective of mouse models. Biochimica et Biophysica Acta (BBA)-Molecular Basis of Disease 1822:1501-1508.

de Brot, S., S. Perez, H. Shivaprasad, K. Baiker, L. Polledo, M. Clark, and L. Grau-Roma. 2016. Wooden breast lesions in broiler chickens in the UK. The Veterinary Record 178:141.

Dean, J. M., and I. J. Lodhi. 2018. Structural and functional roles of ether lipids. Protein & cell 9:196-206.

Deshmukh, A., D. Steenberg, M. Hostrup, J. Birk, J. Larsen, A. Santos, R. Kjøbsted, J. Hingst,

C. Schéele, and M. Murgia. 2021. Deep muscle-proteomic analysis of freeze-dried human muscle biopsies reveals fiber type-specific adaptations to exercise training. Nature communications 12:1-15.

Diaz, B. L., and J. P. Arm. 2003. Phospholipase A2. Prostaglandins, leukotrienes and essential fatty acids 69:87-97.

Doran, P., P. Dowling, J. Lohan, K. McDonnell, S. Poetsch, and K. Ohlendieck. 2004. Subproteomics analysis of Ca2+-binding proteins demonstrates decreased calsequestrin expression in dystrophic mouse skeletal muscle. European Journal of Biochemistry 271:3943-3952.

Dorninger, F., S. Forss-Petter, I. Wimmer, and J. Berger. 2020. Plasmalogens, platelet-activating factor and beyond–Ether lipids in signaling and neurodegeneration. Neurobiology of disease:105061.

Dridi, S., and M. Kidd. 2016. Molecular pathways involved in amino acid and phosphorous utilization. Ch 8:119-128.

Ertbjerg, P., and E. Puolanne. 2017. Muscle structure, sarcomere length and influences on meat quality: A review. Meat science 132:139-152.

Evenseth, L. S. M., M. Gabrielsen, and I. Sylte. 2020. The GABAB Receptor—Structure, Ligand Binding and Drug Development. Molecules 25:3093.

Fajardo, V. A., J. S. Mikhaeil, C. F. Leveille, A. R. Tupling, and P. J. LeBlanc. 2018. Elevated whole muscle phosphatidylcholine: phosphatidylethanolamine ratio coincides with reduced SERCA activity in murine overloaded plantaris muscles. Lipids in health and disease 17:1-8.

Farine, L., and P. Bütikofer. 2013. The ins and outs of phosphatidylethanolamine synthesis in

Trypanosoma brucei. Biochimica et biophysica acta (BBA)-molecular and cell biology of lipids 1831:533-542.

Farine, L., M. Niemann, A. Schneider, and P. Bütikofer. 2015. Phosphatidylethanolamine and phosphatidylcholine biosynthesis by the Kennedy pathway occurs at different sites in Trypanosoma brucei. Scientific reports 5:1-11.

Fu, S., L. Yang, P. Li, O. Hofmann, L. Dicker, W. Hide, X. Lin, S. M. Watkins, A. R. Ivanov, and G. S. Hotamisligil. 2011. Aberrant lipid metabolism disrupts calcium homeostasis causing liver endoplasmic reticulum stress in obesity. Nature 473:528-531.

Fulton, M. H., and P. B. Key. 2001. Acetylcholinesterase inhibition in estuarine fish and invertebrates as an indicator of organophosphorus insecticide exposure and effects. Environmental Toxicology and Chemistry: An International Journal 20:37-45.

Gilbert, H. F. 1997. Protein disulfide isomerase and assisted protein folding. Journal of Biological Chemistry 272:29399-29402.

Girotti, A. W. 1998. Lipid hydroperoxide generation, turnover, and effector action in biological systems. Journal of lipid research 39:1529-1542.

Greene, E., R. Cauble, A. E. Dhamad, M. T. Kidd, B. Kong, S. M. Howard, H. F. Castro, S. R. Campagna, M. Bedford, and S. Dridi. 2020. Muscle metabolome profiles in woody breast-(un) affected broilers: Effects of Quantum Blue phytase-enriched diet. Frontiers in veterinary science 7:458.

Grider, M. H., R. Jessu, and C. S. Glaubensklee. 2019. Physiology, action potential.

Holm, T. H., and K. Lykke-Hartmann. 2016. Insights into the pathology of the α3 Na+/K+-ATPase ion pump in neurological disorders; lessons from animal models. Frontiers in physiology 7:209.

Houenou, L. J., M. V. Sahuqué, and A. P. Villageois. 1993. Calcium influxes and calmodulin modulate the expression and physicochemical properties of acetylcholinesterase molecular forms during developmentin vivo. Cellular and molecular neurobiology 13:217-232.

Inagi, R. 2010. Endoplasmic reticulum stress as a progression factor for kidney injury. Current opinion in pharmacology 10:156-165.

Jiang, H., and X. J. Zhang. 2008. Acetylcholinesterase and apoptosis: a novel perspective for an old enzyme. The FEBS journal 275:612-617.

Kanno, K., M. K. Wu, E. F. Scapa, S. L. Roderick, and D. E. Cohen. 2007. Structure and function of phosphatidylcholine transfer protein (PC-TP)/StarD2. Biochimica et Biophysica Acta (BBA)-Molecular and Cell Biology of Lipids 1771:654-662.

Kim, H.-Y., B. X. Huang, and A. A. Spector. 2014. Phosphatidylserine in the brain: metabolism and function. Progress in lipid research 56:1-18.

Kim, K. M., D. K. Kirn, Y. M. Park, C.-K. Kim, and D. S. Na. 1994. Annexin-I inhibits phospholipase A2 by specific interaction, not by substrate depletion. FEBS letters 343:251-255.

Koohmaraie, M. Year. The role of endogenous proteases in meat tenderness. Proc. Proc. Recip. Meat Conf.

Korbecki, J., I. Baranowska-Bosiacka, I. Gutowska, and D. Chlubek. 2013. The effect of reactive oxygen species on the synthesis of prostanoids from arachidonic acid. J Physiol Pharmacol 64:409-421.

Kurebayashi, N., H. Takeshima, M. Nishi, T. Murayama, E. Suzuki, and Y. Ogawa. 2003.

Changes in Ca2+ handling in adult MG29-deficient skeletal muscle. Biochemical and biophysical research communications 310:1266-1272.

Kuttappan, V., B. Hargis, and C. Owens. 2016. White striping and woody breast myopathies in the modern poultry industry: a review. Poultry Science 95:2724-2733.

Kuttappan, V. A., W. Bottje, R. Ramnathan, S. D. Hartson, C. N. Coon, B.-W. Kong, C. M. Owens, M. Vazquez-Añon, and B. M. Hargis. 2017. Proteomic analysis reveals changes in carbohydrate and protein metabolism associated with broiler breast myopathy. Poultry science 96:2992-2999.

Lambert, I., S. Pedersen, and K. Poulsen. 2006. Activation of PLA2 isoforms by cell swelling and ischaemia/hypoxia. Acta Physiologica 187:75-85.

Lanner, J. T., D. K. Georgiou, A. D. Joshi, and S. L. Hamilton. 2010. Ryanodine receptors: structure, expression, molecular details, and function in calcium release. Cold Spring Harbor perspectives in biology 2:a003996.

Law, S.-H., M.-L. Chan, G. K. Marathe, F. Parveen, C.-H. Chen, and L.-Y. Ke. 2019. An updated review of lysophosphatidylcholine metabolism in human diseases. International journal of molecular sciences 20:1149.

Lee, S., F. Norheim, H. L. Gulseth, T. M. Langleite, A. Aker, T. E. Gundersen, T. Holen, K. I. Birkeland, and C. A. Drevon. 2018. Skeletal muscle phosphatidylcholine and phosphatidylethanolamine respond to exercise and influence insulin sensitivity in men. Scientific reports 8:1-12.

Li, M., C. J. Milligan, H. Wang, A. Walker, L. Churilov, A. J. Lawrence, C. A. Reid, S. C. Hopkins, and S. Petrou. 2017. KCTD12 modulation of GABA (B) receptor function. Pharmacology research & perspectives 5.

Li, Z., L. B. Agellon, T. M. Allen, M. Umeda, L. Jewell, A. Mason, and D. E. Vance. 2006. The ratio of phosphatidylcholine to phosphatidylethanolamine influences membrane integrity and steatohepatitis. Cell metabolism 3:321-331.

Lin, Z., J. Li, T. Ji, Y. Wu, K. Gao, and Y. Jiang. 2021. ATP1A1 de novo mutation-related disorders: clinical and genetic features. Frontiers in Pediatrics 9:329.

Liu, Z., X. Du, C. Yin, and Z. Chang. 2013. Shotgun proteomic analysis of sarcoplasmic reticulum preparations from rabbit skeletal muscle. Proteomics 13:2335-2338.

Manring, H., E. Abreu, L. Brotto, N. Weisleder, and M. Brotto. 2014. Novel excitation-contraction coupling related genes reveal aspects of muscle weakness beyond atrophy—new hopes for treatment of musculoskeletal diseases. Frontiers in physiology 5:37.

McGleenon, B., K. Dynan, and A. Passmore. 1999. Acetylcholinesterase inhibitors in Alzheimer's disease. British journal of clinical pharmacology 48:471.

McNamara, R. K., R. Jandacek, T. Rider, P. Tso, A. Cole-Strauss, and J. W. Lipton. 2010. Omega-3 fatty acid deficiency increases constitutive pro-inflammatory cytokine production in rats: relationship with central serotonin turnover. Prostaglandins, Leukotrienes and Essential Fatty Acids (PLEFA) 83:185-191.

Michalak, M., and M. Opas. 2009. Endoplasmic and sarcoplasmic reticulum in the heart. Trends in cell biology 19:253-259.

Morel, J.-L., L. Rakotoarisoa, L. H. Jeyakumar, S. Fleischer, C. Mironneau, and J. Mironneau. 2004. Decreased expression of ryanodine receptors alters calcium-induced calcium release mechanism in mdx duodenal myocytes. Journal of Biological Chemistry 279:21287-21293.

Mouchlis, V. D., Y. Chen, J. A. McCammon, and E. A. Dennis. 2018. Membrane allostery and

unique hydrophobic sites promote enzyme substrate specificity. Journal of the American Chemical Society 140:3285-3291.

Murakami, M., and I. Kudo. 2002. Phospholipase A2. The journal of biochemistry 131:285-292.

Mutryn, M. F., E. M. Brannick, W. Fu, W. R. Lee, and B. Abasht. 2015. Characterization of a novel chicken muscle disorder through differential gene expression and pathway analysis using RNA-sequencing. BMC genomics 16:399.

Ohkura, M., K.-I. Furukawa, H. Fujimori, A. Kuruma, S. Kawano, M. Hiraoka, A. Kuniyasu, H. Nakayama, and Y. Ohizumi. 1998. Dual regulation of the skeletal muscle ryanodine receptor by triadin and calsequestrin. Biochemistry 37:12987-12993.

Ohlendieck, K. 2013. The pathophysiological role of impaired calcium handling in muscular dystrophy in Madame Curie Bioscience Database [Internet]Landes Bioscience.

Oldham, W. M., and H. E. Hamm. 2008. Heterotrimeric G protein activation by G-protein-coupled receptors. Nature reviews Molecular cell biology 9:60-71.

Papah, M. B., E. M. Brannick, C. J. Schmidt, and B. Abasht. 2018. Gene expression profiling of the early pathogenesis of wooden breast disease in commercial broiler chickens using RNA-sequencing. PLoS One 13:e0207346.

Patel, D., and S. N. Witt. 2017. Ethanolamine and phosphatidylethanolamine: partners in health and disease. Oxidative medicine and cellular longevity 2017.

Periasamy, M., and A. Kalyanasundaram. 2007. SERCA pump isoforms: their role in calcium transport and disease. Muscle & Nerve: Official Journal of the American Association of Electrodiagnostic Medicine 35:430-442.

Pertille, A., C. L. T. De Carvalho, C. Y. Matsumura, H. S. Neto, and M. J. Marques. 2010.

Calcium-binding proteins in skeletal muscles of the mdx mice: potential role in the pathogenesis of Duchenne muscular dystrophy. International journal of experimental pathology 91:63-71.

Petracci, M., S. Mudalal, F. Soglia, and C. Cavani. 2015. Meat quality in fast-growing broiler chickens. World's Poultry Science Journal 71:363-374.

Putney, J. W., and T. Tomita. 2012. Phospholipase C signaling and calcium influx. Advances in biological regulation 52:152.

Quinn, D. M. 1987. Acetylcholinesterase: enzyme structure, reaction dynamics, and virtual transition states. Chemical reviews 87:955-979.

Ranjbar, A., P. Pasalar, and M. Abdollahi. 2002. Induction of oxidative stress and acetylcholinesterase inhibition in organophosphorous pesticide manufacturing workers. Human & experimental toxicology 21:179-182.

Rao, R. V., and D. E. Bredesen. 2004. Misfolded proteins, endoplasmic reticulum stress and neurodegeneration. Current opinion in cell biology 16:653-662.

Ren, X., G. D. Lamb, and R. M. Murphy. 2019. Distribution and activation of matrix metalloproteinase-2 in skeletal muscle fibers. American Journal of Physiology-Cell Physiology 317:C613-C625.

Rossi, A. E., and R. T. Dirksen. 2006. Sarcoplasmic reticulum: the dynamic calcium governor of muscle. Muscle & Nerve: Official Journal of the American Association of Electrodiagnostic Medicine 33:715-731.

Rossi, D., V. Barone, E. Giacomello, V. Cusimano, and V. Sorrentino. 2008. The sarcoplasmic reticulum: an organized patchwork of specialized domains. Traffic 9:1044-1049.

Roth, D., E. Lynes, J. Riemer, H. G. Hansen, N. Althaus, T. Simmen, and L. Ellgaard. 2010. A

di-arginine motif contributes to the ER localization of the type I transmembrane ER oxidoreductase TMX4. Biochemical Journal 425:195-208.

Ruberg, M., F. Rieger, A. Villageois, A. M. Bonnet, and Y. Agid. 1986. Acetylcholinesterase and butyrylcholinesterase in frontal cortex and cerebrospinal fluid of demented and non-demented patients with Parkinson's disease. Brain research 362:83-91.

Rubio, J. M., J. P. Rodríguez, L. Gil-de-Gómez, C. Guijas, M. A. Balboa, and J. Balsinde. 2015. Group V secreted phospholipase A2 is upregulated by IL-4 in human macrophages and mediates phagocytosis via hydrolysis of ethanolamine phospholipids. The Journal of Immunology 194:3327-3339.

Sberna, G., J. Sáez-Valero, K. Beyreuther, C. L. Masters, and D. H. Small. 1997. The amyloid β-protein of Alzheimer's disease increases acetylcholinesterase expression by increasing intracellular calcium in embryonal carcinoma P19 cells. Journal of neurochemistry 69:1177-1184.

Sihvo, H.-K., K. Immonen, and E. Puolanne. 2014. Myodegeneration with fibrosis and regeneration in the pectoralis major muscle of broilers. Veterinary pathology 51:619-623.

Soglia, F., S. Mudalal, E. Babini, M. Di Nunzio, M. Mazzoni, F. Sirri, C. Cavani, and M. Petracci. 2016. Histology, composition, and quality traits of chicken Pectoralis major muscle affected by wooden breast abnormality. Poultry Science 95:651-659.

Soglia, F., Z. Zeng, J. Gao, E. Puolanne, C. Cavani, M. Petracci, and P. Ertbjerg. 2018. Evolution of proteolytic indicators during storage of broiler wooden breast meat. Poultry science 97:1448-1455.

Tasoniero, G., M. Cullere, M. Cecchinato, E. Puolanne, and A. Dalle Zotte. 2016. Technological

quality, mineral profile, and sensory attributes of broiler chicken breasts affected by white striping and wooden breast myopathies. Poultry science 95:2707-2714.

Tijare, V. V., F. Yang, V. Kuttappan, C. Alvarado, C. Coon, and C. Owens. 2016. Meat quality of broiler breast fillets with white striping and woody breast muscle myopathies. Poultry Science 95:2167-2173.

Toyoshima, C. 2009. How Ca2+-ATPase pumps ions across the sarcoplasmic reticulum membrane. Biochimica et Biophysica Acta (BBA)-Molecular Cell Research 1793:941-946.

Trang, A., and P. B. Khandhar. 2020. Physiology, acetylcholinesterase. StatPearls [Internet].

Trocino, A., A. Piccirillo, M. Birolo, G. Radaelli, D. Bertotto, E. Filiou, M. Petracci, and G. Xiccato. 2015. Effect of genotype, gender and feed restriction on growth, meat quality and the occurrence of white striping and wooden breast in broiler chickens. Poultry science 94:2996-3004.

van der Veen, J. N., J. P. Kennelly, S. Wan, J. E. Vance, D. E. Vance, and R. L. Jacobs. 2017. The critical role of phosphatidylcholine and phosphatidylethanolamine metabolism in health and disease. Biochimica et Biophysica Acta (BBA)-Biomembranes 1859:1558-1572.

Vance, J. E. 2015. Phospholipid synthesis and transport in mammalian cells. Traffic 16:1-18.

Vance, J. E., and G. Tasseva. 2013. Formation and function of phosphatidylserine and phosphatidylethanolamine in mammalian cells. Biochimica et Biophysica Acta (BBA)-Molecular and Cell Biology of Lipids 1831:543-554.

Vance, J. E., and D. E. Vance. 2004. Phospholipid biosynthesis in mammalian cells. Biochemistry and cell biology 82:113-128.

Villa, A., P. Podini, A. Nori, M. C. Panzeri, A. Martini, J. Meldolesi, and P. Volpe. 1993. The endoplasmic reticulum-sarcoplasmic reticulum connection. Experimental cell research 209:140-148.

Vu, H. S., R. Roston, S. Shiva, M. Hur, E. S. Wurtele, X. Wang, J. Shah, and R. Welti. 2015. Modifications of membrane lipids in response to wounding of Arabidopsis thaliana leaves. Plant signaling & behavior 10:e1056422.

Wagner, M., E. Rudakova, V. Schütz, M. Frank, H. Ehmke, and T. Volk. 2010. Larger transient outward K+ current and shorter action potential duration in Gα 11 mutant mice. Pflügers Archiv-European Journal of Physiology 459:607-618.

Walsh, M. P. 1983. Review Article Calmodulin and its roles in skeletal muscle function. Canadian Anaesthetists' Society Journal 30:390-398.

Wang, Q., and M. Michalak. 2020. Calsequestrin. Structure, function, and evolution. Cell calcium 90:102242.

Welter, A., W. J. Wu, T. O'Quinn, T. Houser, E. Boyle, M. Chao, D. Boyle, B. Bowker, and H. Zhuang. 2019. A proposed mechanism for texture property of woody breast in broilers. Meat Muscle Biol 3:179.

Welti, R., W. Li, M. Li, Y. Sang, H. Biesiada, H.-E. Zhou, C. Rajashekar, T. D. Williams, and X. Wang. 2002. Profiling membrane lipids in plant stress responses role of phospholipase Dα in freezing-induced lipid changes in Arabidopsis. Journal of Biological Chemistry 277:31994-32002.

Wilkie, G. S., and E. C. Schirmer. 2008. Purification of nuclei and preparation of nuclear envelopes from skeletal muscle. Pages 23-41 in The NucleusSpringer.

Woo, J. S., J.-H. Hwang, M. Huang, M. K. Ahn, C.-H. Cho, J. Ma, and E. H. Lee. 2015.

Interaction between mitsugumin 29 and TRPC3 participates in regulating Ca2+ transients in skeletal muscle. Biochemical and biophysical research communications 464:133-139.

Xiao, S., W. Gao, Q.-F. Chen, S.-W. Chan, S.-X. Zheng, J. Ma, M. Wang, R. Welti, and M.-L. Chye. 2010. Overexpression of Arabidopsis acyl-CoA binding protein ACBP3 promotes starvation-induced and age-dependent leaf senescence. The Plant Cell 22:1463-1482.

Xing, T., X. Pan, L. Zhang, and F. Gao. 2021. Hepatic oxidative stress, apoptosis and inflammation in broiler chickens with wooden breast myopathy. Frontiers in physiology 12:415.

Yadav, R. K., M. Singh, S. Roy, M. N. Ansari, A. S. Saeedan, and G. Kaithwas. 2018. Modulation of oxidative stress response by flaxseed oil: Role of lipid peroxidation and underlying mechanisms. Prostaglandins & other lipid mediators 135:21-26.

Yang, F. w., H. Wang, C. Wang, and G. n. Chi. 2020. Upregulation of acetylcholinesterase caused by downregulation of microRNA-132 is responsible for the development of dementia after ischemic stroke. Journal of cellular biochemistry 121:135-141.

Young, J. F., and M. K. Rasmussen. 2020. Differentially expressed marker genes and glycogen levels in pectoralis major of Ross308 broilers with wooden breast syndrome indicates stress, inflammation and hypoxic conditions. Food Chemistry: Molecular Sciences 1:100001.

Zhang, L., J. Kelley, G. Schmeisser, Y. M. Kobayashi, and L. R. Jones. 1997. Complex formation between junctin, triadin, calsequestrin, and the ryanodine receptor: proteins of the cardiac junctional sarcoplasmic reticulum membrane. Journal of Biological Chemistry 272:23389-23397.

Zhang, X., D. Antonelo, J. Hendrix, V. To, Y. Campbell, M. Von Staden, S. Li, S. P. Suman, W.

Zhai, and J. Chen. 2020. Proteomic Characterization of Normal and Woody Breast Meat from Broilers of Five Genetic Strains. Meat and Muscle Biology 4.

Zheng, B., J. Zhang, T. Zheng, H. Wang, Z. Li, C. Huan, S. Ning, Y. Wang, and W. Zhang. 2020. ATP1B3 cooperates with BST-2 to promote hepatitis B virus restriction. Journal of medical virology 92:201-209.

Zheng, S., N. Abreu, J. Levitz, and A. C. Kruse. 2019. Structural basis for KCTD-mediated rapid desensitization of GABA B signalling. Nature 567:127-131.

Zhou, Z., S. R. Marepally, D. S. Nune, P. Pallakollu, G. Ragan, M. R. Roth, L. Wang, G. H. Lushington, M. Visvanathan, and R. Welti. 2011. LipidomeDB data calculation environment: online processing of direct-infusion mass spectral data for lipid profiles. Lipids 46:879-884.

Zuo, H., I. Glaaser, Y. Zhao, I. Kurinov, L. Mosyak, H. Wang, J. Liu, J. Park, A. Frangaj, and E. Sturchler. 2019. Structural basis for auxiliary subunit KCTD16 regulation of the GABAB receptor. Proceedings of the National Academy of Sciences 116:8370-8379.

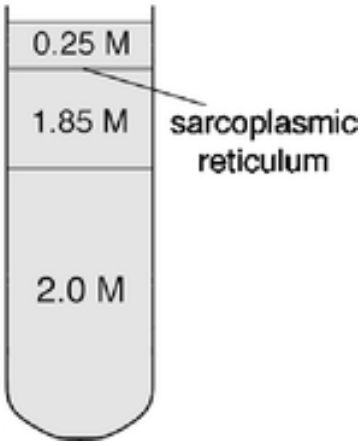

Figure 3.1 Sarcoplasmic reticulum was extracted based on the principle of density gradient centrifugation. The less dense SR was separated from the microsome pellet to the layer with less sucrose while pelleting the denser components of the microsome. Diagram adopted from Wilkie and Schrimer, (2008).

Table 3.1 Scanning conditions of the phospholipid species.

Class	PA	PC and LPC	PE and LPE	PG	PI	PS
Intact ion analyzed	$(M + NH_4)^+$	$(M + H)^+$	$(M + H)^+$	$(M + NH_4)^+$	$(M + NH_4)^+$	$(M + H)^+$
Positive ion scan mode	NL of 115.00	Pre of 184.07	NL of 141.02	NL of 189.04	NL of 277.06	NL of 185.01
m/z range	500–850	450–960	420–920	650–1,000	790–950	600–920
Collision energy (V)	25	40	28	24	25	25
Declustering potential (V)	100	100	100	100	100	100
Entrance potential (V)	14	14	15	14	14	14
Exit potential (V)	14	14	11	14	14	14

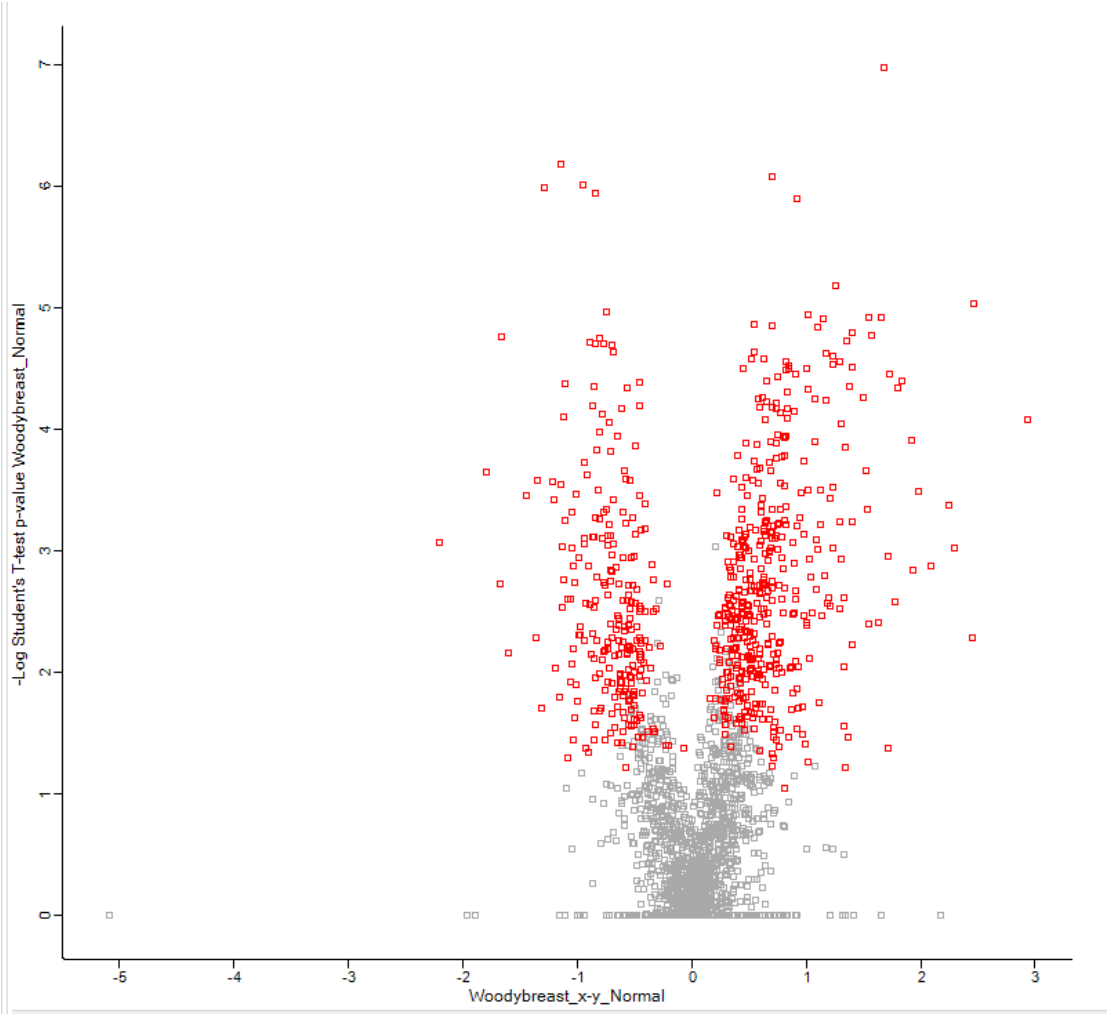

Figure 3.2 Volcanic plot representation of WB and N SR proteome utilizing high-stringency criteria (*FDR* 0.05 and *S0 factor* 0.1) in which red dots correspond to significantly different proteins.

Table 3.2 Representative proteins related to the calcium regulation pathways in sarcoplasmic reticulum between woody and normal breast.

Protein Name	Gene Name	UniProt ID	P-value	Log2 fold changes (WB/N)	Specific Function
Sarcoplasmic/ endoplasmic reticulum calcium ATPase 2	SERCA	Q03669	<0.001	1.68	Calcium transport
Calcium-transporting ATPase	ATP2B4	A0A1D5PU07	0.034	1.37	Calcium transport
Plasma membrane calcium-transporting ATPase 1	ATP2B1	Q98SH2	<0.001	0.73	Calcium transport
Ryanodine receptor 2	RYR2	F1NLZ9	0.001	-0.98	Calcium release
Ryanodine receptor 3	RYR3	A0A1D5PCL0	0.005	-0.64	Calcium release
Calcium load-activated calcium channel	TMCO1	A0A1L1RIN1	0.038	-0.64	Calcium release
Voltage-dependent L-type calcium channel subunit alpha	CACNA1S	A0A1D5PTJ2	0.015	-0.52	Calcium release
Junctophilin 1	JPH1	A0A1D5P1R0	0.001	-0.59	Calcium release
Calsequestrin	CASQ2	A0A3Q2TXF6	0.298	-0.28	Calcium storage
Calmodulin	CALM	P62149	0.327	-0.28	Calcium storage
Sarcalumenin	SRL	A0A1D5P984	<0.001	1.09	Calcium storage

Table 3.3 Representative proteins related to endoplasmic reticulum stress in sarcoplasmic reticulum between woody and normal breast.

Protein Name	Gene Name	UniProt ID	P-value	Log2 fold changes (WB/N)	Specific Function
Protein disulfide-isomerase	P4HB	A0A1D5PV06	0.002	0.51	Response to ER stress
Protein disulfide-isomerase A3	PDIA3	Q8JG64	0.014	0.53	Response to ER stress
Protein disulfide-isomerase A4	PDIA4	A0A1D5PWP7	0.004	0.40	Response to ER stress
Thioredoxin related transmembrane protein 4	TMX4	R4GFY2	0.008	0.52	Response to ER stress

Table 3.4 Representative proteins related to membrane integrity in sarcoplasmic reticulum between woody and normal breast.

Protein Name	Gene Name	UniProt ID	P-value	Log2 fold changes (WB/N)	Specific Function
Phospholipase A2	PLA2G4A	A0A1D5PS91	<0.001	0.75	Enzymatic fatty acid cleavage
Annexin A1	ANXA1	F1N9S7	<0.001	0.84	Phospholipase A2 suppressor
Annexin A2	ANXA2	P17785	<0.001	1.17	Phospholipase A2 suppressor
Annexin A4	ANXA4	A0A1D5PTL7	<0.001	1.41	Phospholipase A2 suppressor
Annexin A5	ANXA5	P17153	0.009	0.69	Phospholipase A2 suppressor
Annexin A6	ANXA6	P51901	<0.001	1.80	Plasma membrane repair
Myoferlin	MYOF	A0A1D5NT41	<0.001	1.22	Plasma membrane repair
Phosphatidylserine synthase 1	PTDSS1	Q5ZM65	0.003	-0.29	Phosphatidylserine biosynthetic process

Table 3.5 Representative proteins related to acetylcholinesterase activity in sarcoplasmic reticulum between woody and normal breast.

Protein Name	Gene Name	UniProt ID	P-value	Log2 fold changes (WB/N)	Specific Function
Cholinesterase	BCHE	A0A3Q2UC01	<0.001	2.93	Acetylcholinesterase activity
Guanine nucleotide binding protein G11 alpha-subunit	GNA11	Q71RI7	<0.001	0.66	G-protein coupled acetylcholine receptor signaling pathway
Guanine nucleotide binding protein, q polypeptide	GNAQ	Q5F3B5	<0.001	0.45	G-protein coupled acetylcholine receptor signaling pathway
Synaptophysin-like protein 2	SYPL2	A0A3Q2UCF9	0.024	-0.59	Calcium homeostasis

Table 3.6 Representative proteins related to the action potential pathways in sarcoplasmic reticulum between woody and normal breast.

Protein Name	Gene Name	UniProt ID	P-value	Log2 fold changes (WB/N)	Specific Function
Sodium voltage-gated channel beta subunit 2	SCN2B	E1BXH9	0.005	-0.70	Sodium channel activity
Potassium channel tetramerization domain containing 12	KCTD12	A0A1D5P9P4	0.001	0.79	Potassium channel activity
Sodium/potassium-transporting ATPase subunit alpha	ATP1A1	A0A1D5PU80	0.008	0.91	Electrochemical gradient homeostasis
Sodium/potassium-transporting ATPase subunit beta 3	ATP1B3	A0A3Q2UED6	0.007	1.03	Electrochemical gradient homeostasis

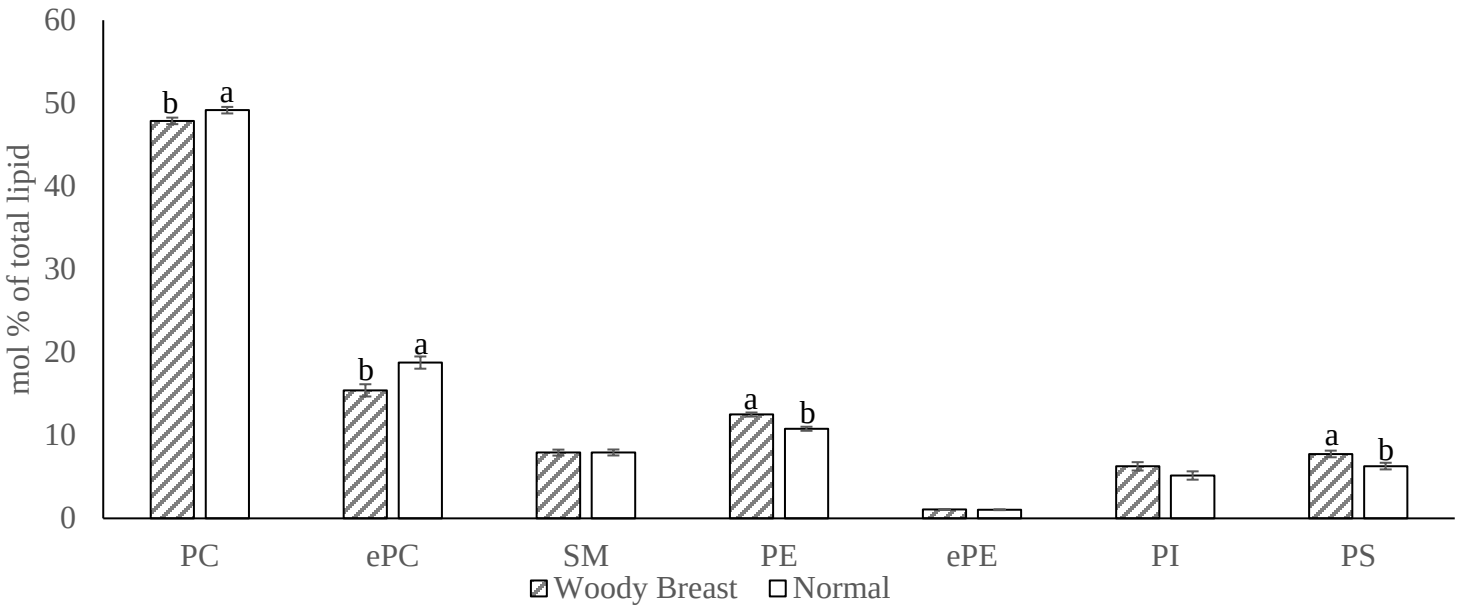

Figure 3.3 WB syndrome effects on phospholipid classes mol % [(nmol of phospholipid class/nmol of total phospholipid)x100] of chicken breast. Each bar represents the mean ± standard error; *n* = 14. Means with different letters within a lipid class are different at *P* < 0.05. PC = phosphatidylcholine; ePC = ether-linked PC; SM = sphingomyelin; PE = phosphatidylethanolamine; ePE = ether-linked PE; PI =phosphatidylinositol; PS=phosphatidylserine.

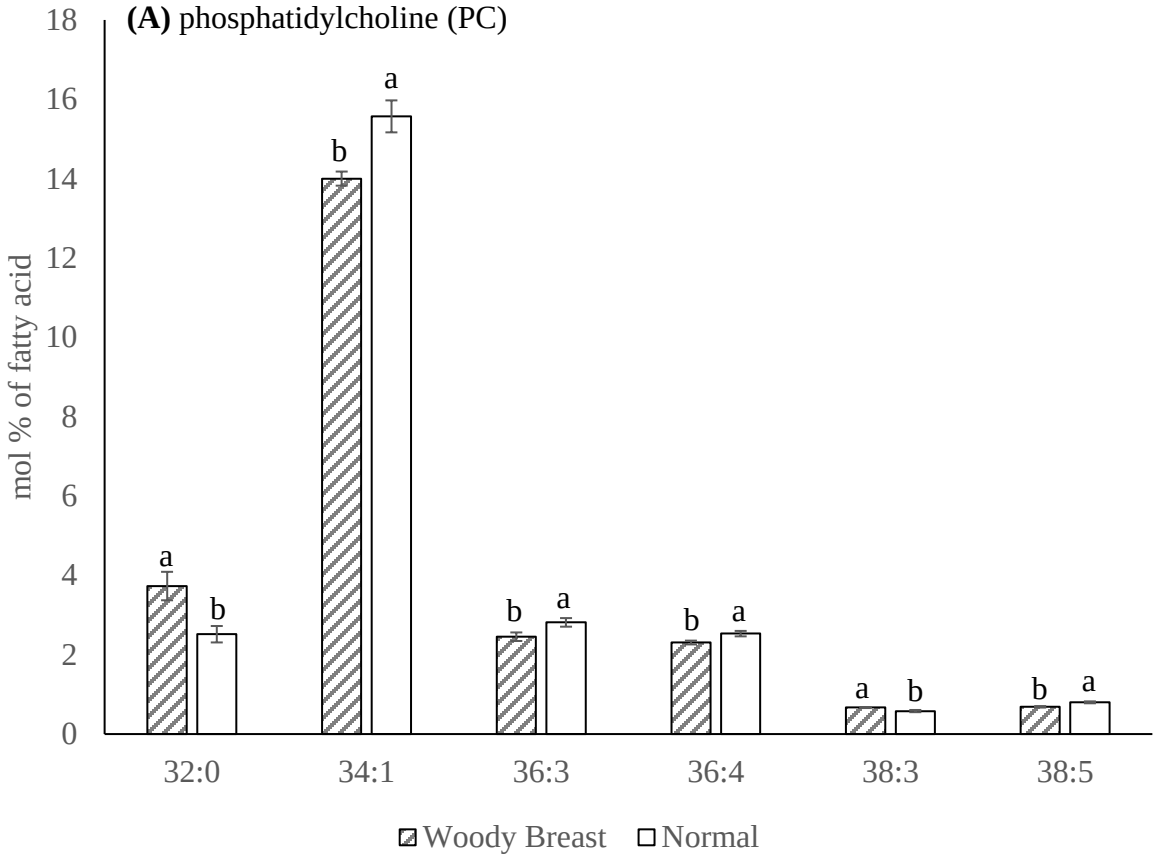
(A) phosphatidylcholine (PC)
mol % of fatty acid
18
16
14
12
10
8
6
4
2
0
a
b
b
a
b
a
b
a
a
b
b
a
32:0
34:1
36:3
36:4
38:3
38:5
Woody Breast
Normal

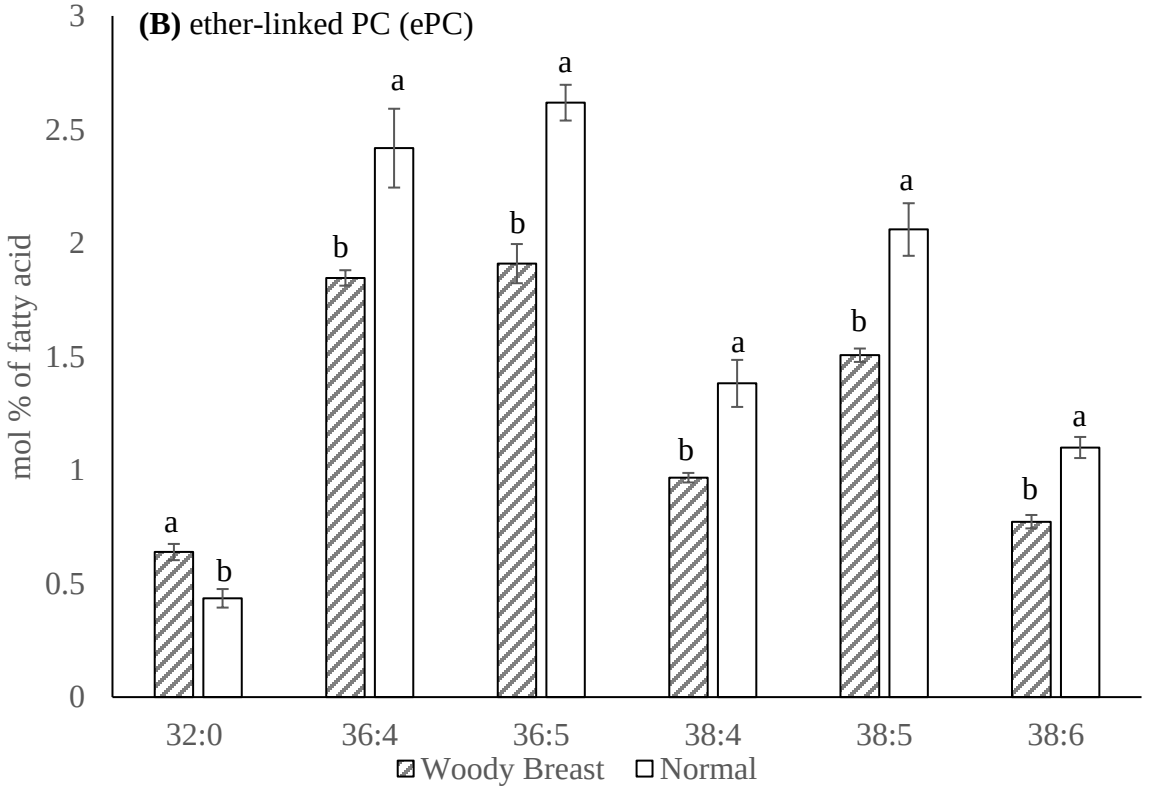
(B) ether-linked PC (ePC)
mol % of fatty acid
3
2.5
2
1.5
1
0.5
0
a
b
b
a
b
a
b
a
b
a
b
a
32:0
36:4
36:5
38:4
38:5
38:6
Woody Breast
Normal

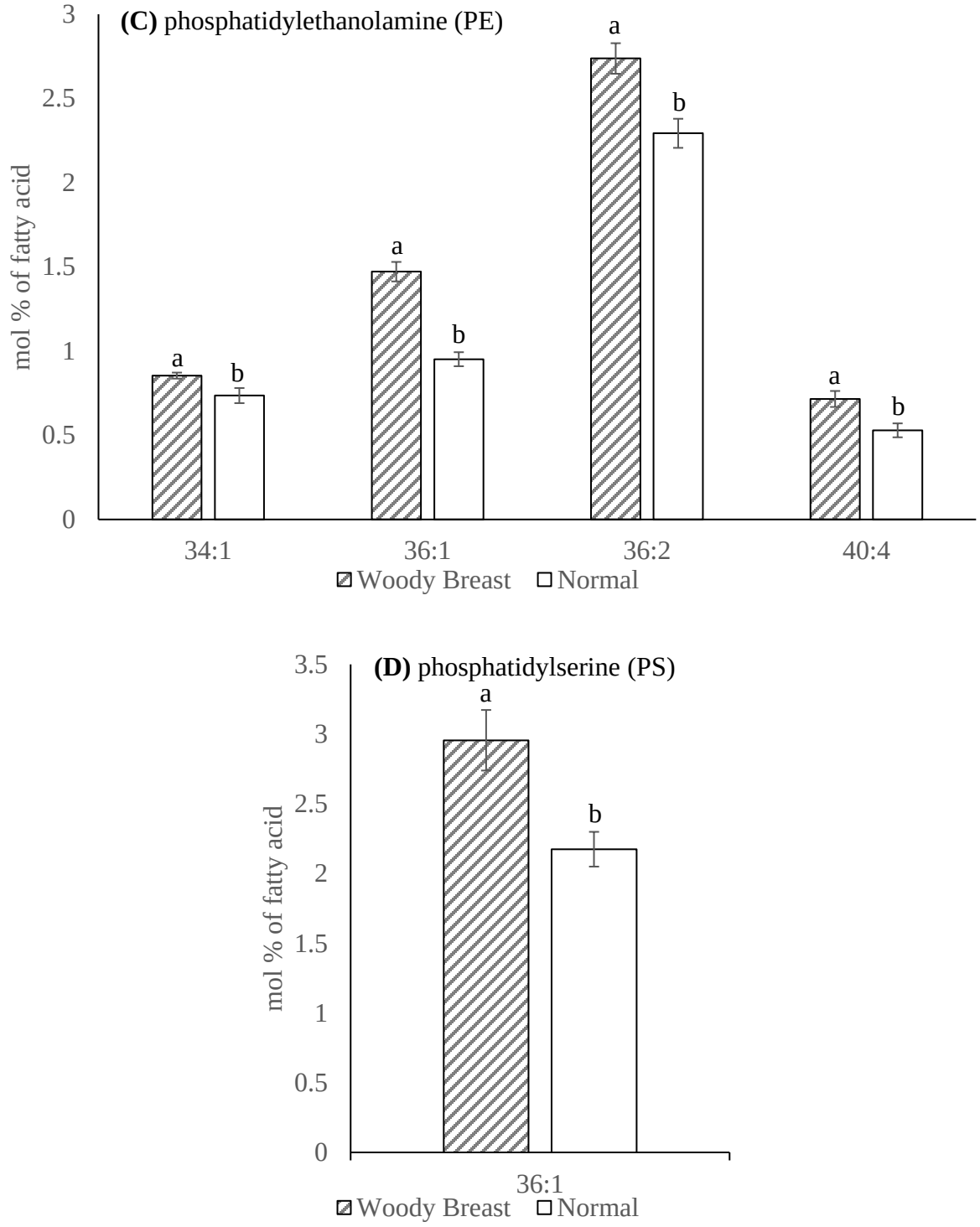

Figure 3.4 WB syndrome effects on lipid molecular species mol % [(nmol of lipid molecular species/nmol of total phospholipid)x100] of (A) phosphatidylcholine (PC) (B) ether-linked PC (ePC) (C) phosphatidylethanolamine (PE) (D) phosphatidylserine (PS). Each bar represents the mean ± standard error; *n* = 14. Means with different letters within a lipid class are different at *P* < 0.05.

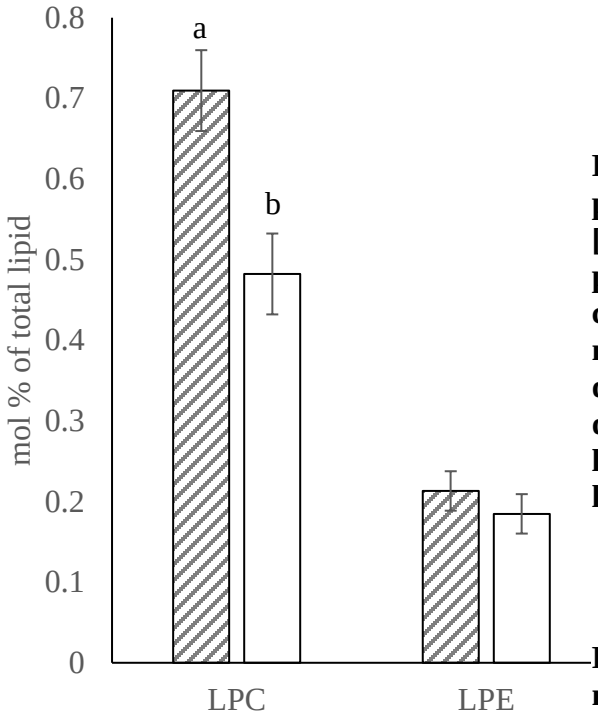

Figure 3.5 WB syndrome effects on phospholipid hydrolysis product mol % [(nmol of phospholipid hydrolysis product/nmol of total phospholipid)x100] of chicken breast. Each bar represents the mean ± standard error; *n* = 14. Means with different letters within a lipid class are different at *P* < 0.05. LPC = lysophosphatidylcholine; LPE = lysophosphatidylethanolamine.

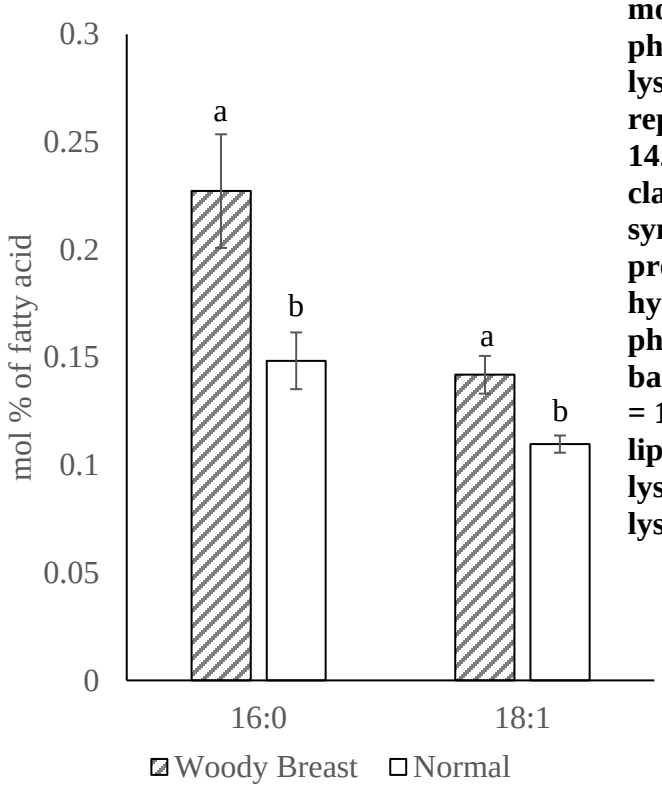

Figure 3.6 WB syndrome effects on lipid molecular species mol % [(nmol of lipid molecular species/nmol of total phospholipid)x100] of lysophosphatidylcholine (PC). Each bar represents the mean ± standard error; *n* = 14. Means with different letters within a lipid class are different at *P* < 0.05.Figure 3.7 WB syndrome effects on phospholipid hydrolysis product mol % [(nmol of phospholipid hydrolysis product/nmol of total phospholipid)x100] of chicken breast. Each bar represents the mean ± standard error; *n* = 14. Means with different letters within a lipid class are different at *P* < 0.05. LPC = lysophosphatidylcholine; LPE = lysophosphatidylethanolamine.

Figure 3.8 WB syndrome effects on lipid molecular species mol % [(nmol of lipid molecular species/nmol of total phospholipid)x100] of lysophosphatidylcholine (PC). Each bar represents the mean ± standard error; *n* = 14. Means with different letters within a lipid class are different at *P* < 0.05.

Figure 3.9 WB syndrome effects on lipid molecular species mol % [(nmol of lipid molecular species/nmol of total phospholipid)x100] of lysophosphatidylcholine (PC). Each bar represents the mean ± standard error; *n* = 14. Means with different letters within a lipid class are different at *P* < 0.05.

Appendix A - Sarcoplasmic Reticulum Extraction Protocol

SR Membrane Extraction
(Wilkie and Schirmer, 2008)

1. Weigh 20 g of raw meat samples (cubed, with all exterior connective tissue and fat removed) to a plastic cup.
2. Add 80 mL of ice cold homogenization buffer: 50 mM HEPES (MW: 238.3 g/mol), 25 mM KCl (MW: 74.55 g/mol), 5 mM of $MgCl_2$ (MW:95.2 g/mol), and 250 mM sucrose (MW: 342.3 g/mol), ice cold, add 1 ml of protease inhibitor/1000 ml of homogenization buffer- if need the SR for protein analysis.
3. Homogenize the muscle on ice with a homogenizer, using 3 x 15 s bursts (Move the pestle all the way down to ensure total homogenization).
4. Transfer the content into 2 separate 50 ml centrifuge tubes.
5. Centrifuge at 1000 x g for 10 min at 4^{o}C (Eppendorf 5810R, A-4-81 rotor).
6. Filter the homogenate from the duplicate tubes with four layers of cheesecloth into a 85 mL Nalgene high-speed centrifuge tube.
7. Change out the rotor to F-34-6-38 rotor and centrifuge the supernatants at 10,000 x g for 20 min at 4^{o}C to pellet mitochondria.
8. Transfer the supernatant to a ultracentrifuge tube for 45 Ti rotor (70 mL, Beckman Coluter, Brea, CA).

9. Centrifuge at 100,000 x g for 45 min at 4°C (Optima XE90 Ultracentrifuge with a Type 45 Ti rotor; Beckman Coluter) to pellet the microsome.
10. Discard the supernatant (**carefully, sometimes the pellet will go with it**), and use a transfer pipet to remove any remaining supernatant.
11. Add 7 mL of icecold homogenization buffer and resuspend the pellet in the solution by pipetting with a 1 mL pipet tip (with the 1cm of tip cut off-easier to scrape off the pellet).
12. Add 19 ml (2.7 volume) of ice cold 2.8M SHKM : 2.8M sucrose, 50 mM HEPES, 25 mM KCl, and 5 mM of $MgCl_2$ (Vigorous stirring and heating are required to dissolve the sucrose, this solution tends to deteriorate quickly due to precipitation, make it the day before and store in room temperature, chill on ice prior use) to make the sucrose concentration 2M SHKM (mix thoroughly).
13. Transfer 26 ml of the microsomal extract to a 38 mL thin wall ultracentrifuge tube. Overlay 7 mL of ice cold 1.85 SHKM : 1.85 M sucrose, 50 mM HEPES, 25 mM KCl, and 5 mM of $MgCl_2$ and then 3 mL of ice cold homogenization buffer.
14. Centrifuge at 57,000 x g for 4 hrs at 4°C (Optima XE90 Ultracentrifuge with a SW32 Ti rotor; Beckman Coluter). This step forces sarcoplasmic reticulum to flow up to the less dense zone, while pelleting other contaminants.
15. The SR will be found at the interphase between the 1.85 M SHKM and homogenization buffer (0.25 M SHKM). Recover the SR with a 5 mL pipet. (Figure 1-c)
16. Transfer the SR to a 32 mL thick wall ultracentrifuge tube and add 25 ml of ice cold homogenization buffer. Centrifuge at 152,000 x g for 75 min at 4°C.
17. Discard the supernatant (remove the remaining supernatant with a transfer pipet) and add 0.5 ml of homogenization buffer.
18. Resuspend the pellet and transfer to a microcentrifuge tube and vortex
19. Split the sample to two microcentrifuge tubes – 250 ul for protein and 250 ul for lipid
20. For the protein tubes, pellet samples at 6,000 × *g* for 10 min at 4°C.
21. Remove the supernatant
22. Resuspend the pellet in 100 ul of PBS + 0.1% (v/v) Triton X-100
23. Add 150 ul 8 *M* urea to the same tube
24. Pellet insoluble material by centrifugation at 6,000×*g* for 2 min
25. Transfer the supernatant to a new tube and determine the protein concentration using BCA
26. Store the sample in -80 °C freezer.

Reference

Wilkie GS, Schirmer EC. Purification of nuclei and preparation of nuclear envelopes from skeletal muscle. Methods Mol Biol. 2008;463:23–41. [PubMed]

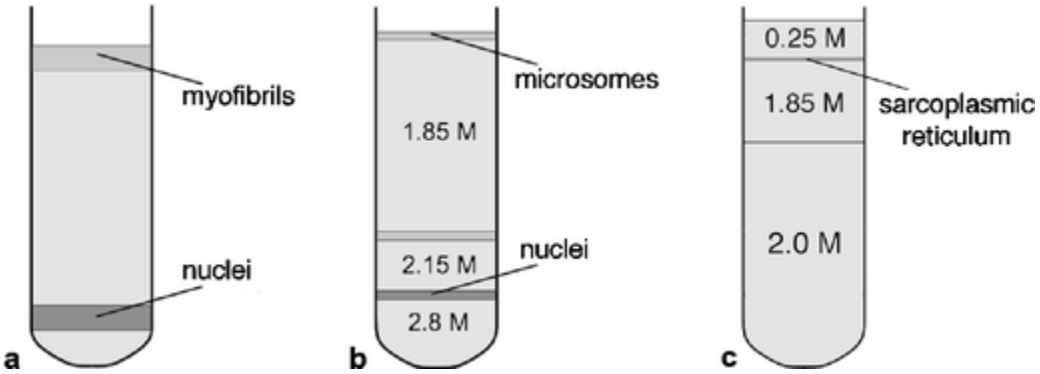
myofibrils
nuclei
a
1.85 M
microsomes
2.15 M
nuclei
2.8 M
b
0.25 M
1.85 M
sarcoplasmic reticulum
2.0 M
c
Figure 1